EBC

Energy in Buildings and Communities Programme

International Energy Agency, EBC Annex 68

Indoor Air Quality Design and Control in Low-Energy Residential Buildings
Subtask 2: Pollutant loads in residential buildings

Energy in Buildings and Communities Technology Collaboration Programme

June 2020

EBC
Energy in Buildings and Communities Programme

International Energy Agency, EBC Annex 68

Indoor Air Quality Design and Control in Low-Energy Residential Buildings Subtask 2: Pollutant loads in residential buildings

Energy in Buildings and Communities Programme

June 2020

Editors

Menghao Qin (menqin@byg.dtu.dk), Technical University of Denmark, Denmark

Jianshun Zhang (jszhang@syr.edu), Syracuse University, USA

Contributing Authors

Zhenlei Liu (zliu138@syr.edu), Syracuse University, USA

Weihui Liang (liangwh@nju.edu.cn), Nanjing University, China

Xudong Yang (xyang@tsinghua.edu.cn), Tsinghua University, China

John Grunewald (john.grunewald@tu-dresden.de), Dresden University of Technology, Germany

Andreas Nicolai (andreas.nicolai@tu-dresden.de), Dresden University of Technology, Germany

Marc Abadie (marc.abadie@univ-lr.fr), University of La Rochelle, France

Reviewed by

Carsten Rode (car@byg.dtu.dk), Technical University of Denmark, Denmark

© Copyright Technical University of Denmark 2020

All property rights, including copyright, are vested in Technical University of Denmark, Operate agent for EBC Annex 68, on behalf of the Contracting Parties of the International Energy Agency Implementing Agreement for a Programme of Research and Development on Energy in Buildings and Communities.

In particular, no part of this publication may be reproduced, stored in a retrieval system or transmitted in any form or by any means, electronic, mechanical, photocopying, recording or otherwise, without the prior written permission of Technical University of Denmark.

Published by the Department of Civil Engineering,Technical University of Denmark, Anker Engelunds Vej 1, 2800 Kgs. Lyngby, Denmark. Report BYG R-428-1.

Disclaimer Notice: This publication has been compiled with reasonable skill and care. However, neither Technical University of Denmark, the Contracting Parties of the International Energy Agency's Implementing Agreement for a Programme of Research and Development on Energy in Buildings and Communities, nor their agents make any representation as to the adequacy or accuracy of the information contained herein, or as to its suitability for any particular application, and accept no responsibility or liability arising out of the use of this publication. The information contained herein does not supersede the requirements given in any national codes, regulations or standards, and should not be regarded as a substitute for the need to obtain specific professional advice for any particular application.

ISBN 978-8-77-877527-6

Participating countries in EBC:

Austria, Belgium, Canada, P.R. China, Denmark, France, Germany, Japan, Republic of Korea, New Zealand, Norway, United Kingdom and the United States of America.

Additional copies of this report may be obtained from:

EBC Bookshop
C/o AECOM Ltd
The Colmore Building
Colmore Circus Queensway
Birmingham B4 6AT
United Kingdom
Web: www.iea-ebc.org
Email: essu@iea-ebc.org

Preface

The International Energy Agency

The International Energy Agency (IEA) was established in 1974 within the framework of the Organisation for Economic Co-operation and Development (OECD) to implement an international energy programme. A basic aim of the IEA is to foster international co-operation among the 30 IEA participating countries and to increase energy security through energy research, development and demonstration in the fields of technologies for energy efficiency and renewable energy sources.

The IEA Energy in Buildings and Communities Programme

The IEA co-ordinates international energy research and development (R&D) activities through a comprehensive portfolio of Technology Collaboration Programmes. The mission of the IEA Energy in Buildings and Communities (IEA EBC) Technology Collaboration Programme is to develop and facilitate the integration of technologies and processes for energy efficiency and conservation into healthy, low emission, and sustainable buildings and communities, through innovation and research. (Until March 2013, the IEA EBC Programme was known as the IEA Energy Conservation in Buildings and Community Systems Programme, ECBCS.)

The R&D strategies of the IEA EBC Programme are derived from research drivers, national programmes within IEA countries, and the IEA Future Buildings Forum Think Tank Workshops. These R&D strategies aim to exploit technological opportunities to save energy in the buildings sector, and to remove technical obstacles to market penetration of new energy efficient technologies. The R&D strategies apply to residential, commercial, office buildings and community systems, and will impact the building industry in five areas of focus for R&D activities:

- Integrated planning and building design
- Building energy systems
- Building envelope
- Community scale methods
- Real building energy use

The Executive Committee

Overall control of the IEA EBC Programme is maintained by an Executive Committee, which not only monitors existing projects, but also identifies new strategic areas in which collaborative efforts may be beneficial. As the Programme is based on a contract with the IEA, the projects are legally established as Annexes to the IEA EBC Implementing Agreement. At the present time, the following projects have been initiated by the IEA EBC Executive Committee, with completed projects identified by (*) and joint projects with the IEA Solar Heating and Cooling Technology Collaboration Programme by (☼):

Annex 1: Load Energy Determination of Buildings (*)
Annex 2: Ekistics and Advanced Community Energy Systems (*)
Annex 3: Energy Conservation in Residential Buildings (*)
Annex 4: Glasgow Commercial Building Monitoring (*)
Annex 5: Air Infiltration and Ventilation Centre
Annex 6: Energy Systems and Design of Communities (*)
Annex 7: Local Government Energy Planning (*)
Annex 8: Inhabitants Behaviour with Regard to Ventilation (*)
Annex 9: Minimum Ventilation Rates (*)
Annex 10: Building HVAC System Simulation (*)
Annex 11: Energy Auditing (*)
Annex 12: Windows and Fenestration (*)
Annex 13: Energy Management in Hospitals (*)
Annex 14: Condensation and Energy (*)
Annex 15: Energy Efficiency in Schools (*)
Annex 16: BEMS 1- User Interfaces and System Integration (*)
Annex 17: BEMS 2- Evaluation and Emulation Techniques (*)
Annex 18: Demand Controlled Ventilation Systems (*)

Annex 19: Low Slope Roof Systems (*)
Annex 20: Air Flow Patterns within Buildings (*)
Annex 21: Thermal Modelling (*)
Annex 22: Energy Efficient Communities (*)
Annex 23: Multi Zone Air Flow Modelling (COMIS) (*)
Annex 24: Heat, Air and Moisture Transfer in Envelopes (*)
Annex 25: Real time HVAC Simulation (*)
Annex 26: Energy Efficient Ventilation of Large Enclosures (*)
Annex 27: Evaluation and Demonstration of Domestic Ventilation Systems (*)
Annex 28: Low Energy Cooling Systems (*)
Annex 29: ☼ Daylight in Buildings (*)
Annex 30: Bringing Simulation to Application (*)
Annex 31: Energy-Related Environmental Impact of Buildings (*)
Annex 32: Integral Building Envelope Performance Assessment (*)
Annex 33: Advanced Local Energy Planning (*)
Annex 34: Computer-Aided Evaluation of HVAC System Performance (*)
Annex 35: Design of Energy Efficient Hybrid Ventilation (HYBVENT) (*)
Annex 36: Retrofitting of Educational Buildings (*)
Annex 37: Low Exergy Systems for Heating and Cooling of Buildings (LowEx) (*)
Annex 38: ☼ Solar Sustainable Housing (*)
Annex 39: High Performance Insulation Systems (*)
Annex 40: Building Commissioning to Improve Energy Performance (*)
Annex 41: Whole Building Heat, Air and Moisture Response (MOIST-ENG) (*)
Annex 42: The Simulation of Building-Integrated Fuel Cell and Other Cogeneration Systems (FC+COGEN-SIM) (*)
Annex 43: ☼ Testing and Validation of Building Energy Simulation Tools (*)
Annex 44: Integrating Environmentally Responsive Elements in Buildings (*)
Annex 45: Energy Efficient Electric Lighting for Buildings (*)
Annex 46: Holistic Assessment Tool-kit on Energy Efficient Retrofit Measures for Government Buildings (EnERGo) (*)
Annex 47: Cost-Effective Commissioning for Existing and Low Energy Buildings (*)
Annex 48: Heat Pumping and Reversible Air Conditioning (*)
Annex 49: Low Exergy Systems for High Performance Buildings and Communities (*)
Annex 50: Prefabricated Systems for Low Energy Renovation of Residential Buildings (*)
Annex 51: Energy Efficient Communities (*)
Annex 52: ☼ Towards Net Zero Energy Solar Buildings (*)
Annex 53: Total Energy Use in Buildings: Analysis and Evaluation Methods (*)
Annex 54: Integration of Micro-Generation and Related Energy Technologies in Buildings (*)
Annex 55: Reliability of Energy Efficient Building Retrofitting - Probability Assessment of Performance and Cost (RAP-RETRO) (*)
Annex 56: Cost Effective Energy and CO2 Emissions Optimization in Building Renovation (*)
Annex 57: Evaluation of Embodied Energy and CO2 Equivalent Emissions for Building Construction (*)
Annex 58: Reliable Building Energy Performance Characterisation Based on Full Scale Dynamic Measurements (*)
Annex 59: High Temperature Cooling and Low Temperature Heating in Buildings (*)
Annex 60: New Generation Computational Tools for Building and Community Energy Systems (*)
Annex 61: Business and Technical Concepts for Deep Energy Retrofit of Public Buildings (*)
Annex 62: Ventilative Cooling (*)
Annex 63: Implementation of Energy Strategies in Communities (*)
Annex 64: LowEx Communities - Optimised Performance of Energy Supply Systems with Exergy Principles (*)

Annex 65: Long-Term Performance of Super-Insulating Materials in Building Components and Systems (*)
Annex 66: Definition and Simulation of Occupant Behavior in Buildings (*)
Annex 67: Energy Flexible Buildings
Annex 68: Indoor Air Quality Design and Control in Low Energy Residential Buildings
Annex 69: Strategy and Practice of Adaptive Thermal Comfort in Low Energy Buildings
Annex 70: Energy Epidemiology: Analysis of Real Building Energy Use at Scale

Annex 71: Building Energy Performance Assessment Based on In-situ Measurements
Annex 72: Assessing Life Cycle Related Environmental Impacts Caused by Buildings
Annex 73: Towards Net Zero Energy Resilient Public Communities
Annex 74: Competition and Living Lab Platform
Annex 75: Cost-effective Building Renovation at District Level Combining Energy Efficiency and Renewables
Annex 76: ☼ Deep Renovation of Historic Buildings Towards Lowest Possible Energy Demand and CO_2 Emissions
Annex 77: ☼ Integrated Solutions for Daylight and Electric Lighting
Annex 78: Supplementing Ventilation with Gas-phase Air Cleaning, Implementation and Energy Implications
Annex 79: Occupant -Centric Building Design and Operation
Annex 80: Resilient Cooling
Annex 81: Data-Driven Smart Buildings

Working Group - Energy Efficiency in Educational Buildings (*)
Working Group - Indicators of Energy Efficiency in Cold Climate Buildings (*)
Working Group - Annex 36 Extension: The Energy Concept Adviser (*)
Working Group - HVAC Energy Calculation Methodologies for Non-residential Buildings
Working Group - Cities and Communities
Working Group - Building Energy Codes
Working Group - International Building Materials Database

IEA EBC Annex 68 – Indoor Air Quality Design and Control in Low-energy Residential Buildings

SUBTASK 2:

Pollutant loads in residential buildings

Editors:
Menghao Qin (menqin@byg.dtu.dk), Technical University of Denmark, Denmark
Jianshun Zhang (jszhang@syr.edu), Syracuse University, USA

Co-authors and Participants:
Zhenlei Liu (zliu138@syr.edu), Syracuse University, USA
Weihui Liang (liangwh@nju.edu.cn), Nanjing University, China
Xudong Yang (xyang@tsinghua.edu.cn), Tsinghua University, China
John Grunewald (john.grunewald@tu-dresden.de), Dresden University of Technology, Germany
Andreas Nicolai (andreas.nicolai@tu-dresden.de), Dresden University of Technology, Germany
Marc Abadie (marc.abadie@univ-lr.fr), University of La Rochelle, France

Annex 68 Operating Agent:
Carsten Rode (car@byg.dtu.dk), Technical University of Denmark, Denmark

Executive Summary

A major obstacle to integrating energy and Indoor Air Quality (IAQ) strategies is the lack of reliable methods and data for estimating pollutant loads in residential buildings in the way heating/cooling loads are routinely estimated. This subtask is to collect existing data and to a limited extent provide new data about properties for transport, retention and emission of chemical substances in new and recycled materials in residential buildings under the influence of heat, airflow and moisture conditions. Collection of results from lab tests on material and room level is part of this study. Specifically, results are collected and analyzed from tests of emission of harmful compounds under various temperature, humidity and airflow conditions, since such data under combined exposures generally are not available for use today.

In Subtask 2, these targets were approached by the following main activities.

- A critical literature survey was carried out to gather relevant data and existing knowledge on major pollutant sources and loads in residential buildings due to building materials and assemblies, including existing Volatile Organic Compound (VOC) emission source and sink models and data.
- Experimental measurements were carried out to study the combined effects of temperature and humidity on VOC emissions from different building materials. Additional small-scale environmental chamber tests were conducted to investigate the adsorption and desorption of VOCs and SVOCs on building materials and furnishing.
- Regarding the mathematical modelling part, first a theoretical correlation between the emission rate and indoor temperature and relative humidity was derived. Second, in order to evaluate the impacts of VOCs emissions from building materials on the indoor pollution load beyond the standard chamber test conditions and test period, mechanistic emission source models were developed. A new procedure was proposed to estimate the model parameters using VOC emission data from standard small chamber tests.
- Three common exercises (CE) were developed.
    - CE1: A procedure for the definition of reference buildings for estimating the pollution loads, IAQ and energy analysis for different countries/climates.
    - CE2: A method and procedure of using a full-scale chamber to evaluate the effects of emission sources and sinks, ventilation and air cleaning on IAQ.
    - CE3: Development of a procedure for estimating the parameters of mechanistic emission source models using emission data from standard small chamber tests.
- A database of model parameters for the estimation of VOC emission rates for IAQ simulations was developed.

CONTENTS

1 Introduction

1.1 About IEA EBC Annex 68

The overall objective of the IEA EBC Annex 68 is to provide scientific basis usable for optimal and practically applicable design and control strategies for **better Indoor Air Quality (IAQ)** in residential buildings. These strategies are intended to minimize possible energy use while ensuring good IAQ. The aim of Annex 68 is to gather the existing data and provide new data on pollution sources in buildings, to model the indoor hygrothermal conditions, air quality and thermal systems, and to find the methods to optimize ventilation and air-conditioning. Annex 68 is focused on **low-energy residential buildings**.

There are numerous different national definitions and concepts describing low-energy buildings. Some, for example, focus on the renewable energy production on-site (NorthPass, 2012) and discuss not only the reduction of energy use. All definitions have in common that a low-energy building should achieve better or significantly better energy performance compared to a traditional contemporary building practice to reduce the use of fossil fuels such as oil, gas and coal (Thullner, 2010). In some countries or regions, low-energy buildings are defined by the building codes or in relation to the energy standard. It may happen that one building, which can be classified as low-energy in one country, uses more energy than a standard building in another country. Also, standards have improved with time and the low-energy standards from the past are likely to be a standard today (Laustsen, 2008). In the present project, a building is considered as low-energy when it has a better energy performance than the typical new building following the minimum standards defined in building regulations at a given point of time in a given country.

The work of the Annex 68 was organized in five subtasks (Figure 1-1): **Subtask 1** developed the metrics to assess the performance of low-energy buildings as regards indoor air quality combining the aspirations to achieve very high energy performance without compromising indoor environmental quality. **Subtask 2** gathered the existing knowledge and provided new data about indoor air pollutants in relation to combined heat, air and moisture transfer. **Subtask 3** identified and developed modelling tools that can assist designers and managers of buildings in accounting for IAQ. **Subtask 4** developed design and control strategies for energy efficient ventilation in residential buildings that will not lessen indoor air quality. **Subtask 5** conducted field measurements to examine and optimize different control and design strategies.

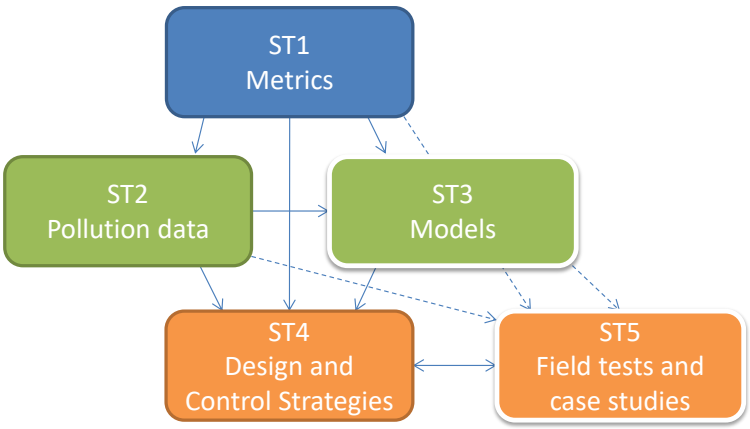

Figure 1-1: Schematic overview of the subtasks in Annex 68 and their interrelations.

In ST2, the focus was to collect / provide data about properties for transport, retention and emission of chemical substances in new and recycled materials in residential buildings under the influence of heat, airflow and moisture conditions. This report summarizes the work done in ST2.

1.2 Outline of the work under Subtask 2

The objective of Subtask 2 was to develop methods and procedures to estimate the pollution loads for VOCs in residential houses. The pollution loads are defined as the total emission rates of VOCs to the conditioned air space in the house, including pollutants from both indoors and out. They vary from one pollutant to another. In analogy to the heating or cooling loads, the pollution loads need to be removed by ventilation or air cleaning in order to maintain the concentrations below threshold values.

1.2.1 Activities

- The subtask organized a literature survey and contacted researchers to gather relevant data and existing knowledge on major pollutant sources and loads in residential buildings due to building materials and assemblies, including existing VOC emission source and sink models and data. A series of datasets have been identified including data from NRC's MEDB-IAQ project, SU/MIT/Tsinghua's ASHRAE projects, University of La Rochelle's PANDORA, databases from Shenzhen IBR and Tsinghua University, etc.
- Several experimental measurements were carried out.
  1) The first one was to study the combined effects of temperature and humidity on VOC emissions from different building materials. Different VOCs were measured for two different materials. The data were used to validate the existing models as well as suggesting new models for correlations between the emission factors and environmental conditions.
  2) The second was a field measurement in the P+ building in Wujin, Jiangsu, China to study the relationship between IAQ and different ventilation/ air cleaning strategies and building energy consumption. The following indoor atmospheric and energy performance parameters were measured: T, RH, VOC, particles, ventilation (mechanical + natural), energy consumption. The test data were also be used to validate the models developed in subtask 3, and provided a case study for Subtasks 4 and 5.
  3) Additional small-scale environmental chamber tests were conducted at Syracuse University to investigate the adsorption and desorption of VOCs and SVOCs on building materials and furnishing. The data were combined with previous data to further evaluate and develop sink models.
- A theoretical correlation between the emission rate and indoor temperature and relative humidity was derived.
  1) A procedure for the definition of reference buildings for estimating the pollution loads, IAQ and energy analysis for different countries/climates was proposed. An example was provided for a detached house in Northeast region of U.S. including house specification, DesignBuilder/E+ simulation results for energy consumption, and IAQX simulation results for VOCs. The test case was used for Common Exercise 1.
  2) A method and procedure of using a full-scale chamber to evaluate the effects of emission sources and sinks, ventilation and air cleaning on IAQ was developed. Two cases were defined with experimental data, one for a simple source (particle board), and the other for a mock up of a room

with vinyl floor, ceiling tiles, painted gypsum wallboards, and a desk. The first test case was used for Common Exercise 2.

- In order to evaluate the impacts of VOCs emissions from building materials on the indoor pollution load beyond the standard chamber test conditions and test period, mechanistic emission source models have been developed in the past. However, very limited data are available for the required model parameters including the initial concentration (C_{m0}), in-material diffusion coefficient (D_m), partition coefficient (K_{ma}), and convective mass transfer coefficient (k_m). In the project, a procedure was developed for estimating the model parameters by using VOC emission data from standard small chamber tests. In the procedure, the measured data was used to estimate initial values of the model parameters and then refine the estimates by multivariate regression analysis of the measured data. The measured concentration data were first normalized by the average value of air concentration. The Least Square and Global search algorithm with multi-starting points were used to achieve a good agreement in the normalized VOC concentrations between the model prediction and experimental data. The procedure was used to analyze emission datasets obtained to develop a database of C_{mo}, D_m and K_{ma} for typical building materials, which were used in the modelling effort of Subtask 3.
- Three Common Exercises were published.
    1) A procedure for definition of reference buildings for estimating the pollution loads, IAQ and energy analysis for different countries/climates.
    2) A method and procedure of using a full-scale chamber to evaluate the effects of emission sources and sinks, ventilation and air cleaning on IAQ.
    3) Development of a Procedure for Estimating the Parameters of Mechanistic Emission Source Models from Chamber Testing Data.

1.2.2 Deliverables

1. The Report on Indoor Pollution Loads Due to Building Materials and Assemblies.
2. A database of VOC emission model parameters for IAQ simulations.
3. High quality journal articles and conference papers on relevant topics.

1.2.3 Stakeholders involved

Stakeholders are partners from academia, manufacturers of building materials and inventory products, and public health authorities, health organizations and technological institutes who make testing for industry and run their labelling systems.

2 Definition of a reference residential building prototype

(Zhenlei Liu and Jensen Zhang)

2.1 Introduction

Many energy efficiency strategies have been used to improve the energy performance of residential buildings, and simulation models are available for evaluating the effectiveness of these strategies. A reference residential building prototype is needed to set a base line IAQ and energy consumption to which the performance of the proposed building (referred to as the target building) with the design and operation strategies can be compared. The reference building needs to be defined for the local region or country, it should represent a typical enclosure design, HVAC operation, occupancy and other internal equipment and activities, and the local climate and practice. In this section, we present a procedure for defining such a reference building using the standard reference specifications for single family houses in the Northeast Region of the US as an example (Case1.1). The method and procedure used in this example have been applied in the Annex 68 Subtask2 Common Exercise 1 to establish respective local reference buildings for other regions and countries.

2.2 Methodologies

The design of the reference house is necessary to represent a typical design in this region that satisfies the requirements of the local building standards and reflect the local practices. Relevant national and local standards already exist for establishing reference building energy consumption (e.g., RESNET and IECC in the U.S.), or for IAQ design (e.g., CDPH 2007), but not both. The intent of this activity was to define a reference residential house for both energy and IAQ analysis.

Based on the review and analysis of the relevant standards in the local region, we specified the building materials, HVAC system settings, equipment settings, and occupancy schedules. For the reference house in the Northeast region of the US, we chose a two-story single-family house design at Syracuse, NY, US as an illustrative case in a cold climate. We reviewed the Building America Benchmark House (NREL, 2014) definition and the relevant ASHRAE Standards 90.2 and 62.2 (ASHRAE, 2007; ASHRAE, 2010) to specify the design and operational condition.

As an example for assessing the energy efficiency strategies, we simulated energy performance of four cases (with/without natural ventilation, with/without lighting control) for the Syracuse reference house by Designbuilder/EnergyPlus. The case without natural ventilation and lighting control was defined as the reference case. Detailed specifications and simulation results can be found in PART II Report of Annex 68 Subtask 2.

To analyze IAQ for the reference house, it is necessary to specify the pollution load which is the summation of products of emission areas time the emission factor (*EF*) of source surfaces. The following approaches can be used to determine the emission factors (*EF*) for the materials used in the reference house:

A) Assuming that pollution loads are constant over time and equal to the initial emission rates (which is considered as the "worst-case" conditions for design because the actual emission rates typically decrease over time), we can use:

1. Threshold concentration limits, material quantity and ventilation rate of the residential scenario defined in the local IAQ standard with the assumption that each material should contribute no more than *1/n* of the total pollution load for a given compound *(*where *n* is the number of materials used in the reference house). In the Syracuse reference house, the allowable concentrations specified in the CDPH standard guide for selecting low-emitting materials (CDPH, 2017) was used to determine the allowable emission factors for each material. Note that in the CDPH Standard, *n* was set to 2, which resulted over limit concentrations in the simulated house when the number of materials were more than 2 as expected.
2. Threshold *EF* limits in emission standards for low-emission materials (e.g., the maximum *EFs* defined in the Green Label Plus Emission Criteria for carpet).
3. Measured material *EFs* from standard environmental chamber testing at a specified time point (e.g., *EFs* at 14 days in the NRC emission database).

B) Assuming variable pollution loads as more realistic conditions, we can use:

4. Empirical model representation of material emission test data: *EF(t)*.
5. Mechanistic model calculation with necessary model parameters (Section 4 and Section 5).

Once the pollution loads are specified, an IAQ simulation model such as IAQX1.1, CONTAM or CHAMPS-BES can be used to evaluate the resulting pollution levels in the house under the reference and proposed ventilation conditions. Details about the procedure to define the reference conditions for the Syracuse reference house are described in Part II Case 1.1.

2.3 Results from the Syracuse Reference House Study

In this section, we use the Syracuse reference house study to illustrate how the above methodologies can be applied to define a local reference house, and how to use it as a baseline to evaluate energy and IAQ strategies.

The Syracuse reference house was intended to be an economical modest size with three bedrooms, two bathrooms, a kitchen, a dining room and a family/living room, and has no garage. It had two floors plus an unconditioned basement. The front door faced North in this particular configuration.

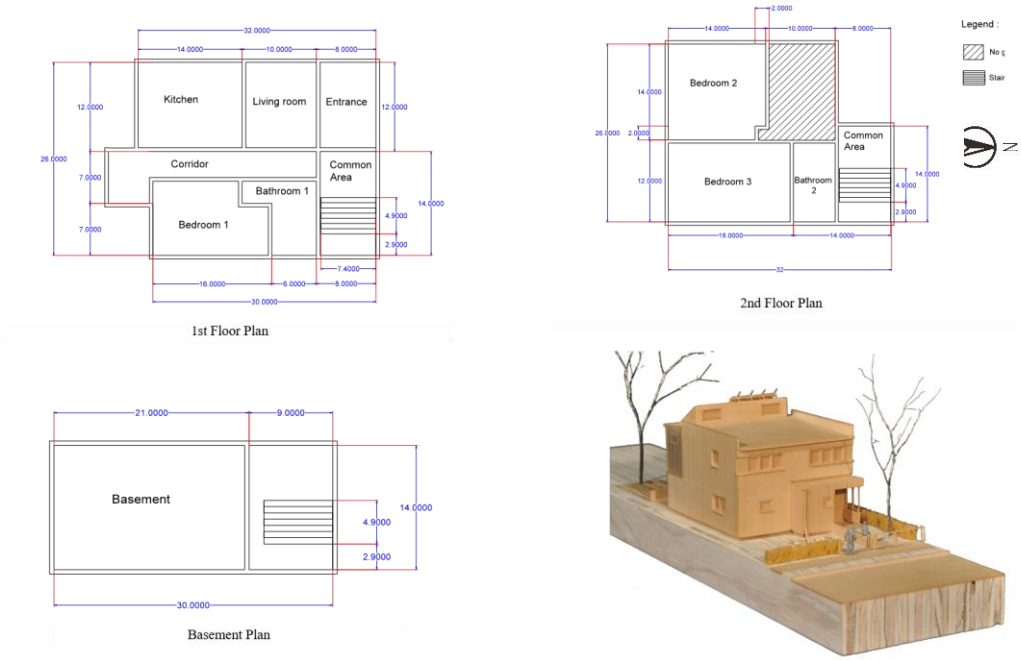

Figure 2-1 Layout of Syracuse reference house. Two conditioned floors with a total of 137.6 m^2 (1481 ft^2)(calculated from wall central to wall central by original floor plans) of conditioned space. All rooms have the same height 2.43 m (8 ft*)) except that the living/family room has a double room height.

Building envelope assembly compositions and material properties are provided in Table 2-1. They follow the specifications in the Building America B10 Benchmark house design.

Table 2-1 : Building Envelope Assembly Composition and Material Properties

Building Envelope					
Assembly	Materials (exterior to interior)	Thickness mm	Conductivity W/(m K)	Specific Heat* J/(Kg K)	R-value (m^2 K)/W
Flat Roof (simplified for modeling purpose)	Asphalt shingles			1255.20	
	Roofing felt underlayment	4.1			
	Plywood	19.1	0.12	1213.36	0.16
	Air	76.2		1004.16	0.18
	R38 fiberglass	88.9	0.04	962.32	2.07
	Gypsum board	15.9	0.16	1087.84	0.10
	Total R value				2.51
External Wall	Cement panel	9.5	0.72	1004.16	0.01
	Air layer	19.1		1004.16	0.18
	Vapor Permeable	0.2			0.005

	Plywood	19.1	0.12	1213.36	0.16
	R13 fiberglass	88.9	0.05	962.32	1.93
	Vapor retarder	0.2			0.21
	Gypsum board	15.9	0.16	1087.84	0.10
	Total R value				2.60
Below Grade wall	R11 EPS	50.8	0.04	-	1.43
	CMU	203.2	0.86	920.48	0.24
	R10 fiberglass	88.9	0.04	1338.88	2.07
	Gypsum wall board (GWB)	15.9	0.16	1213.36	0.10
	Total R value				3.84
Ground Floor	Cast Concrete	152.4	1.13	836.8	0.14
	Vapor Barrier	0.2			0.21
	R11 Glass-fiber batt insulation	50.8	0.04	1338.88	1.18
	Crushed stone	152.4	3.49		0.04
	Total R value				1.57
Ground Floor (basement)	Vapor Barrier	0.2			0.21
	R11 Glass-fiber batt insulation	50.8	0.04	1338.88	1.18
	Crushed stone	152.4	3.49		0.04
	Total R value				1.42
Name	Total Solar transmission (SHGC)		Light transmission		U value
Vertical glazing, 0%-40% of wall, U-0.35 (1.99), SHGC-0.45	0.45		0.56		0.35

HVAC system operation and ventilation rate:

In accordance with ASHRAE 90.2, the temperature set points were specified as:

6:00 a.m. – 23:00 p.m.:

- Set point for cooling: 25.6 ℃ (78 °F)
- Set point for heating: 20 ℃ (68 °F)

23:00 p.m. – 6:00 a.m.:

- Set point for cooling: 25.6 ℃ (78 °F)
- Set point for heating: 15.6 ℃ (60°F)

For single family house, there is typically only one thermostat in living room in most cases, so we used same heating/cooling schedule and setpoint for the entire house. It should be noted that such a single zone

assumption for the entire house can be a significant over-simplification for houses where spatial nonuniformity in temperature exist. A multizone approach should be considered when more accurate prediction is required. The same problem exits for IAQ simulation for houses where spatial concentration gradients are significant among the different zones.

For the reference house, the heating and cooling devices were modeled as an ideal system, and were auto sized by the simulation software with the default inputs for the HVAC system. Fan energy consumption was assumed to be 0.18 W/(m^3 h^{-1}) (0.3 W/cfm) according to Building America B10 Prototype (2014) and ASHRAE Standard 90.2.

E+ simulation results:

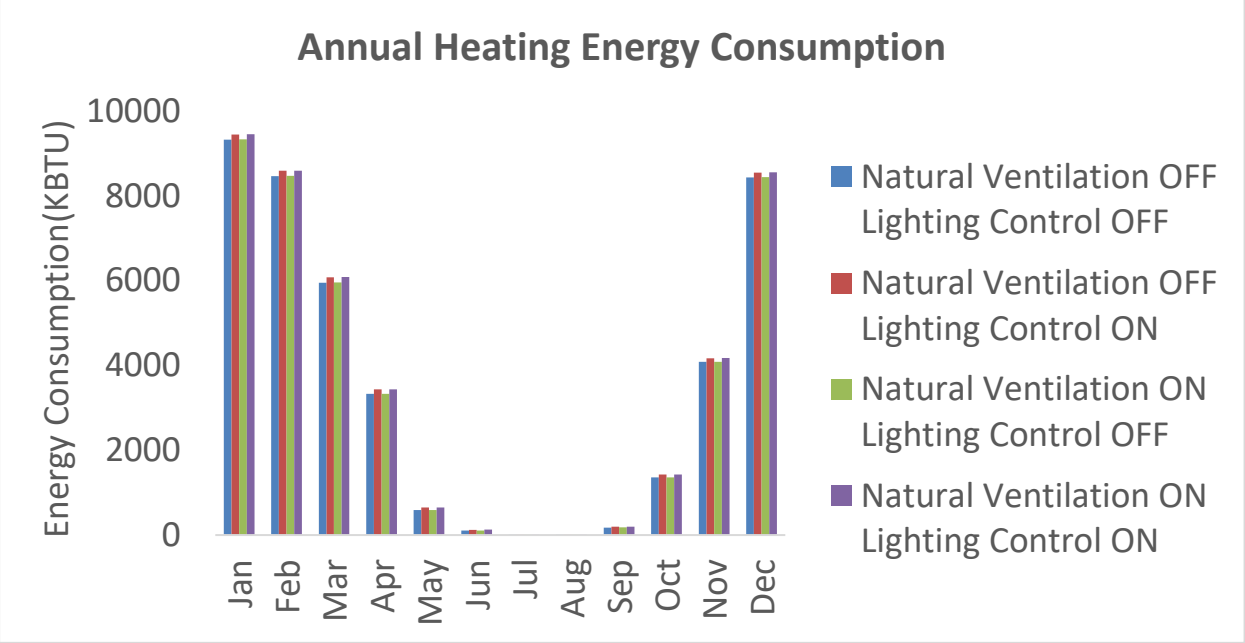

Figure 2-2 Monthly heating energy consumption for the four cases (Unit conversion: 1 BTU = 0.00029 kWh)

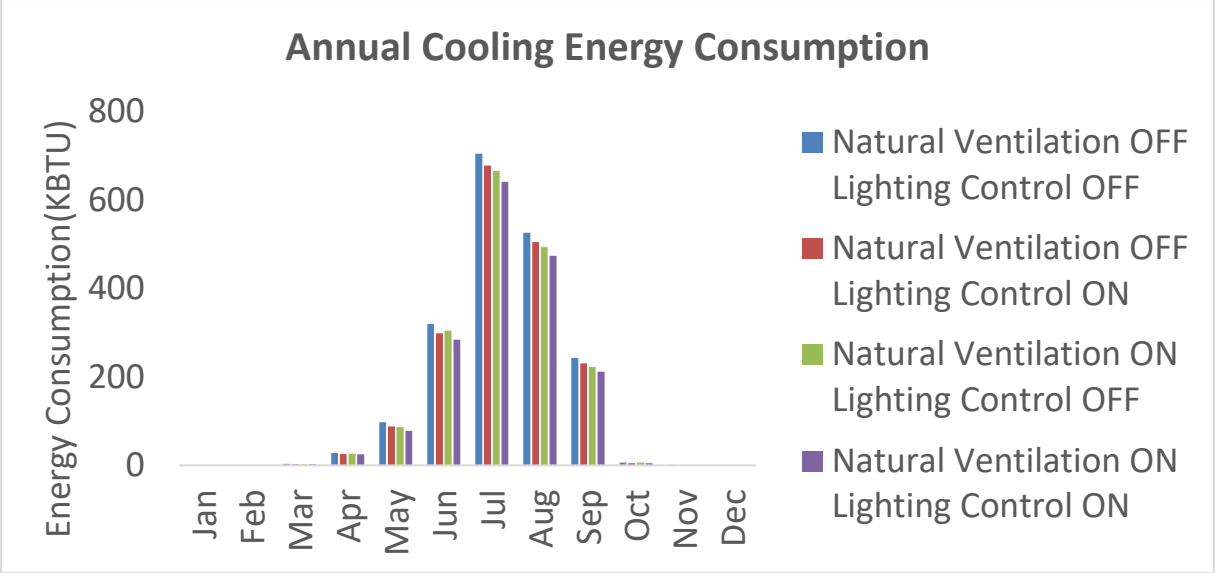

Figure 2-3 Monthly cooling energy consumption for the four cases (Unit conversion: 1 BTU = 0.00029 kWh)

From the results shown in Figure 2-2 and Figure 2-3, the baseline model with no natural ventilation and natural lighting had an energy consumption intensity of 134.07 kWh/m^2 (47.68 kBtu/ft) per year, which is 23% less than the 2005 survey value for detached single-family houses that is 173.50 kWh/m^2 (55 kBtu/ft) per year. Natural ventilation reduced the monthly cooling energy consumption by 5% - 11% from the baseline model. The case with natural ventilation was simulated as follows: For the heating season, it was activated when the outdoor temperature was above 20.6 ℃ (0.6 ℃ or 1 ℉ above heating setpoint). For the cooling season, it was activated when the outdoor temperature was less than 25 ℃ (0.6 ℃ or 1 ℉ below cooling setpoint). When it was activated, an additional 5.4 ACH was infiltrated and exfiltrated in the house. So, natural ventilation saves more cooling in spring and autumn than summer. The lighting control was simulated as follows: the lighting is controlled by the setpoint of lighting level and the availability of natural daylight. The overhead lights dim continuously from the maximum light output to minimum light output as the daylight illuminance increases. The corresponding electrical power required for artificial lighting decreases accordingly. Lighting control reduced the lighting energy consumption by 15% - 21% from the baseline model (not shown here). But only about 10% of the total energy over a year was consumed by the lighting equipment. So, the contribution of lighting control is not significant in reducing total energy consumption. It also reduced the cooling energy consumption due to the reduction in the heat from the artificial lights (Figure 2-3). It also led to slight increase in heating energy consumption (Figure 2-2).

In the cases of constant pollutant loads, the “worst” case scenario can predict the performance for different material selection and house design strategies (Figure 2-4, where formaldehyde was used as an example due to its low threshold concentration). For Method 1, the constant pollutant load was defined with the threshold concentrations from the CDPH standard. The resulting concentrations at steady state reached the allowable levels in the CDPH standard as expected. For Method 2 and 3, the constant pollutant load was defined with threshold of building material emission standards, which is maximum acceptable emission factor for each material. So, the simulated VOC concentration could exceed the CDPH standards. Therefore, the constant

pollution load approach could be considered as the "worst" case. Method 4 uses empirical models to estimate the decay of emission rates over time, and hence reflects the "Age effect" of the material (Figure 2-5, where toluene was used as an example since it is typically used as a reference compound for TVOC quantitation).

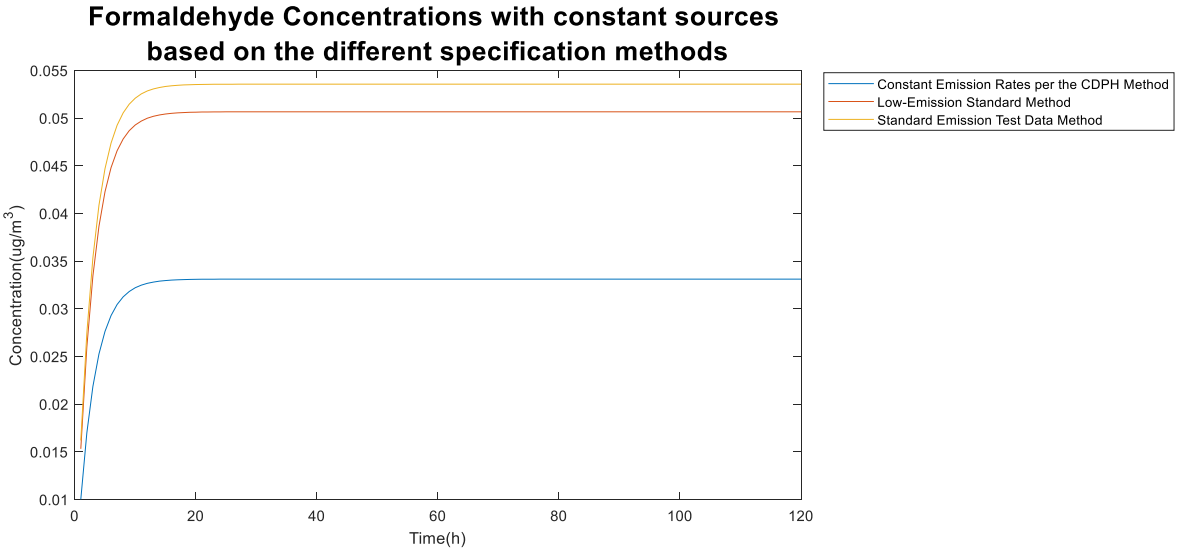

Figure 2-4 120 hours IAQ simulation for formaldehyde under constant emission factor (*EF*)

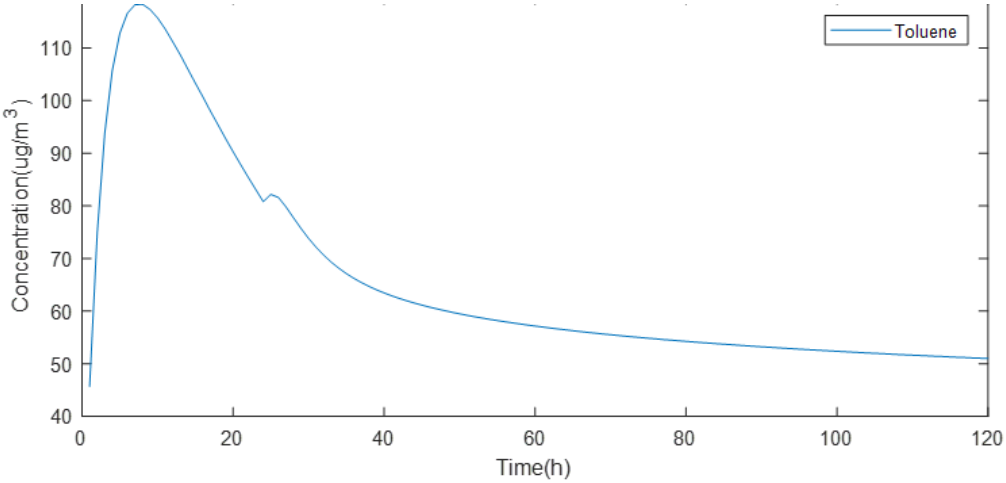

Figure 2-5 120 hours IAQ simulation for toluene by empirical model (power-law model)

The above results illustrate that the different constant emission rate specification methods led to different predicted formaldehyde/toluene concentrations in the prototype house. Which specification method should be used depends on the availability of standards and test data, with the preference given to Method 4 if actual emission data are available. In any case, the same Method should be used throughout in evaluating various IAQ design and operation strategies. Empirical models based on emission tests can be used to evaluate the effects of the emission rate decay over time on the VOC concentrations in the house *under standard test conditions*. In real houses, temperature and relative humidity vary over time. Evaluations of the effects of temperature and relative humidity on the VOC concentrations and IAQ require the use of

mechanistic models and associated model parameters, i.e., using a model-based testing and evaluation approach as discussed in the next.

3 Model-based testing and evaluation of VOC emission and sorption

(Zhenlei Liu, Andreas Nikolai, John Grunewald and Jensen Zhang)

3.1 Introduction

Model-based testing and evaluation (MBTE) refers to a methodology in which modelling and standard testing are combined to evaluate the performance of a product not only under the standard test condition, but also future usage condition (Zhang et al., 2004). It involves three steps (Figure 3-1): First, a physics-based model of the emission processes was developed and the essential model parameters are identified. Second, tests are performed to determine the model parameters. Third, the parameters are used in the model to evaluate the rates of the emissions and their impact on the VOC concentrations and indoor air quality (section 5).

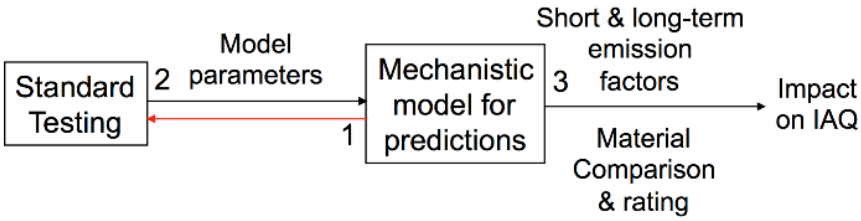

Figure 3-1 Model-based testing and evaluation of material emissions and their impact on IAQ

Standard test methods have been established and widely used for characterizing VOC emissions from building materials, indoor furnishings, and office equipment by using small or full-scale environmental chambers (ASTM, 1997; ASTM, 2001; ANSI/BIFMA M7.1, 2011). With standardized procedures for specimen collection, preparation, testing and data analyses, these existing methods are suitable for identifying the compounds emitted from the test specimen, and their emission rates over time under pre-defined conditions. The test specimens can be either individual materials or material assemblies. Empirical or semi-empirical equations/models are often used to represent the test results with the model parameters being determined by regression analyses of the VOC concentrations measured in the chamber. However, the equations and their coefficients obtained in such a manner may not be suitable for extrapolating the test results beyond the test period, from smaller scale to full-scale, or from testing of individual materials to material assemblies or product systems. Adopting a model-based testing and evaluation methodology would allow prediction of long-term emissions based on short term testing, and of emissions from assemblies or systems based on the testing of their individual materials or components.

3.2 Theory

3.2.1 Source and sink models and the parameters

Consider a homogeneous dry material source that has only the top surface exposed to the air in a well-mixed chamber while the other surfaces sealed (Figure 3-2). The experiment facility was presented in Section 4.3. Here, we limit the discussion to cases where VOC emission and adsorption are governed by the VOC transport in the material and through the boundary layer as well as the sorption equilibrium at the material-air interface:

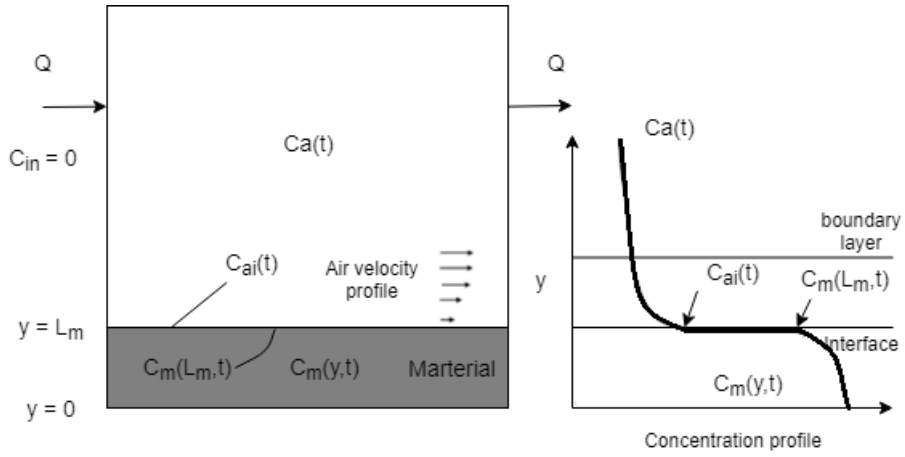

Figure 3-2 Schematic of an emission source inside a ventilated environmental chamber.

Material Layer: Assuming 1-D diffusion inside the material., the following diffusion model can be used to describe the VOC transport inside the material (Christiansson et al., 1993; Little et al., 1994; Bodalal, 1999; Yang, 1999):

$$\frac{dC_m}{dt} = D_m \frac{d^2C_m}{dy^2} \quad \text{(3-1a)}$$

Where, C_m = VOC concentration in the material., kg/m^{3}REV (representative element volume of the material); t = time, s; D_m = effective VOC diffusivity in the material., m^2/s; and y = coordinate, m. The model applies to both non-porous and porous materials. For porous materials, it is often assumed that the VOC transfers via the inter-connected pores driven only by the gas phase concentration gradient in the pore air:

$$j'' = -D_p \frac{dC_{pa}}{dy} = -D_m \frac{dC_m}{dy} \quad \text{(3-1b)}$$

Where, j'' = diffusion flux, kg/(m^{2}s); D_p is the VOC diffusivity in the material through the pore air; C_{pa} is the VOC concentration in the pore air, kg/m^3 (Note that at equilibrium in a sealed chamber, C_{pa}=C_a). It is further assumed that the equilibrium between the gas and adsorbed phase of a VOC in a control volume is achieved instantaneously, and is governed by:

$$C_m = K_{ma} C_{pa} \quad \text{(3-1c)}$$

Where, K_{ma} = partition coefficient between the adsorbed and gas phase. Insert Eq. (3-1c) in Eq. (3-1b), we have,

$$D_p = K_{ma} D_m \quad \text{(3-1d)}$$

Material-air Interface: The equilibrium condition at the material-air interface can be described by:

$$C_{m,i} = K_{ma} C_{a,l}, \text{ at the interface} \quad \text{(3-2)}$$

Where, $C_{m,i}$ and $C_{a,i}$ are the adsorbed and gas phase concentration at the interface, respectively, kg/m^3.

Air boundary layer: The mass transfer of VOCs from the interface to the ambient air is described by:

$$E(t) = h_m \left[C_{a,i}(t) - C(t) \right] \quad \text{(3-3)}$$

Where, E = emission factor, kg/(m^{2}s); t = time, s; h_m = convective mass transfer coefficient, m/s; C = concentration in the chamber air, kg/m^3. The VOC mass balance in the chamber is represented by:

$$V \frac{dC(t)}{dt} = AE(t) - QC(t) \quad \text{(3-4)}$$

Where, V = chamber volume, m^3; A = material's top surface area, m^2; Q = clean airflow rate in m^3/s.

Boundary Conditions: Boundary conditions for the forgoing governing equations are:

$$-D_m \frac{\partial C_m}{\partial y} = -D_a \frac{\partial C_a}{\partial y} = E(t) \text{ at the material-air interface } (y=l) \quad \text{(3-5a)}$$

$$-D_m \frac{\partial C_m}{\partial y} = 0 \text{ at the bottom of the material layer } (y=0) \quad \text{(3-5b)}$$

Initial Conditions: At t=0:

$$C_a(0) = C_{a0},\ C_m(0) = C_{m0} \quad \text{(3-6)}$$

Equations (3-1) through (3-6) can be solved numerically given the model parameters and initial and boundary conditions. The above model applies to emission sources and reversible sinks in which the adsorption is considered a reverse of the emission, and both are governed by the same transport and storage processes. This model distinctly describes the sorption equilibrium between air and surfaces, in-material diffusion, and the convective mass transfer across the boundary layer. Each model parameter has distinct physical meaning. Alternatively, indoor sinks had also been frequently described by the 1st order surface adsorption and desorption rates model in which the net flux onto the surface is assumed to be equal to the adsorption flux minus the desorption flux, and the adsorption flux is equal to the gas phase concentration times an adsorption rate constant, and the desorption flux is proportional to the surface concentration times a desorption rate constant. However, such a model is an empirical one that only applies to sinks that are dominated by the surface phenomenon, and is not appropriate for sinks where internal diffusion process is also important (Zhang et al. 2002a, 2002b, 2003). The adsorption and desorption rate constants are empirical coefficients that involve the effects of both sorption equilibrium and convective mass transfer processes.

3.2.2 Model parameters and methods of determination

The forgoing model has 7 parameters: $C_m(0)$, D_m, K_{ma}, h_m, A, V and Q. Of these, $C_m(0)$, D_m, K_{ma}, and A are source parameters, whereas h_m, V, and Q are environmental parameters. A, V and Q can be determined based on the exposed surface area of the material used, chamber volume and ventilation rate. The mass transfer coefficient h_m may be estimated by CFD simulations (Yang, 1999) or from established correlations between the mass transfer coefficient and air velocity over the surface (Sparks et al., 1996).

$C_m(0)$, D_m and K_{ma} are more difficult to determine. Different experimental methods have been developed including: 1) a static dual-chamber/cup (Bodalal et al., 1999); 2) a C-history method (Huang et al., 2013); 3) a regression method that makes use of the emission data from both static and dynamic small-scale chamber tests (Yang, 2005); 4) a dynamic dual-chamber test method (Xu et al., 2009); 5) a similarity theory-based approach in which the D_m is estimated based on the similarity between the VOC and water vapor transport in the porous media (Section 5) (Xu et al., 2009); 6) a cyclic emission testing approach in which the alternate static and dynamic chamber tests are performed to estimate the D_m, K_{ma} and the initial C_{mo} (Zhou et al., 2018); 7) a procedure involving grinding of the material followed by VOC extraction and composition analysis (Cox et al., 2002; Smith et al., 2009); and 8) screening approach based on the VOC concentration data from the standard small chamber testing of emissions (Ye et al., 2004).

Most recently, a refined procedure has been developed to estimate the C_{m0}, D_m and K_{ma} based on the VOC concentration data from standard small-scale chamber tests (Section 5) (Liu et al., 2018). The model parameters obtained under the standard chamber test conditions (typically at 23°C, 50% RH, 0.41 m^2/m^3 of sample loading ratio and 1 ACH of supply airflow rate) are regarded as reference values. In the following section, we introduce a systematic approach to account for the effects of the media (material composition and structure), environment (T, RH), and species (VOC properties) on the model parameters. This would extend the application of the physics-based model beyond the emission test condition and period.

3.2.3 Effects of the media, environment and species (MES) on the model parameters

The media: Material's composition and structure directly affect the initial VOC concentrations in the material and its storage and transport properties. Building materials can be classified into dry, wet coating and wet installation materials (Zhang et al., 1999). In this section we limit the discussion to dry building materials and dried coating materials as they represent the majority of materials used in buildings. More complex physics-based models are needed to describe the in-material transport processes in wet coating and wet installation materials because the in-material diffusion coefficient changes during the drying period (Zhang et al., 1999; Yang et al., 2001). Since emission rates vary significantly among different building materials, the initial VOC concentration of a material is best estimated from the standard emission test data using the recently refined procedure (Liu et al., 2018).

Material's composition and structure also affect the diffusion and partition coefficients. The porosity and tortuosity affect the pore diffusion coefficient, D_p. The pore size distribution (and hence the internal surface area) affects the partition coefficient, K_{ma}. Assuming that initial VOC content is uniformly distributed inside the material and moisture transfer is primarily by vapor transfer, the transport mechanism for VOCs is similar to that of water vapor. A similarity coefficient has been introduced to represent the ratio between the VOC diffusion resistance factor and the water vapor diffusion resistance factor (Xu et al., 2009). However, it is not clear if a similarity can be readily established between the VOC and water vapor adsorption since the

concentration level of VOCs are several orders of magnitude lower than the water vapor concentration. The polarity of the compounds also plays a role in the similarity behavior, which needs to be further investigated.

At present, we recommend the use of the C_{m0}, D_m and K_{ma} estimated from the standard small-scale chamber tests as the reference values, C_{m0_ref}, D_{m_ref} and K_{ma_ref}, and then extend the dataset to other VOCs based on the VOC properties, and to other temperature and RH conditions as discussed below.

Species: The molecular weight and vapor pressure were found to correlate well with the diffusion and partition coefficient, respectively when applied to the compounds with similar polarity (non-polar, semi-polar and polar, respectively) (Bodalal et al., 1999):

$$D_m = a_1 M_w^{-a_2} \tag{3-7}$$

$$K_{ma} = b_1 P_{v,sat}^{-b_2} \tag{3-8}$$

Where a_1, a_2, b_1 and b_2 are empirical constants; M_w is the molecular weight; and $P_{v,sat}$ the vapor pressure at saturation under the test temperature. Given any new set of reference D_{m_ref} and K_{am_ref} determined from the standard chamber emission tests, these coefficients can be determined for each group of VOCs separately according to their polarity. For porous materials, since $D_p = K_{ma} D_m$, we have,

$$D_p = K_{ma} D_m = K_{ma} a_1 M_w^{-a_2} = b_1 P_v^{-b_2} a_1 M_w^{-a_2} \tag{3-9}$$

Li (2007) applied Equation (3-9) to Bodalal (1999)'s data, and found that D_p had very weak dependence on the molecular weight for each material and the VOCs tested. This suggests that the diffusion occurred primarily through the pore air, an assumption typically accepted in modelling the water vapor transfer in porous media when there is no significant capillary condensation.

Environment: An increase in air temperature would increase the vapor pressure of the VOC (Li, 2007):

$$\ln P_v = A \ln(T) + \frac{B}{T} + C + DT^2 \tag{3-10}$$

Where A, B, C, and D are constants (collected data from literature are provided in the Appendix Table 1), T = absolute temperature, K; $P_{v,sat}$ = VOC saturation vapor pressure at T, kPa. Knowing the vapor pressure at T and reference temperature, the partition coefficient at T can then be determined from:

$$\frac{K_{ma,T}}{K_{ma,ref}} = \left(\frac{P_{v\_T}}{P_{v\_ref}}\right)^{-b_2} \tag{3-11}$$

A higher temperature also leads to more active VOC molecules with a higher kinetic energy and hence a higher diffusion coefficient. Assuming that the pore diffusion is the dominant mechanism for VOC transport in the material and the range of temperature change considered here does not alter the porosity and tortuosity of the media, the pore diffusion coefficient is then proportional to the VOC diffusivity in air, which is proportional to $T^{1.75}/P$ (where P is the total pressure in atm) (Lyman, 1990). The ratio between the pore diffusion coefficients at T and T_{ref} can then be expressed by:

$$\frac{D_{p\_T}}{D_{p\_ref}} = \left(\frac{T}{T_{ref}}\right)^n \left(\frac{P_{ref}}{P}\right) \tag{3-12}$$

Where, T and T_{ref} are temperature and reference temperature, K; P and P_{ref} are the total pressure at T and the reference total pressure, respectively, kPa; D_{p_T} and D_{p_ref} are pore diffusion coefficients at T and T_{ref}, m^2/s; and n is a constant ($n=1.75$). Therefore,

$$\frac{D_{m\_T}}{D_{m\_ref}}\frac{K_{ma\_T}D_{p\_T}}{K_{ma\_ref}D_{p\_ref}} = \left(\frac{P_{v\_T}}{P_{v\_ref}}\right)^{-b_2}\left(\frac{T}{T_{ref}}\right)^{n}\left(\frac{P_{ref}}{P}\right) \quad (3\text{-}13)$$

Equation (3-13) can be used to estimate the diffusion coefficient at a given temperature based on the diffusion coefficient determined under the reference condition (i.e., the chamber test condition). Relative humidity (RH)'s effect on the VOC emission and sorption strongly depends on the moisture content of the material and the polarity of the VOCs. Definitive relationship between the D_p, K_{ma} and RH are yet to be determined, though some studies on the RH effects have been carried out.

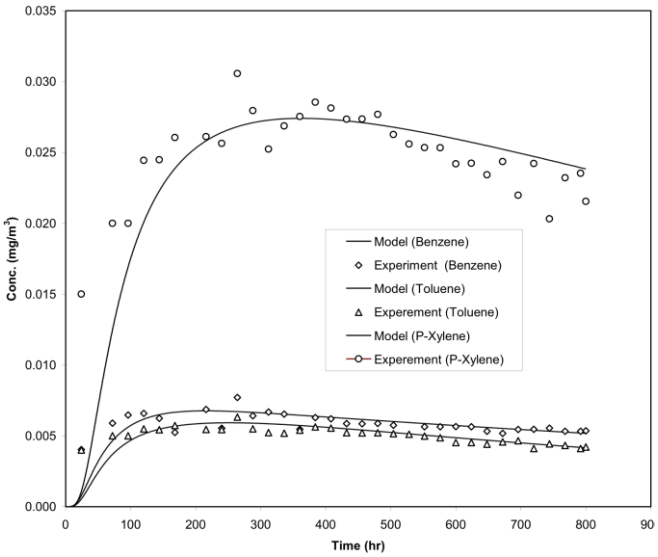

Figure 3-3 Emissions from a floor tile assembly

3.3 Application

3.3.1 Emissions from a sub-floor assembly

The model-based testing and evaluation (MBTE) method was first applied to evaluate the contribution of a rubber floor tile to the indoor concentration (Zhang et al., 1999). The diffusion and partition coefficients for each material were first determined by using the static-dual chamber test method, and the initial VOC concentrations in the rubber material were determined from the headspace analysis. They were then used in a multi-layer 1-D diffusion model to predict the concentration in a full-scale (Figure 3-3).

3.3.2 Pollution load from a residential wall assembly and effect of air infiltration

The method was applied to a typical wood-framed wall assembly to evaluate its impact on the pollution load to the indoor space due to the VOC emitted from the OSB under three different outdoor to indoor pressure differences: 0, 2 and 4 Pa (Li, 2007). Figure 3-4 shows that the air infiltration significantly increased the

emission factor during the first 20 days but had relatively smaller effect afterwards. The results also show that the air gap (leakage pass) played an important role in VOC transport. Even under no airflow condition (0 Pa pressure difference), the air gap is still the primary pass for the transport of VOCs emitted from the OSB because the VOC diffusivity in air is much larger than in the materials.

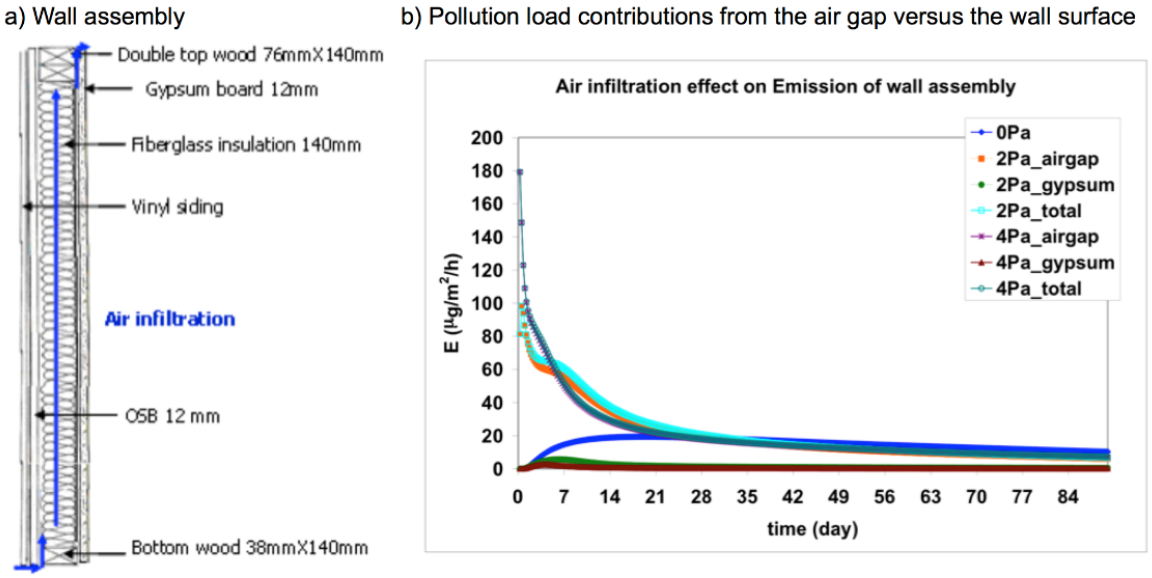

Figure 3-4 Pollution loads due to the emissions from the OSB in a residential wall assembly

3.3.3 Effects of Sorption on IAQ

A material in contact with indoor air will act as a sink if the gas-phase VOC concentration in the air is higher than the corresponding concentration on the material surfaces. Emissions from time-limited events such as paint jobs, cleaning or smoking can result in elevated gas phase concentration in indoor air and cause adsorption on indoor surfaces. The adsorbed pollutants would re-emit when the gas phase concentrations are later reduced (e.g., due to continuous ventilation). Such re-emission is also referred to as secondary emission, can cause poor air quality in a building for an extended period. Building materials especially those containing sorptive materials can also affect the transport and removal of indoor VOCs by sorption (adsorption and desorption) in the interior surface.

The sorption rate depends on the material properties, the VOC type, and environmental conditions, including temperature, relative humidity, air velocity, and VOC concentration in the air. Zhang et al. (2002a, 2002b and 2003) compared different sorption models and performed experiments to investigate the effects of temperature, RH and velocity on the sorption. Existing sorption models that are derived from experimental data obtained under the test condition have been evaluated. An integration method was used to calculate the total mass amount of VOC adsorbed by unit surface area during the test period, which can be considered as an index to characterize the sink strength. The linear Langmuir model was used to model the sorption process as a surface phenomenon, involving VOCs from the bulk air adsorbed on the surface and VOCs from the surface desorbed to the bulk air. It describes the sorption process by the adsorption coefficient k_a and equilibrium coefficient k_e. The diffusion model was used to model the sorption as a diffusion-controlled process, involving the VOCs partitioning at the material-air interface and the diffusion of VOCs into the

interior of the material. It was also found that increasing temperature decreased the partition coefficient, while it increased the diffusion coefficient, and hence decreased the sink capacity of the building materials.

In this study, the diffusion model was applied to simulate and illustrate the effects of short-time painting work on the indoor concentrations after the painting due to sorption on the carpet. We simulated for the small-chamber test condition with fresh painted gypsum wall boards on all walls and the whole floor covered with a carpet (chamber volume: 0.05 m^3, loading ratio (ratio between exposure area of material and volume of test chamber) for the painted surface and carpet are 10.5 and 4, respectively, air change rate: 1 ACH). Figure 3-5 shows the reduction of the gas-phase concentration by the sorption of the carpet at the early stage, and higher gas-phase concentration at the slow-decay period due to the desorption/re-emission.

Table 2: Diffusion model parameters of dodecane

Compound	Material	D_m (m^2/s)	K_{ma}	C_{m0} (mg/m^3)
Dodecane	Painted wall	6.58E-10	753	1.09E+03
	Carpet	1.18E-11	15300	-

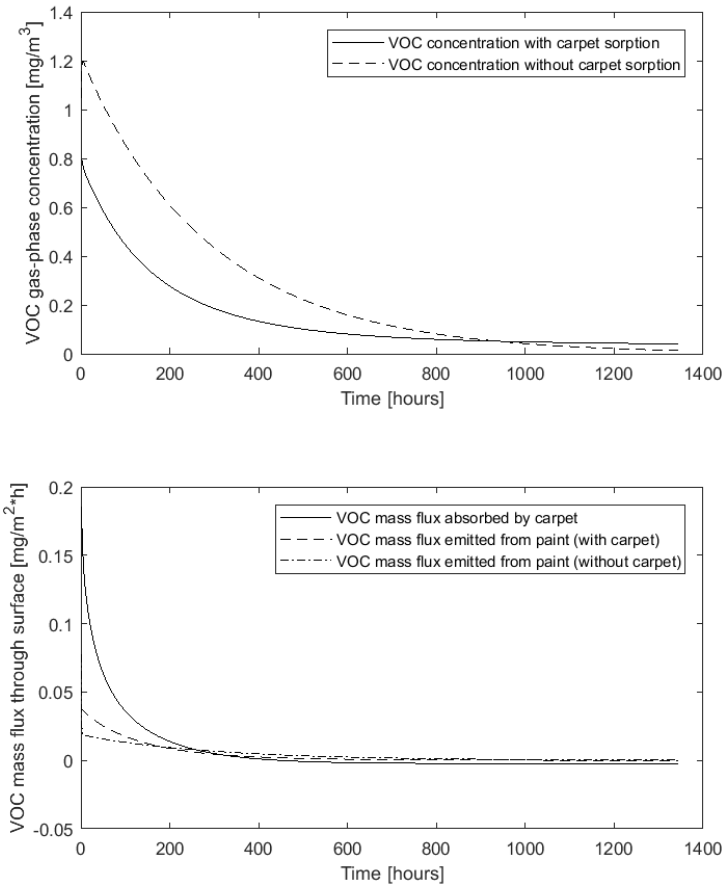

Figure 3-5 Effect of sorption on the concentrations and net flux of dodecane emitted from the painted dry wall

3.3.4 Effects of solar radiation on the emissions from the floor material of a reference house

A reference house has been developed for the evaluation of IAQ and energy performance of low-energy residential buildings in Section 2. With the framework established above for model-based testing and evaluation, one can predict how the different materials in the enclosure will affect the VOC transport into the indoor space more realistically, the resulting contribution to the indoor pollution loads, and how the daily and seasonal variations of outdoor air temperature and solar radiation would affect the pollution loads and IAQ. We limit the discussion to conditions that all materials do not have significant capillary condensation so that the model parameters derived from the standard emission test condition (23 °C and 50%RH) as well as the model described above is applicable.

For the purpose of illustration, we also limit the discussion here to a case where only the emissions from the floor materials are considered (Figure 3-6). The reference house is modeled as a single zone being subjected to the mechanical ventilation, infiltration, convective heat fluxes on the interior surfaces of the walls, roof, internal heat gains and the air conditioning by the HVAC system as simulated in the reference house under the Syracuse weather condition. VOCs emitted from the floor in a summer day was investigated to illustrate how the surface temperature variation due to the variation of the transmitted solar radiation affects the VOC emission from the floor, which is assumed to consist of plywood and a particleboard.

Table 3-1 and Table 3-2 show the model parameters and floor material properties and dimensions.

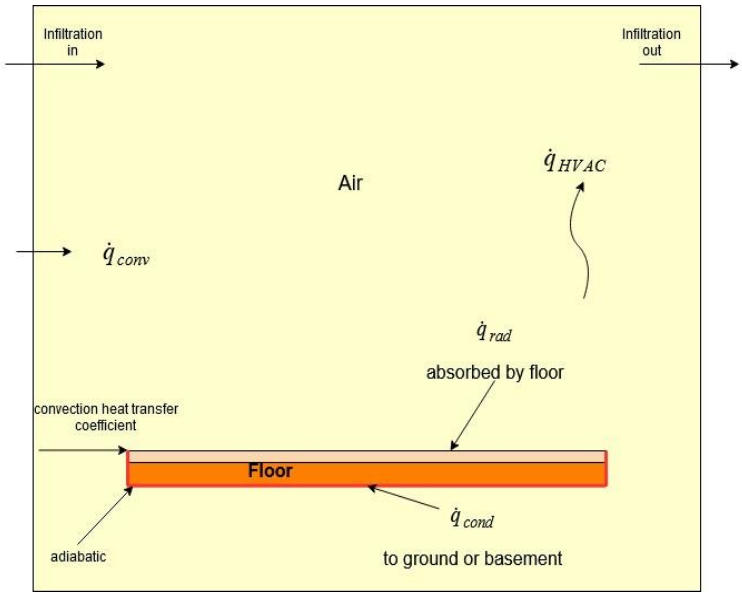

Figure 3-6 Schematic of the case of VOC emissions from the floor materials of a reference house

Table 3-1: Diffusion model parameters of VOC compounds in reference house IAQ simulation

(Garcıa et al., 2011, Cox et al., 2001)

Compound	Material	D_m (m^2/s)	K_{ma}	C_{m0} (mg/m^3)
Hexanal	plywood	3.58E-11	1528	-
	particleboard	7.65E-11	3289	1.15E+04

Table 3-2: Properties of floor materials

Materials	Thickness mm	Density kg/m^3	Heat conductivity w/m*K	Heat capacity J/kg*K
plywood	9	427	0.11	1600
particleboard	16	700	0.15	1421

We first used EnergyPlus to obtain the transmitted solar radiation on the floor and all the heat flow rates shown in Figure 3-6, which were then used as boundary conditions or source/sink conditions in Delphin 6.0 to simulate the VOC emissions from the floor assembly.

Figure 3-7 shows the heat flow rates from external walls and roof, the heat flow rate extracted by the HVAC system and the zone air temperature. Note that the heat flow rates decreased at 9:00 am as occupants enter the zone, leading to the increase of the zone air temperature when the heat flow rate to HVAC system was maintained the same from 9:00 am to 7:00 pm. The pattern of the solar radiation absorbed by the floor reflected the variation in the cloudiness of the day simulated. The HVAC was turned off during unoccupied period of the day, which is reflected by the zero heat flow extracted by HVAC. During the occupied period, the ideal HVAC system extracted the sufficient amount of heat to maintain the zone air temperature at the setpoint.

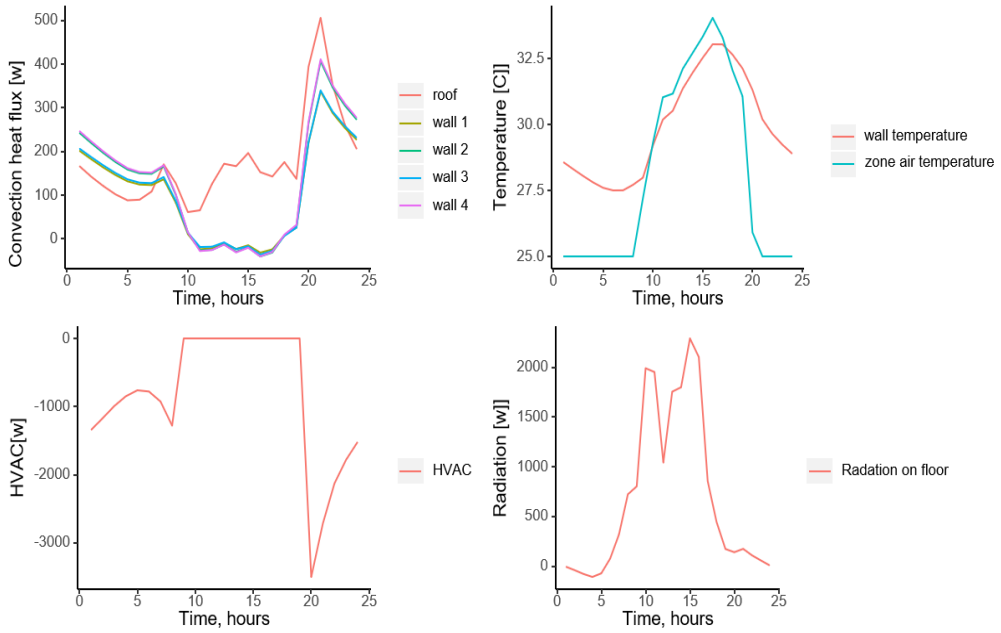

Figure 3-7 Boundary conditions extracted from EnergyPlus

Figure 3-8 shows that the average zone air temperature obtained by Delphin 6.0 agreed well with that from the EnergyPlus, confirming that the thermal conditions in the reference house modeled was properly reproduced.

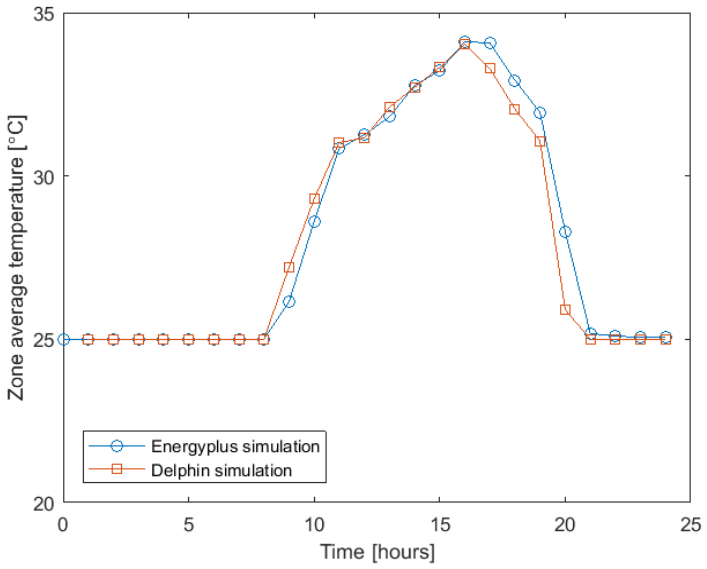

Figure 3-8 Average zone air temperatures from Delphin6.0 and Energyplus

As shown in Figure 3-9, the emission rate of hexanal increased with the increase of the floor surface temperature. There was a rapid reduction in emission factor at 12 pm due to reduction in the floor surface temperature corresponding to the increase in sky cloudiness from 11 am to 12 pm in the weather data.

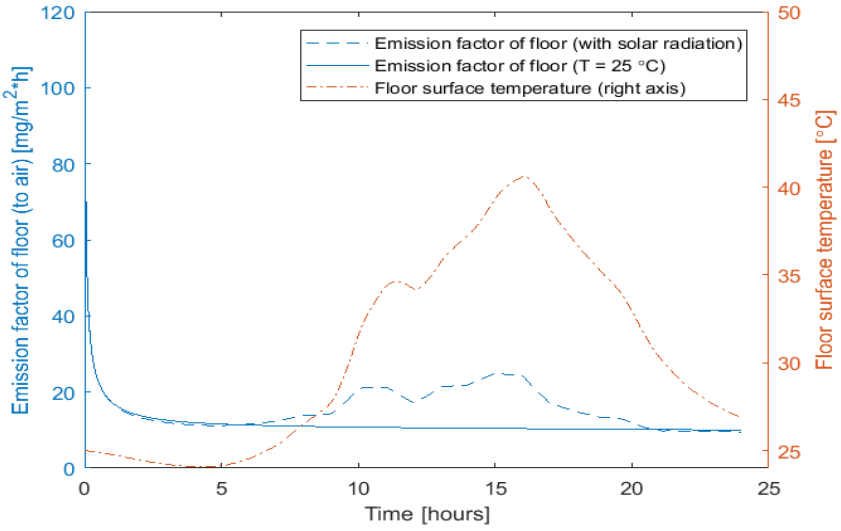

Figure 3-9 Emission factor of hexanal from floor surface to zone air and floor temperature. Reference emission factor is the emission with floor surface temperature = 25 °C

3.4 Summary

A model-based testing and evaluation method has been introduced and an implementation procedure established for the prediction of the impact of material emissions and sorption on indoor pollution loads, indoor VOC concentrations and IAQ. Several application examples are briefly discussed including emissions from a sub-floor assembly and a typical residential wall assembly, effects of sorption on re-emission and effects of the floor surface temperature on the emission rates from the floor in a residential reference house.

4 Effects of temperature and relative humidity on emissions

(Weihui Liang, Menghao Qin, and Xudong Yang)

In actual buildings, indoor temperature and humidity are generally not constant, and vary with outdoor environmental conditions as well as occupant behavior. Consequently, VOCs are emitted under variable temperature and humidity conditions. Understanding the VOC emission characteristics of building materials in different temperature and humidity conditions is needed to model indoor exposures and mitigate health risks. This could either be done by the field studies or environmental chamber studies. In this study, we focused our effort on formaldehyde because it has very low allowable indoor concentration and many building and furnishing materials in residential houses emit it.

4.1 Literature review

4.1.1 Field studies

Wolkoff et al. (1991) measured formaldehyde concentrations in two semi-detached twin apartments for one year. They found that formaldehyde concentrations were higher in summer in the vacant apartment, while decreased and then increased during autumn in the occupied one. Pollutant transport occurred between these two apartments, which complicated the situation. Brown (2001) measured formaldehyde concentrations 4 times over 8 months in an occupied dwelling. Formaldehyde concentrations were found to decay double exponentially. However, the above studies could not directly characterize emissions from materials because human activities may also have contributed to the observed formaldehyde concentrations and multiple emission sources may have been present in the studied spaces. Crump et al. (1997) measured formaldehyde in four unoccupied test houses for 24 months to investigate the relationship between sources and indoor concentrations. As multiple materials were present in the house, it was difficult to distinguish emission from each individual source. Thus, long-term measurements conducted in actual houses without interference by human behavior and multiple sources are needed to understand realistic materials emission characteristics. Existing field studies also have not continuously measured environmental conditions. The frequency of concentration measurements and the lengths of the studies may also have been insufficient considering the long-term effects of formaldehyde emissions on indoor air quality.

4.1.2 Environmental chamber studies

Research about the effect of temperature and humidity was mainly conducted experimentally in the environmental chamber, in which the materials were measured with constant temperature and humidity case-by-case. Myers and Nagaoka (1981) measured a urea-formaldehyde (UF)-bonded particleboard from relative humidity (RH) 30% to 75%. They found formaldehyde emissions increased 2-fold and 6-fold at 25 °C and 40 °C when RH increased from 30% to 75%, respectively. Myers (1985) reviewed some available data and proposed a linear relation between steady state formaldehyde emission rate and RH. Frihart et al. (2012) measured formaldehyde emissions from a UF-bonded particleboard and concluded that the emission rate increased 6-9 times when RH increased from 30% to 100%. Parthasarathy et al. (2011) measured the steady state formaldehyde concentrations in a small environmental chamber and found that the increase of RH from

50% to 85% yielded a 1.8-3.5 times increase in formaldehyde emission rate. Generally speaking, existing studies about the humidity effect on formaldehyde emissions were mainly focused on the analysis of steady state concentration or emission rate. Results obtained may not be applicable to actual buildings in which the environmental conditions are variable and the steady state precondition would be barely held (Liang et al. 2015). Limited studies had reported the humidity effect on emission parameters. Farajollahi et al. (2009) measured the diffusion coefficient (D_m) of octane, isopropanol, cyclohexane, ethyl acetate and hexane of a ceiling tile and concluded that the effect of humidity on D_m was negligible. Xu and Zhang (2011) measured the D_m and partition coefficient (K) of formaldehyde and toluene of a porous building material and claimed that RH had no significant effect on D_m. Higher K was found when RH increased from 50% to 80% while no significant difference was observed between RH of 25% and 50%. Very limited studies have been done on the correlation between initial emittable coefficient (C_0) and humidity. Although researchers have been making efforts to explore the mechanism to explain the humidity effect on formaldehyde emission, theoretical correlations between the emission parameters and humidity have not been derived yet. Additionally, it should be mentioned that experimental studies regarding the humidity effect were mainly focused on the analysis of RH. Absolute humidity (AH), which represents the absolute quantity of free water content in the air, was seldom analyzed. Measurement results and correlation analysis of a recent field study in a full-scale experimental room suggested that AH was more likely the parameter affecting formaldehyde emission than RH (Liang et al. 2015). Moreover, the representative parameter of humidity effect was significant on the environmental parameter settings in the temperature effect and the combined effects experimental studies. The differences between the individual effect of temperature and the combined effects of temperature and representative parameter of humidity (AH vs. RH) are still unknown.

Traditional experimental studies about the temperature effect on formaldehyde emissions were conducted with identical RH. Andersen et al. (1975) noted that equilibrium concentration of formaldehyde in the chamber was directly proportional to temperature. Wiglusz et al. (2002) measured formaldehyde emissions from a laminate flooring and found that emission increased 18-fold when temperature increased from 29 °C to 50 °C. Xiong et al. (2010) found that C_0 increased by 507% when temperature increased from 25.2 °C to 50.6 °C. These experimental studies have verified the positive effect of temperature on formaldehyde emissions. However, emissions other than the test temperature could not be estimated by this approach. Thus, correlation equations would have more practical values. Myers (1985) reviewed the available data together with his measurement results and reported that temperature changes could be described by an exponential relation with steady state emission rate. Zhang et al. (2007) derived a theoretical correlation between K and temperature. Deng et al. (2009) proposed a theoretical correlation between D_m and temperature. Theoretical correlation between steady state emission rate and temperature has been derived by Xiong et al. (2013). Huang et al. (2015) established a correlation between C_0 and temperature. These correlations were validated by the measurement results in the chamber with identical RH. However, no experimental studies and validations with identical AH have been done yet.

Despite the many studies that exist regarding the individual effects of temperature and humidity on formaldehyde emissions, there is still a knowledge gap between the conclusions and their applications in actual buildings. In actual buildings, indoor temperature and humidity are generally not constant (Korjenic et al. 2010; Soutullo et al. 2014), and would vary with outdoor environmental conditions as well as occupant behaviors (Fabi *et al.*, 2013; Saeki *et al.*, 2014). The combined effects rather than the individual effects of

temperature and humidity need to be considered when materials emitted under the variable environmental conditions. However, the aforementioned correlations and conclusions of the individual effect of temperature or humidity can only be applied to the conditions with identical RH or temperature, which is quite different from that in actual buildings. Consequently, correlations between emission parameters and the combined effects of temperature and humidity are well needed. Sensitivity analysis suggested that C_0 is the most important parameter determining the emission behaviors of building materials among the three emission parameters (Yang *et al.*, 2001). And there were studies emphasizing the importance to distinguish the total concentration ($C_{0,total}$) from the initial emittable concentration (C_0) for formaldehyde when labeling the building material emissions (Xiong et al. 2013; Huangd et al. 2015). The correlation between C_0 and the combined effects of temperature and humidity will be helpful in the simulation of formaldehyde emissions in actual buildings as well as the development of the low emission building materials.

4.2 Field study

The main objectives of this field study are to investigate the long-term formaldehyde emission characteristics of building materials under variable temperature and humidity conditions, to explore the extent to which formaldehyde emissions vary by season. We measured formaldehyde emissions from a medium-density fiberboard (MDF) for more than 29 months using a full-scale experimental room. Indoor formaldehyde concentrations and air ventilation rates were measured frequently throughout the study. Temperature and humidity were monitored continuously over the entire time period.

4.2.1 Study design

4.2.1.1 The full-scale experimental room

Dimension of the full-scale experimental room was 4 m × 3 m × 3 m (length × width × height). It was located in the corner of an experimental base in a rural district of Beijing. The total area of the experimental base was 5000 m^2 and a 2.5 m high enclosure was built around it. There was only one door in the south wall of the room, which remained closed during the entire measurement period. Figure 4-1 gives the digital images and schematic illustration of the experimental room and its wall assembly.

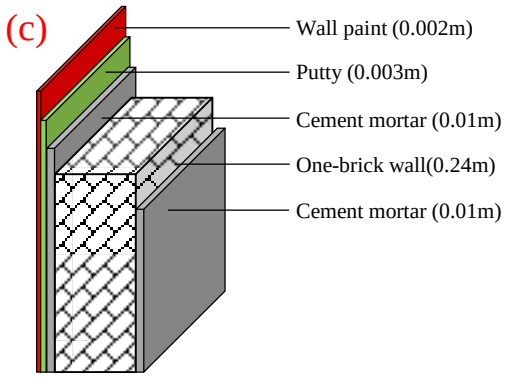

Figure 4-1 : Digital images of the interior and exterior of the full-scale experimental room and the schematic illustration of the wall assembly. (a) Interior image of the MDF**; (b) Exterior image** of the experimental room**; (c) Wall assembly**

The room layout and interior surface materials shared similar features as a typical room in China. But the room possessed several key features to better serve the goal of this particular study, as described below.

(1) The room was unoccupied. Thus, all human-related interferences to emissions could be eliminated. Another advantage was that measurements could be conducted at any time without disturbing occupants or requiring permission.

(2) The construction of the room was completed two years before the experiment began and only latex wall paint and ceramic floor tiles were used as interior construction materials. There were no formaldehyde emissions from the ceramic floor tiles, and emissions from the latex wall paint were negligible by the time the experiment began. Thus, the only formaldehyde emission source in this room was the MDF introduced. Formaldehyde is a small molecule compound whose adsorption capacity is not as strong as other VOCs and aldehydes (Petitjean *et al.*, 2010). Previous experimental studies indicated that sorption of formaldehyde by wall paint was insignificant (Salthammer and Fuhrmann, 2007).

(3) Temperature and humidity were allowed to vary naturally in the room, without the use of heating or air conditioning equipment. In this way, temperature and humidity ranges were much larger than that commonly observed in actual homes. This would allow better investigation of the possible impact of temperature and humidity on material emissions.

(4) A fan was operated to ensure good mixing of air in the room, with the same design purpose as the fan in an environmental chamber (ASTM, 2008).

4.2.1.2 Studied material

The studied material was a typical MDF directly purchased from the manufacturer. It was transported and placed inside the room immediately after being received. Hence, it could be considered as a new material at the beginning. The boards were leaned against the interior walls with an angle. Both the front and back surfaces of the boards emitted formaldehyde, which could be simplified to a one-dimensional material with half thickness and double emission area to the original board. Key features of the studied MDF are listed below.

(1) Dimension of the original full-size MDF is 2.44 m × 1.2 m × 0.012 m (length × width × thickness). Three full-size boards together with a small piece (dimension of 0.18 m × 1.2 m × 0.012 m) were placed in the room, resulting in a loading ratio of 0.5 m^2/m^3. This value was comparable to that of densely furnished spaces such as a small room or kitchen, but higher than most living or bedrooms in actual residential buildings (Yao 2011). A relatively large loading ratio was selected to allow higher room concentrations over a long period of time, so as to minimize the error caused by measurement uncertainty.

(2) The MDF was directly exposed to air, different from its typical use as chairs surrounded by foam or tables and countertops laminated by a plastic cover. This could simplify the emission process and better fit to the main purpose of this study. More complicated and realistic features could be added later after the fundamental emission characteristics of the material were understood.

(3) Headspace analysis of the MDF indicated that formaldehyde was the dominant emitted compound. Headspace concentrations of other aldehydes and ketones were one or two orders of magnitude lower than formaldehyde, and the sum of other aldehydes and ketones was less than 5% of formaldehyde mass. The total VOC concentration in the MDF headspace was as low as 15.7 $\mu g/m^3$. Thus, potential generation of formaldehyde from chemical oxidation of terpenes, alkenes, or hydrocarbons could be eliminated (Nazaroff and Weschler, 2004; Nørgaard *et al.*, 2014).

The above features of the experimental room and studied material will benefit the understanding of long-term formaldehyde emission characteristics as well as the quantification of temperature and humidity effects. On the other hand, formaldehyde concentrations in the experimental room were much higher than that in actual homes due to large loading ratio, elimination of the retard resistance from the cover surrounding the MDF, and extreme summertime environmental conditions. Concentration differences in different seasons could also be more pronounced due to larger indoor temperature and humidity ranges across seasons. The formaldehyde concentrations measured in this experimental room should not be considered as typical in actual homes.

4.2.1.3 Formaldehyde measurements

Entry into the experimental room could cause air exchange between outdoor and indoor air, affecting the indoor formaldehyde concentration. To eliminate human interference in the concentrations, a sampling portal was placed near the door frame so that samples could be collected from outside the room without opening the door and entering. The portal was located 1.2 m above the floor. Formaldehyde was measured using the 3-methyl-2-benzothiazolinone hydrazone (MBTH) spectrophotometric method, in accordance with the Chinese national standard (GB/T18204.26-2000). To collect formaldehyde samples, a stainless steel tube was extended into the center of the room through the sampling portal. Indoor air samples were pumped through the stainless steel tube into a glass sampling tube using a QC-2 pump (Beijing Institute of Labor Protection) at a flow rate of 100–200 mL/min. Formaldehyde in the air was absorbed into a solution in the glass tube containing 5.0 mL of 50 μg/mL MBTH. The sampling time was 5–30 min, depending on the estimated formaldehyde concentration in the air, with less volume collected at higher concentrations. To analyze the formaldehyde concentrations, 0.4 mL of 10 g/L ferric ammonium sulfate solution was added to the sampling tube. The tube was shaken and then held for 15 min, during which formaldehyde was converted into a blue cationic dye by the MBTH. The light absorbance was measured using a spectrophotometer at 630 nm (Unic 7200, China).

Frequent sampling (ranging from a few days to a few weeks) was conducted to evaluate variations and trends over time. Three duplicate samples were taken for each measurement. The measurement period was 9 October 2012 to the end of February 2015. The indoor background formaldehyde concentration was also measured before introducing MDF. Outdoor formaldehyde concentrations were also occasionally measured.

4.2.1.4 Environmental measurements

Indoor temperature and RH were measured by an automatic data logger (WSZY-1 sensor, Beijing, China) placed in the center of the room. The instrument measurement ranges were -40–100 °C for temperature and 0–100% for RH with measurement errors of 0.5 °C for temperature and 3% for RH, respectively. The sampling interval was 10 min. The ventilation rate was measured monthly in 2013 using the CO_2 decay method to analyze annual variations (Van Hoof and Blocken 2013).

4.2.2 Results and Discussion

4.2.2.1 Formaldehyde concentration

The measured indoor formaldehyde concentrations are illustrated in Figure 4-2. Relative standard deviations (RSD) were within 10% for most measurements, indicating good repeatability of the results. The mean value for each test was used for data analysis. The year was divided into spring (March–May), summer (June–August), autumn (September–November), and winter (December–February) seasons. Indoor formaldehyde concentration ranges and means for each season are listed in Table 4-1. Indoor formaldehyde concentrations did not decrease continuously, instead having different trends in different seasons. A monotonic increase in the concentration occurred in spring, reaching a maximum value of 4.78 mg/m^3 in summer 2013 and 3.19 mg/m^3 in summer 2014. Concentrations then decreased throughout mid-late summer and autumn and reached a minimum in winter. Both the levels and ranges differed in different seasons, with summer > spring > autumn > winter. The maximum concentration was 30–50 times the minimum, exhibiting significant differences in the same year. The mean concentration in summer was 20 times that in winter. Therefore, indoor formaldehyde concentrations and trends were strongly seasonal.

Both the formaldehyde concentrations and ranges decreased from one year to the next. The mean concentration was 3.59 mg/m^3 in the summer of 2013 and decreased to 2.52 mg/m^3 in the summer of 2014. Similar concentration decreases were measured in other seasons from 2013 to 2014. Generally speaking, the formaldehyde concentration decreased 20–65% in corresponding months of the second year. Concentration ranges also narrowed, e.g. from 1.32–4.78 mg/m^3 in the summer of 2013 to 2.17–3.19 mg/m^3 in the summer of 2014. The above results indicate that formaldehyde emissions decreased annually within the seasonal trends noted above.

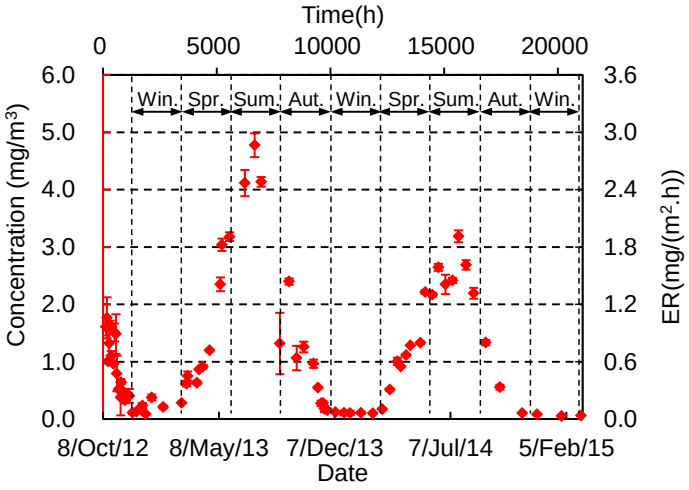

Figure 4-2: Indoor formaldehyde concentration and emissions rate profiles in the experimental room. Aut., Win., Spri., and Sum. are abbreviations for autumn, winter, spring, and summer, respectively. Error bars are the standard deviations of the formaldehyde concentration results

Table 4-1. Indoor formaldehyde concentrations, formaldehyde emissions rates, temperature, relative humidity (RH), and absolute humidity (AH) in different seasons

Time period	Season	Concentration (mg/m^3)			Emission rate ($mg/m^2 \cdot h$)			Temperature (°C)			RH (%)			AH (g/kg_{air})		
		Mean	Min.	Max.	Mean	Min.	Max.	Mean	Min.	Max.	Mean	Min.	Max.	Mean	Min.	Max.
9/10/2012-30/11/2012	Autumn*	1.00	0.33	1.77	0.57	0.18	1.02	8.7	-0.3	19.3	63.5	55.3	71.2	4.6	2.3	8.2
1/12/2012-28/2/2013	Winter	0.19	0.09	0.38	0.10	0.04	0.23	-4.18	-10.9	4.3	66.3	58.7	73.6	1.9	1.1	3.4
1/3/2013-31/5/2013	Spring	1.38	0.28	3.18	0.80	0.16	1.84	14.7	2.5	26.9	60.1	49.1	69.1	6.7	2.9	13.5
1/6/2013-31/8/2013	Summer	3.59	1.32	4.78	2.07	0.76	2.76	27.0	19.1	31	75.2	55.1	83.6	17.2	10.2	23.1
1/9/2013-30/11/2013	Autumn	0.79	0.15	2.4	0.45	0.08	1.38	14.2	0	24.7	67.3	49.9	78.2	7.8	1.9	14.7
1/12/2013-28/2/2014	Winter	0.11	0.1	0.12	0.06	0.05	0.06	-1.3	-5.6	4.5	58.6	50.9	68.3	2.1	1.3	3.4
1/3/2014-31/5/2014	Spring	1.07	0.17	2.21	0.61	0.09	1.28	17.1	3.2	30	55.3	46.5	62.8	7.2	2.7	14.5
1/6/2014-31/8/2014	Summer	2.52	2.17	3.19	1.46	1.25	1.84	28.1	22.7	31.4	64.3	51.4	72.9	15.6	10.8	21.1
1/9/2014-30/11/2014	Autumn	0.66	0.1	1.33	0.38	0.05	0.77	14.0	2.6	26.1	66.7	55.8	76.1	7.4	2.8	15.1
1/12/2014-28/2/2015	Winter	0.07	0.05	0.08	0.03	0.02	0.04	-1.2	-4.0	4.8	54.8	49.4	59.9	1.9	1.5	2.8

* Measurement data for 2012 only partially covered the autumn season (9 October–30 December). These data were not used for comparison with data for autumn 2013 and 2014.

4.2.2.2 Formaldehyde emission characteristics

4.2.2.2.1 Emission rate calculation

In the time-scale of several hours or a day, indoor temperature and humidity varied in a small range. Indoor environmental conditions were relatively stable. Consequently, a short-term steady state emission rate could be assumed. The formaldehyde emission rate from MDF at a certain time *t* was estimated based on the following equation:

$$ER(t) = VR \times (C(t) - C_{amb}) / L \qquad (4\text{-}1)$$

where *ER*(*t*) is the emission rate (mg/m^2·h) at time *t*, *VR* is the ventilation rate of the experimental room (h^{-1}), *C*(*t*) is the measured indoor formaldehyde concentration (mg/m^3) at time *t*, C_{amb} is the outdoor formaldehyde concentration (mg/m^3), and *L* is the loading ratio of the source material (0.5 m^2/m^3).

The background formaldehyde concentration in the experimental room was 0.021 mg/m^3. The outdoor formaldehyde concentration varied only slightly within 0.012 ± 0.010 mg/m^3 during the entire study period. Thus, there was no significant difference between the outdoor and background formaldehyde concentration and the assumption that there were no other formaldehyde emission sources in the experimental room was confirmed. Additionally, no seasonal trends were observed in the outdoor formaldehyde concentration.

The monthly measured ventilation rates for 2013 are illustrated in Figure 4-3. It varied randomly between 0.21–0.35 h^{-1}. The relatively stable ventilation rate was ideal for direct comparison purposes. The main reason for the small variation was that no heating or cooling equipment was operated in the experimental room; thus, indoor-outdoor temperature differences were small during all of the seasons. Moreover, the effect of outdoor wind pressure on the ventilation rate was minimized by an enclosure around the room. No seasonal variations in ventilation rate would be expected. The mean and standard deviation (SD) of the ventilation rate throughout the year were 0.29 h^{-1} and 0.046 h^{-1}, respectively. Ventilation conditions over the entire test period were assumed to follow the pattern observed in 2013.

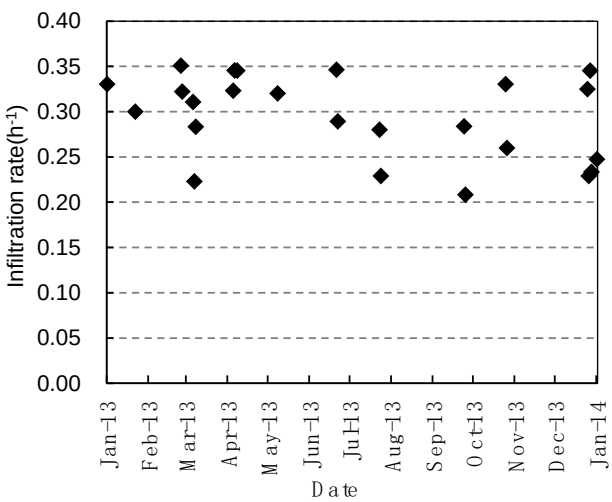

Figure 4-3: Ventilation rate results for the experimental room in 2013

The loading ratio (*L*) was constant and outdoor formaldehyde concentrations (C_{amb}) were much lower than indoor formaldehyde concentrations (*C*(*t*)). Uncertainty or the RSD of the emission rate for each measurement may be larger than that for the concentration considering the variations in the ventilation rate (*VR*). However, the overall trends in emission rates would not be affected by this factor. Thus, the mean emission rate for each measurement would vary in a similar manner as did the indoor formaldehyde concentration, as illustrated in the right-hand y-axis of Figure 4-2. Means and ranges for emission rates in the different seasons are listed in Table 4-1

4.2.2.2.2 Comparison of emission characteristics between environmental chambers and the experimental room

The emission rate from MDF decreased from the beginning of the measurement until 1 December 2012, consistent with that observed in an environmental chamber with constant environmental conditions. One might draw the conclusion that MDF emission in actual buildings would be similar to those in the chambers based on such data. However, this trend did not continue over time and an entirely different emission pattern occurred in the experimental room compared to that in the environmental chamber, as discussed below.

(1) Material emission rates in an environmental chamber should decrease continuously (Little and Hodgson 2002). However, in the experimental room, an apparent increase in the emission rates occurred in spring and summer. Annual cyclical seasonal variations were observed.

(2) In an environmental chamber, the highest emission rates usually occur at the beginning when materials are introduced. However, in the experimental room, maximum emissions occurred in summer instead of at the beginning of the study. For example, the highest emission rates in the summer of 2013 and 2014 were 2.76 and 1.84 mg/m^2·h respectively, much higher than the 0.93 mg/m^2·h initial emission rate. These results suggest that environmental conditions should be considered in estimating formaldehyde emission rates from MDF.

(3) When materials are tested in an environmental chamber, a “steady state” could be achieved with prolonged emission time (Qian *et al.*, 2007). The emission rates change little after that (Xiong et al. 2013). However, when the MDF was placed in the experimental room, no such “steady state” could be assumed for the long time scale.

Due to apparent differences in emission characteristics observed between environmental chambers and the experimental room, emission models developed based on constant environmental conditions should not be directly applied to actual buildings. Adjustments to the model or model parameters are required to represent the more complex situation in actual buildings.

4.2.2.3 Influencing factors

The main differences between the experimental room and environmental chambers were the temperature and humidity conditions. The impacts of these two factors are examined below.

4.2.2.3.1 Influence of temperature

The overall trends in formaldehyde concentration and temperature were consistent (**Figure 4-4**). Obvious seasonal variations were also observed in indoor temperature. Indoor formaldehyde concentrations increased in spring and decreased in autumn as did the temperature. The same patterns in concentration and temperature were observed in summer and winter. Based on this qualitative analysis, temperature was likely one of the key factors inducing seasonal variations in formaldehyde concentrations. The Pearson correlation coefficient between the formaldehyde concentration and temperature was 0.84, indicating a strong positive correlation between these two parameters.

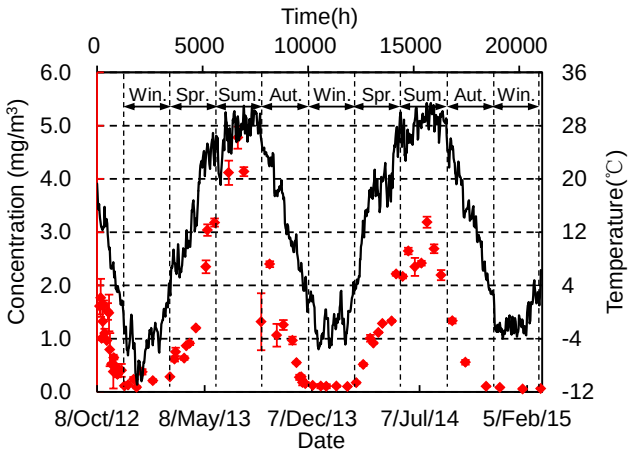

Figure 4-4: Indoor formaldehyde concentration and temperature profiles for the experimental room

Temperature ranges for each season are listed in Table 4-1. The annual variations were -10.9–31 °C in 2013 and -5.6–31.4 °C in 2014, respectively. This broad range goes beyond all possible temperature situations in actual buildings, and inclusive. In particular, it is interesting to compare emissions at high- and low-temperature extremes. The magnitude of indoor temperature variations in summer were nearly the same as or smaller than those in winter (19.1–31 °C vs. -10.9–4.3 °C); however, the formaldehyde concentration ranges were much larger in summer than in winter (1.32–4.78 mg/m^3 vs. 0.09–0.38 mg/m^3). Thus, formaldehyde emissions were more sensitive to temperature changes at higher temperatures.

Temperatures and ranges over the next year did not change substantially from the first year (Table 4-1, **Figure 4-4**). However, formaldehyde concentrations and ranges decreased significantly (0.09–4.78 mg/m^3 vs. 0.10–3.19 mg/m^3). The same correlations between temperature and concentration in each season were observed. These results demonstrate the reduced effect of temperature on formaldehyde emissions over the long term, which was not revealed in previous studies using environmental chambers (Xiong et al. 2013; Parthasarathy et al. 2011; Frihart et al. 2012).

4.2.2.3.2 Influence of humidity

Ranges for RH in each season are presented in Table 4-1Table 4-1 and indoor RH and formaldehyde concentration profiles are illustrated in Figure 4-5(a). Indoor RH mainly varied between 55–70%. RH began to increase at the end of May 2013 and reached a maximum of 83.6% in the middle of August 2013. This increase in RH was due to rainy weather during that period. Indoor RH decreased and returned to almost the same level as before after 15 October 2013. Unlike formaldehyde concentration and temperature, RH was relatively stable without strong seasonal variations. The Pearson correlation coefficient between the indoor formaldehyde concentration and RH was 0.33, indicating that seasonal variations in the formaldehyde concentration were not strongly associated with RH.

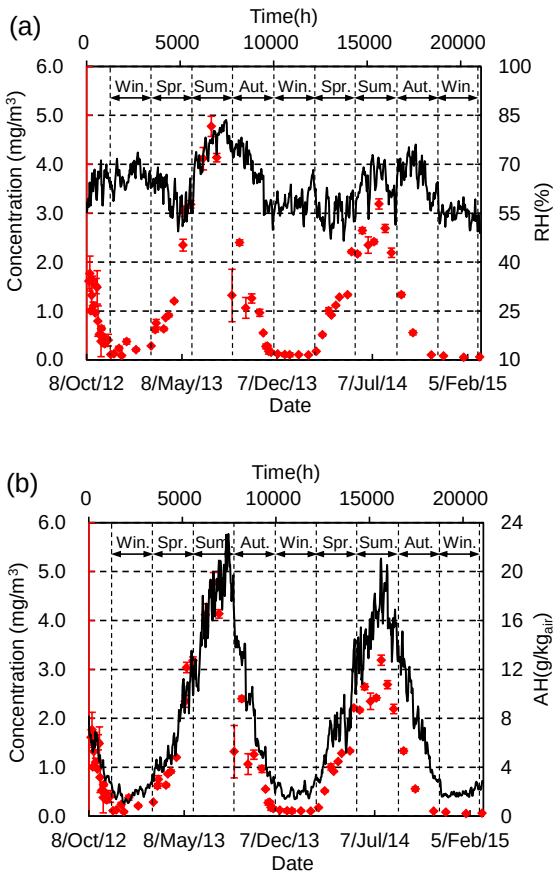

Figure 4-5: Indoor formaldehyde concentration and humidity profiles for the experimental room. (a) Formaldehyde concentration and relative humidity (RH); (b) Formaldehyde concentration and absolute humidity (AH)

The absolute humidity (AH) profile, on the other hand, exhibited clear seasonal variations (Figure 4-5 (b)). The maximum AH occurred in summer and the minimum in winter, with a range of 1.1–23.1 g/kg_{air}. The Pearson correlation coefficient between the formaldehyde concentration and AH was 0.89, indicating a strongly positive correlation between them.

Previous studies on the influence of humidity on formaldehyde emissions were mainly conducted in environmental chambers and focused on analysis of RH. The influence of humidity on formaldehyde emissions has also been neglected in field studies (Wolkoff et al. 1991; Brown 2001; Crump et al. 1997). However, Parthasarathy et al. (2011) found that the emission rate increased when RH increased from 50% to 85%. Similar conclusions were obtained in other studies (Frihart et al. 2012; Sidheswaran et al. 2013). Given the apparent discrepancies between the results of this and previous studies, it is important to consider the fundamental mechanism of formaldehyde emissions from MDF. A common explanation about the mechanism of humidity effect on formaldehyde emissions is that free formaldehyde would increase due to urea-formaldehyde depolymerization and hydrolysis in the presence of free water (Frihart et al. 2012; Sidheswaran et al. 2013; Myers 1985). Competition between pollutant and water molecules for free adsorption sites of the building material is another possible mechanism (Lin et al. 2009; Huang et al. 2006; Suzuki et al. 2014). However, it is the molar amount of free water that determines the amount of hydrolysis. The absolute quantity of free water in the air (AH) is a better approximation of the molar amount of free water than the RH. Moreover, RH changes with temperature even when the molar amount of free water remains the same in the air. Thus, from the standpoint of the hydrolysis reaction mechanism, AH is a more appropriate metric for evaluating the influence of humidity on formaldehyde emissions than RH.

4.2.2.4 Comparison with other studies

The measurement settings and results of this and several other studies are briefly compared in Table 4-2. The unique features and advantages of this study are summarized as follows.

(1) Human-related emissions, as well as disturbances by the testing personnel, were eliminated in this unoccupied experimental room. Other formaldehyde sources and interactions were not present, so that the measured concentrations were solely due to emissions by the MDF studied. In other studies, the measurement results may represent the cumulative contributions of several factors.

(2) The overall study period using the experimental room was 29 months, far longer than previous controlled laboratory or field studies. Formaldehyde concentrations, as well as temperature, humidity, and ventilation rate data, were all obtained over this long study period. Annual cyclical seasonal variations in formaldehyde concentrations and emission rates were observed along with annual attenuation. Positive correlations between the formaldehyde concentration and temperature and the formaldehyde concentration and AH were also clearly identified based on the detailed long-term data. Due to the shorter durations and sometimes confounding data in other studies, these interesting variations and correlations were not reported.

(3) Temperature and humidity varied naturally and the ranges for these variables were deliberately allowed to be much larger than typically occur in occupied buildings. Thus, the effects of temperature and humidity on formaldehyde emissions could be fully represented and analyzed. In particular, the effects of low extremes in temperature and AH were analyzed in the field for the first time.

Thus, this study had several advantages, including elimination of multiple interferences, long-term detailed measurement of data, and incorporation of broader temperature and humidity ranges. Thus, the results provide a meaningful contribution to characterization of long-term formaldehyde emissions and can be used to guide factor analysis as well as emission model validation for actual buildings.

Table 4-2. Summary of the measurement conditions and results of this study with those of previous studies

Studies	Wolkoff et al. (1991)		Brown (2001)	Crump et al. (1997)	This study
House occupancy	Occupied	Unoccupied	Occupied	Unoccupied	Unoccupied
Testing person position	Indoor	Indoor	Indoor	Indoor	Outdoor
Building materials number	Multiple	Multiple	Multiple	Multiple	Only MDF
Other VOCs existences	Yes (21)*	Yes (21) *	Yes (27) *	Yes (>5) *	None
Time duration	12 months	12 months	8 months	24 months	29 months
Total number of concentration tests	10 times	10 times	4 times	28 times	71 times
Duplicated samples	No duplicate	No duplicate	Two duplicates	No duplicate	Three duplicates
Temperature interval	Not reported	Not reported	Not reported	Not reported	10 min
RH interval	Not reported	Not reported	Not reported	Not reported	10 min
Temperature range (°C)	14.9-23.9	17-33	21-29	20-30	-10.9-31.4
RH range (%)	40-56	24-67	32-54	33-40	46.5-83.6
AH range (g/kg_{air})	Not reported	Not reported	6.6-10.8	Not reported	1.1-23.1
Ventilation measurement period	March to May	March to May	Not measured	Not reported	A whole year

Ventilation measurement frequency	Not reported	Not reported	Not measured	One time	Monthly

* Numbers in parentheses are the reported number of VOCs in the corresponding references.

4.2.3 Conclusions on field study

We studied formaldehyde emissions from the medium-density fiberboard (MDF) in a full-scale experimental room to approximate emissions in actual buildings. Detailed indoor formaldehyde concentrations and temperature and humidity data were obtained for about 29 months. Temperature, relative humidity (RH), and absolute humidity (AH) ranged over -10.9–31.4 °C, 46.5–83.6%, and 1.1–23.1 g/kg_{air}, respectively. Annual cyclical seasonal variations were observed for indoor formaldehyde concentrations and emission rates, exhibiting entirely different characteristics than that in an environmental chamber under constant environmental conditions. The maximum concentration occurred in summer rather than at initial introduction of the material. The concentrations in summer could be a few up to 20 times higher than that in winter, depending on the indoor temperature and humidity conditions. Concentrations decreased by 20–65% in corresponding months of the second year. Indoor formaldehyde concentrations were positively correlated with temperature and AH, but were poorly correlated with RH. It is understood that other VOCs may or may not follow the same trend. Additional quantitative studies are needed in the future. Nevertheless, this field work provides a complete procedure in understanding the complex impact of temperature and humidity on VOC emissions.

These findings indicate that: 1) it is important to factor in the effects of temperature and humidity even during the design stage where data from the standard chamber tests (typically done at 23 C and 50% RH) are used as basis of specifying the pollution loads; 2) demand-based ventilation or air cleaning can be applied to provide the required ventilation and clean air delivery rate to keep the formaldehyde concentration below the threshold limits, and save energy comparing to constant ventilation. This support the needs of developing demand-based ventilation strategies as discussed in Subtask 4 report.

4.3 Laboratory studies

The field study indicated that both temperature and humidity have effects on formaldehyde emissions. The main objectives of this laboratory study are to investigate and obtain the correlation between C_0 and the combined effects of temperature and humidity on formaldehyde emissions, to compare the differences between the different representative parameters of humidity in the individual effect of temperature and the combined effects studies.

4.3.1 Measurement methods

4.3.1.1 Environmental chamber measurement system

A dynamic environmental chamber is the most commonly used equipment in material emission test and it is of advantage in the accurate control of the temperature and humidity conditions. The emission parameters can be regressed according to the measurement results of the chamber air. The measurement system is illustrated in Figure 4-6. A 53 L stainless steel chamber with a fan on the top to mix the air and emitted formaldehyde was used. Temperature in the air of the chamber was controlled by a water bath equipped at the outer surface of the chamber. Humidity was regulated by adjusting the valves at the wet and dry clean air flow paths. An automatic data logger (WSZY-1 sensor, Beijing, China) was installed in the chamber to measure the temperature and humidity continuously. Ventilation rate was controlled by the valves in the flow paths.

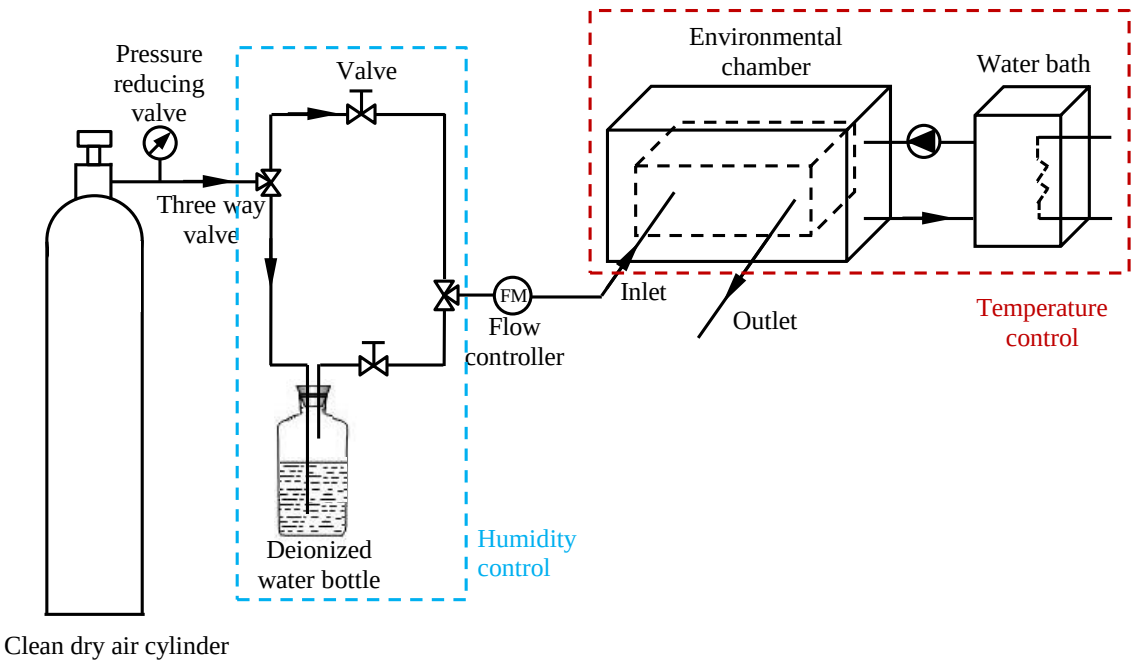

Figure 4-6: Schematic of the environmental chamber measurement system.

4.3.1.1.1 Measurement scenarios

Three series of experiments S1-S3 with four cases each were conducted. Experimental parameter settings of each case are specified in Table 4-3. Temperatures were set from 5.2 °C to 35 °C, which could cover the most common range happening in actual buildings. Temperature of S1, absolute humidity (AH) of S2 and relative humidity (RH) of S3 were almost identical between the cases among the series. Additionally, temperature and RH of S2, temperature and AH of S3 were changed case by case. Thus, either AH or RH was used as the representative parameter of humidity effect, these three series of experiments could be used to analyze the individual effect of humidity, temperature and the combined effects of them on formaldehyde emissions.

Table 4-3. Environmental parameter settings based on ventilated environmental chambers at different scenarios

Series No.	Temperature (°C)	Relative humidity (%)	Absolute humidity (g/kg_{air})	Ventilation rate (h^{-1})	Dimensions (mm×mm×mm)
S1	**25.5±0.5**	20±5	4.0±0.5	1±0.05	245×140×12
	25.5±0.5	30±5	6.1±0.5	1±0.05	245×140×12
	25.5±0.5	50±5	10.4±0.5	1±0.05	245×140×12
	25.5±0.5	80±5	16.7±0.5	1±0.05	245×140×12
S2	7.0±0.5	62.0±5	**4.0±0.5**	1±0.05	245×140×12
	15.0±0.5	38.6±5	**4.0±0.5**	1±0.05	245×140×12
	25.5±0.5	20.0±5	**4.0±0.5**	1±0.05	245×140×12
	34.1±0.5	12.0±5	**4.0±0.5**	1±0.05	122×140×12
S3	5.2±0.5	**50.0±5**	2.8±0.5	1±0.05	245×140×12
	15.0±0.5	**50.0±5**	5.2±0.5	1±0.05	245×140×12
	25.5±0.5	**50.0±5**	10.4±0.5	1±0.05	245×140×12
	35.0±0.5	**50.0±5**	17.8±0.5	1±0.05	122×140×12

A typical MDF, which is the same material as was used in the field study, was chosen for test. It was placed in the center of the chamber. All four edges of the sample were sealed by aluminum foil, so that only the front and back surfaces of the MDF emitted formaldehyde. Hence, the emission could be simplified as a one-dimensional., double-sided diffusion process.
Formaldehyde concentrations in the air of the chamber were measured at the outlet by a bubble absorption tube containing 5.0 mL of 50 µg/mL 3-methyl-2-benzothiazolinone hydrazone (MBTH). Samples were taken at a flow rate of 200 mL/min. The sampling time was 5 min. Duplicate samples were taken at the emission time of 12 h in each case to estimate the measurement errors.

4.3.1.1.2 Method of emission parameters regression

The diffusion emission model and expression of the time-varying pollutant concentration in the air of the chamber was presented in detail by Deng and Chang (2004). Emission parameters of different humidity scenarios were regressed according to the grid-mesh searching method introduced by He et al. (2005). The idea of the regression method is to fit the model predicted concentration result to the measurement data by adjusting the emission parameters. When the relative least squares in the following equation is obtained, the best match is reached.

$$R = \frac{1}{N_s}\sum_{i=1}^{N}\left(\frac{C_{a\_pi} - C_{a\_mi}}{C_{a\_mi}}\right)^2 \qquad \textbf{(4-2)}$$

Where C_{a_pi} is the i^{th} predicted result by the emission model. C_{a_mi} is the i^{th} measurement data point. N_s is the total number of the measurement data.
This regression method is slow but reliable and could ensure the global optimum point to be found (He et al. 2005). As multiple parameters need to be searched at the same time, this may contribute some uncertainty to the regressed emission parameters. He et al. (2005) had compared the differences between the searched values and the corresponding desired values and concluded that they were less than 5%. Thus the 5% uncertainty of the regressed parameters was adopted in this study.

4.3.2 Results and Discussion

4.3.2.1 Humidity effect on formaldehyde emissions

4.3.2.1.1 Measurement results

Figure 4-7 illustrates the measurement results of different humidity scenarios. Formaldehyde concentrations increased to the peak value in the first a few hours and then decreased continuously. Remarkable differences have occurred among the cases. Formaldehyde concentrations in the air of the chamber were higher at the high humidity scenarios, suggesting a positive effect of humidity on formaldehyde emissions. More specifically, concentrations at the RH (AH) of 80% (16.7 g/kg_{air}) were about three times as that at 20% (4.0 g/kg_{air}) at the same emission time. Despite the differences in concentration levels, the general variation trends of these four scenarios were similar.

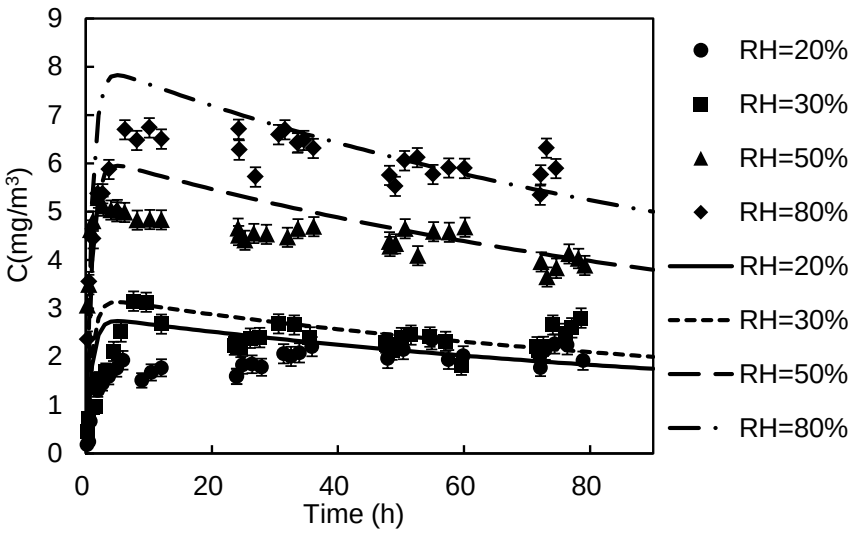

Figure 4-7: Time-varying formaldehyde concentrations in the air of the chamber at different humidity levels. Dots are the measurement data and lines are the regression curves. Error bars are the estimated measurement errors.

4.3.2.1.2 Emission parameters

The regression curves are illustrated in the lines of Figure 4-7 and the estimated emission parameters are shown in Table 4-4. Discrepancies between the regression and measurement results were relatively large at the beginning of emission. This was a common phenomenon reported in the literature, which could be explained by the instability of environmental conditions and partial mixing of the chamber air at the initial stage (Huang and Haghighat 2002).

Table 4-4. Regressed emission parameters based on ventilated environmental chambers at different humidity conditions

Series No.	Temperature (°C)	Relative humidity (%)	Absolute humidity (g/kg_{air})	C_0 (mg/m^3)	D_m (m^2/s)	K (—)
S1	25.5±0.5	20±5	4.0±0.5	1.75×10^{6}	3.40×10^{-14}	6340
	25.5±0.5	30±5	6.1±0.5	2.00×10^{6}	3.36×10^{-14}	5514
	25.5±0.5	50±5	10.4±0.5	3.80×10^{6}	3.50×10^{-14}	5340
	25.5±0.5	80±5	16.7±0.5	5.20×10^{6}	3.14×10^{-14}	6128

As presented in Table 4-4, initial emittable concentration (C_0) was the most sensitive parameter influenced by humidity. A positive effect of humidity on C_0 was verified. C_0 increased from 1.75×10^{6} mg/m^3 to 5.20×10^{6} mg/m^3, which is a 2.97-fold increase that happened when RH changed from 20% to 80% (AH changed from 4.0 g/kg_{air} to 16.7 g/kg_{air}). By plotting the regressed results of C_0 with RH and AH in the same figure (Figure 4-8), a linear regression was obtained between C_0 and RH, C_0 and AH, respectively. The empirical linear relations could be expressed as the following equations.

$$C_0 = a_1 \times RH + b_1 \quad (4\text{-}3)$$

$$C_0 = a_2 \times AH + b_2 \quad (4\text{-}4)$$

where a_1, b_1, a_2, b_2 are empirical constants obtained from the regressed results. R-squared (R^2) of the regressions between C_0 and RH, C_0 and AH were respectively 0.976 and 0.977, suggesting the empirical linear relation fit well for them. Only the empirical constants presented some differences (Figure 4-8). The effects of AH and RH on formaldehyde emissions are similar and consistent.

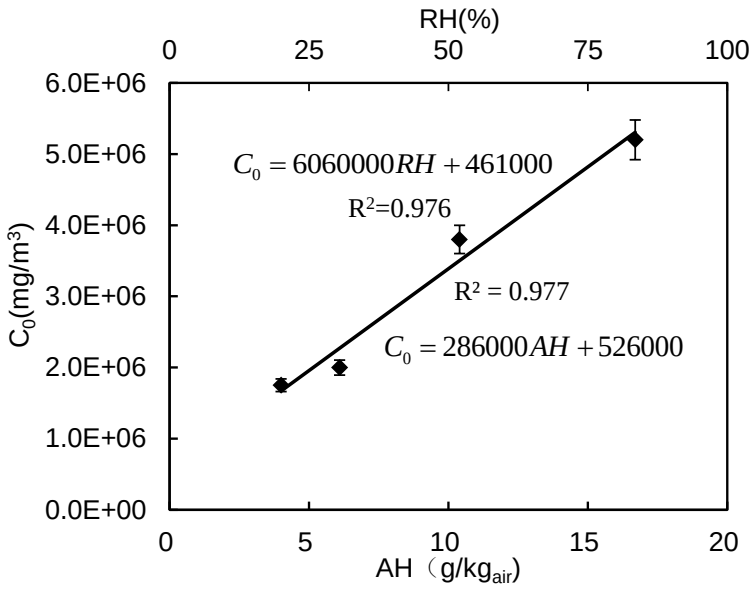

Figure 4-8: The linear relation between initial emittable concentration (C_0) and relative humidity (RH), C_0 and absolute humidity (AH). Error bars are the calculated standard deviation of C_0 with 5% uncertainty.

Humidity effects on D_m and K were not obvious compared to C_0, neither consistent trends with humidity had been identified. D_m of the MDF was small and varied between 3.14×10^{-14} - 3.50×10^{-14} m^2/s and K varied between 5340 - 6340 at the RH range of 20 - 80%. Differences of D_m and K between these four cases were within 11% and 17%, respectively. Such small variations of D_m and K should have little effect on the emission results (Yang *et al.*, 2001). Therefore humidity effects on these two emission parameters of the MDF were neglected. Xu and Zhang (2011) measured the D_m and K of a porous building material and found that RH had no significant effect on D_m. Higher K occurred when RH increased from 50% to 80% while no significant difference was observed for RH between 25% and 50%. Wei et al. (2013) analyzed the influence of humidity on D_m and K and concluded that humidity had a negative effect on D_m while the effect on K was unclear.

4.3.2.1.3 Mechanism explanations

The mechanism of humidity effect on formaldehyde emission from MDF is very complicated. One of the most common explanations was that there was hydrolysis inside the materials, which could yield formaldehyde with the presence of free water (Sidheswaran *et al.*, 2013). The use of formaldehyde-based polymeric resins (e.g. UF and phenol-formaldehyde) in the manufacturing of the artificial wood-based panels was the main reason of formaldehyde emission from these products. UF resin was the most widely used adhesive and it was known for releasing free formaldehyde upon reversible hydrolytic degradation (Frihart et al. 2012). Other possible chemical reactions that may occur in the material were hydrolysis of formaldehyde polymer and formaldehyde-wood polymer. When humidity in the mainstream air changed, moisture mass transfer would happen between the air and material. Thus, water molecules inside the material would increase with humidity

ascending in the air. Consequently, hydrolysis of the resins and polymers was induced and formaldehyde generated in the material. Formaldehyde content and emissions thus increased with the ascending humidity. The formaldehyde generated from the decompositions of these resins and polymers most likely acted as an internal source in addition to the formaldehyde existed during the board manufacturing process.

Another possible explanation of humidity effect on formaldehyde emission was that competitions for the adsorption sites between formaldehyde and water molecules may exist on the structure surface. For a porous material, the adsorption site on the surface of the solid-matrix was limited and immutable according to the Langmuir monolayer adsorption theory (Langmuir, 1918; Liu *et al.*, 2015). Formaldehyde molecules had to compete for the same adsorption sites with water molecules. Thus raising humidity was unfavorable to formaldehyde adsorption, which would lead to the decrease of formaldehyde at the adsorption sites (Sun et al. 2010; Yu et al. 2015). Consequently, more formaldehyde molecules will transfer from adsorbed-phase to gas-phase and contribute to a higher emittable concentration in the materials when humidity increased. Different from the hydrolysis reaction aforementioned, this mechanism would not generate extra formaldehyde because there was only phase transfer of formaldehyde molecules inside the material. Moreover, adsorption on the material surface was a very quick process (Yu et al. 2015), thus formaldehyde molecules at the adsorption sites would be replaced very quickly when moisture level increased. This might explain the instantaneous responses of formaldehyde emission to humidity changes in the experiment. It should be noticed that the adsorption of a porous material is related to the microstructural properties such as porosity, pore size distribution and gas permeability of it (Hamami et al. 2012). And statistic variability of the adsorptivity property of building materials can modify results obtained from deterministic approach (Trabelsi *et al.*, 2011).

These mechanisms mentioned above could give a qualitative explanation of the humidity effect on formaldehyde emission. But the quantitative and theoretical correlations between emission parameters and humidity are yet to be studied.

4.3.2.2 Temperature effect on formaldehyde emission

4.3.2.2.1 Measurement results

Formaldehyde measurement data of S2 and S3 are shown in **Figure 4-9**. When AH was used as the representative parameter of humidity effect, cases of S2 with identical AH and changed temperature could be used to discuss the individual effect of temperature, while cases of S3 with changed temperature and AH could be used to analyze the combined effects of temperature and AH. Although the humidity setting was quite different from the traditional approach on the studies about the individual effect of temperature, formaldehyde concentration increased with temperature increase (**Figure 4-9**(a)). Qualitative conclusion about the positive effect of temperature on formaldehyde concentration was consistent with that reported in the literature by the traditional study approach with identical RH (Wiglusz *et al.*, 2002; Xiong and Zhang, 2010).

When RH was used as the representative parameter of humidity effect as the traditional study approach, cases of S3 for the individual effect of temperature. Formaldehyde emission increased at higher temperature at the individual effect of temperature (**Figure 4-9**(b)).

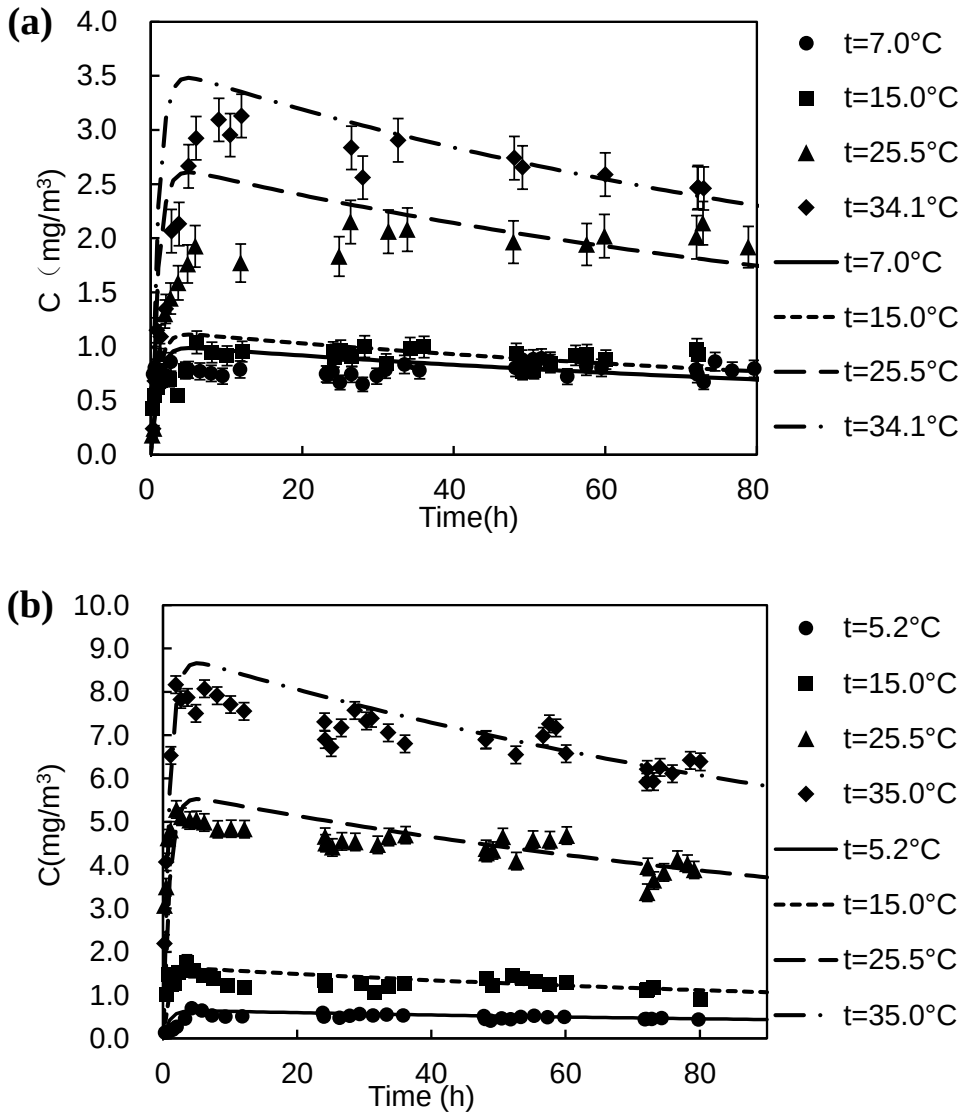

Figure 4-9: Formaldehyde concentration results in the chamber air with different temperature and humidity conditions. Dots are the measurement data, lines are the regression curves: (a) measurement results of S2 with identical absolute humidity (AH), (b) measurement results of S3 with identical relative humidity (RH). Error bars are the estimated measurement errors.

For the individual effect of temperature as shown in Figure 4-9, no matter whether AH or RH are being used as the representative parameter of the humidity effect, formaldehyde emission increased with temperature. The qualitative conclusion about the positive effect of temperature on formaldehyde concentration becomes the same for these two different approaches. However, concentration differences at identical RH were larger than that at identical AH, suggesting formaldehyde emission at identical RH was more sensitive to temperature variation.

4.3.2.2.2 Emission parameters

The regression curves are illustrated in the lines of Figure 4-9 and the estimated emission parameters are shown in

Table 4-5. At the individual effect of temperature, C_0 and D_m increased and K varied the same way with temperature either AH or RH being set as identical, and C_0 was the most sensitive parameter influenced by

temperature. It increased from 7.90×10^5 mg/m^3 to 4.30×10^6 mg/m^3, which means that a 5.4-fold increase occurred when temperature increased from 7.0 °C to 34.1 °C at the identical AH of 4.0 g/kg$_{air}$. The differences of C_0 among different temperatures were more pronounced at identical RH than AH

Table 4-5. Regressed emission parameters based on ventilated environmental chambers at different temperature conditions

Series No.	Temperature (°C)	Relative humidity (%)	Absolute humidity (g/kg$_{air}$)	C_0 （mg/m^3）	D_m （m^2/s）	K （—）
S2	7.0±0.5	62.0±5	**4.0±0.5**	7.90×10^5	3.00×10^{-14}	9467
	15.0±0.5	38.6±5	**4.0±0.5**	8.50×10^5	3.15×10^{-14}	7844
	25.5±0.5	20.0±5	**4.0±0.5**	1.75×10^6	3.40×10^{-14}	6340
	34.1±0.5	12.0±5	**4.0±0.5**	4.30×10^6	3.57×10^{-14}	4570
S3	5.2±0.5	**50.0±5**	2.8±0.5	4.93×10^5	2.90×10^{-14}	9752
	15.0±0.5	**50.0±5**	5.2±0.5	1.14×10^6	3.15×10^{-14}	7280
	25.5±0.5	**50.0±5**	10.4±0.5	3.80×10^6	3.50×10^{-14}	5340
	35.0±0.5	**50.0±5**	17.8±0.5	1.10×10^7	3.60×10^{-14}	3450

As humidity has little effect on D_m and K, the values at the same temperature can be supposed to be close to each other regardless of the humidity conditions. More specifically, D_m and K at t=25.5 °C, AH=10.4 g/kg$_{air}$ were 3.50×10^{-14} m^2/s and 5340, respectively. While D_m and K at t=25.5 °C, AH=4.0 g/kg $_{air}$ were 3.40×10^{-14} m^2/s and 6340. These two pairs are close to each other when taking the measurement and regression errors into account.

4.3.2.2.3 Theoretical correlation

Generally speaking, building material like wood-based panels could be treated as porous media consisting of gas pores and solid matrix. Formaldehyde-based polymeric resins (e.g. UF and phenol-formaldehyde) are commonly used to integrate the wood fibers together in the manufacturing process of artificial wood-based panels. Thus, the resins acted as the connection agent of wood fibers and both of them were solid once the manufacturing process was completed. To simplify the situation, the homogenous assumption of formaldehyde concentration between the resins and wood fibers was adopted in this study. Both of them constituted the solid matrices of the porous material, while the interspaces between the fibers or resins were gas pores. Moreover, the use of the polymeric resins was also the main reason of formaldehyde emissions from these products (Kim *et al.*, 2006). On one hand, formaldehyde would be left in the material because of the manufacturing process using formaldehyde-based resins. On the other hand, extra formaldehyde would also be induced upon reversible hydrolytic degradation of the polymeric resins with the presence of free water (Frihart et al. 2012; Sidheswaran et al. 2013). Thus, total formaldehyde concentration in the material ($C_{0,\,total}$ (mg/m$^3_{material}$)) is constituted by two parts. One is the residual formaldehyde concentration (m_1) from manufacturing, which is supposed to be constant once the manufacturing process was complete. Another part is the yielded formaldehyde concentration (m_2) from hydrolysis reactions of resins, which is dependent on the humidity in the material (Sidheswaran et al. 2013; Myers 1985). From the microcosmic point of view, the formaldehyde molecules in the porous material are presented as gas-phase in the pore and the adsorbed-

phase at the solid matrix surface (Haghight et al. 2005; Lee 2003). A schematic illustration of the porous material and molecular phases is presented in Figure 4-10.

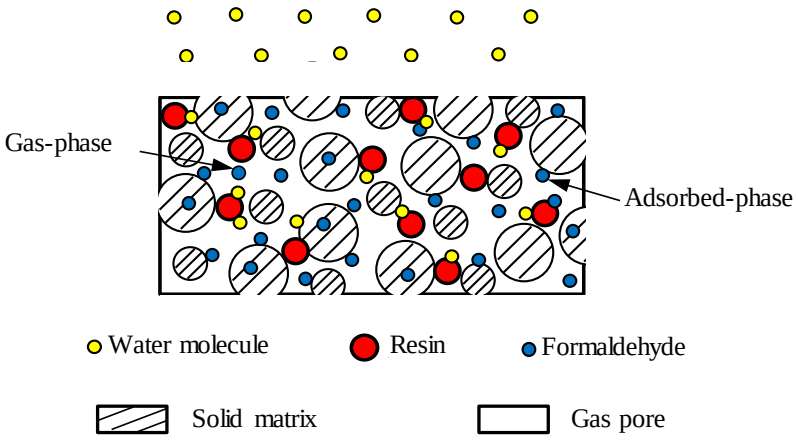

Figure 4-10: Microcosmic schematic illustration of the structure and molecular phases in the porous material

Mass transfer in the porous material could be described by the multi-phase diffusion model, which consists of gas-phase diffusion through the pore, and adsorbed-phase diffusion or diffusion through the solid matrix (Haghight et al. 2005; Lee 2003). Mass transfer in the porous material is mainly dominated by gas-phase diffusion. The adsorbed-phase diffusion is much smaller compared to gas-phase diffusion and thus assumed to be negligible in many studies (Deng et al. 2009; Lee 2003; Blondeau et al. 2003). Consequently, only the molecules in the gas-phase contribute to the initial emittable concentration (C_0) for formaldehyde in the one-phase diffusion model. Thus, correlation between the gas-phase concentration and C_0 could be expressed as

$$C_0 = \varepsilon C_a \quad (4\text{-}5)$$

where C_0 is the initial emittable concentration of the material (mg/m$^3_{material}$), C_a is the gas-phase concentration in the pore (mg/m$^3_{gas}$), ε is the porosity of the porous material (m^3 of gas/m^3 of material). The porosity ε is related to the property and structure of the porous material and it is constant once the material is determined. In the multi-phase approach, an instantaneous equilibrium is assumed to be established between the gas-phase and adsorbed-phase, which is given as (Haghight et al. 2005; Lee 2003; Deng et al. 2009):

$$C_s = K_s C_a \quad (4\text{-}6)$$

Where C_s is the adsorbed-phase concentration (mg/m$^3_{material}$), K_s is the multi-phase partition coefficient between the gas-phase and adsorbed-phase at the solid matrix surface. Total formaldehyde concentration in the material ($C_{0,\,total}$ (mg/m$^3_{material}$)) is the sum of the gas-phase (C_a) and adsorbed-phase concentration (C_s). For a given material with porosity of ε, $C_{0,\,total}$ could be expressed as the following equation

$$C_{0,\,total} = \varepsilon C_a + C_s \quad (4\text{-}7)$$

By inserting Eq. 4-6 into Eq. 4-7, we have

$$C_{0,\,total} = \varepsilon C_a + K_s C_a = (\varepsilon + K_s) C_a \quad (4\text{-}8)$$

Haghighat et al. (2005) have interpreted the correlation between one-phase partition coefficient K and the multi-phase partition coefficient K_s, which is given as

$$K = \varepsilon + K_s \quad (4\text{-}9)$$

Where, K is the partition coefficient at the material-air interface of the one-phase diffusion model. Equation 9 has also been used in the derivation of the correlation between diffusion coefficient (D_m) and temperature (Deng et al. 2009). By substituting Eq. 4-9 into Eq. 4-8, $C_{0,\,total}$ could be expressed as Equation 4-10:

$$C_{0,\,total} = KC_a \quad (4\text{-}10)$$

The correlation between C_a and $C_{0,\,total}$ could be derived according to Eq. 4-10.

$$C_a = \frac{C_{0,\,total}}{K} \quad (4\text{-}11)$$

As ε is constant for a determined material, the initial emittable concentration (C_0) would present the same pattern as the gas-phase concentration (C_a) according to Eq. 4-5. Previous studies suggested that if kinetic energy of the adsorbed-phase molecules is large enough to overcome the bonding force from the solid matrix, the molecules will transfer to gas-phase and become emittable. Based on the kinetic theory, kinetic energy of the molecules will increase with the increase of temperature and more molecules would transfer from adsorbed-phase to gas-phase, which means more molecules would release from the solid matrix to the pore inside the material. Consequently, C_0 and C_a will ascend with temperature increase. But no matter how the molecules transfer between adsorbed-phase and gas-phase, no extra formaldehyde will be generated inside the material. $C_{0,\,total}$ should be in accordance with the law of mass conservation and remains constant regardless of temperature change and molecular phase transfer in the material. The individual effect of temperature on formaldehyde emission was mainly revealed on the ratio of molecules distributed between the adsorbed-phase and gas-phase. Consequently, with stabilized humidity, the effect of temperature on C_0 shared the inverse correlation as K according to Eq. 4-11. By applying the correlation between K and temperature established by Zhang et al. (2007), a correlation between C_0 and temperature could be derived as:

$$C_0 = \varepsilon C_a = \frac{\varepsilon C_{0,\,total}}{K} = \frac{\varepsilon C_{0,\,total}}{A_1 T^{0.5} \exp\frac{A_2}{T}} = C_1 T^{-0.5} \exp(-\frac{C_2}{T}) \quad (4\text{-}12)$$

Where C_1 and C_2 are constants. C_2 in Eq. 4-12 determines the rate of C_0 change with temperature, such that a larger C_2 indicates that C_0 is more sensitive to the temperature change. The correlation between C_0 and temperature presented the same form as the theoretical correlation derived by Huang et al. (2015). This supports the notion that the derivation process and assumptions in this paper were reasonable. Another aspect we could draw from this derivation process was that even when the total formaldehyde concentration in the material is not the parameter that directly determines the actual emission behavior, it is still a good index in the emission control from building materials. Because of that, some adsorbed-phase formaldehyde molecules would transfer to gas-phase and emit into room air at a higher temperature.

A theoretical correlation between D_m and temperature was derived by Deng et al. (2009), which is given as:

$$D_m = B_1 T^{1.25} \exp\frac{B_2}{T} \quad (4\text{-}13)$$

A correlation between *K* and temperature was established by Zhang et al. (2007), which is expressed as follows:

$$K = A_1 T^{0.5} \exp\frac{A_2}{T} \quad (4\text{-}14)$$

where A_1, A_1, B_1, B_2 are constants, which are independent of temperature. Regression results of the correlations between C_0 and temperature, D_m and temperature, *K* and temperature at identical AH are presented in Figure 4-11. The good fitting between the correlations and the experimental results demonstrated the effectiveness of the correlations at identical AH. These implied that it may be reasonable to use AH as the representative parameter of humidity effect. Regression results of the correlations between C_0 and temperature, D_m and temperature, *K* and temperature at identical RH are presented in Figure 4-12.

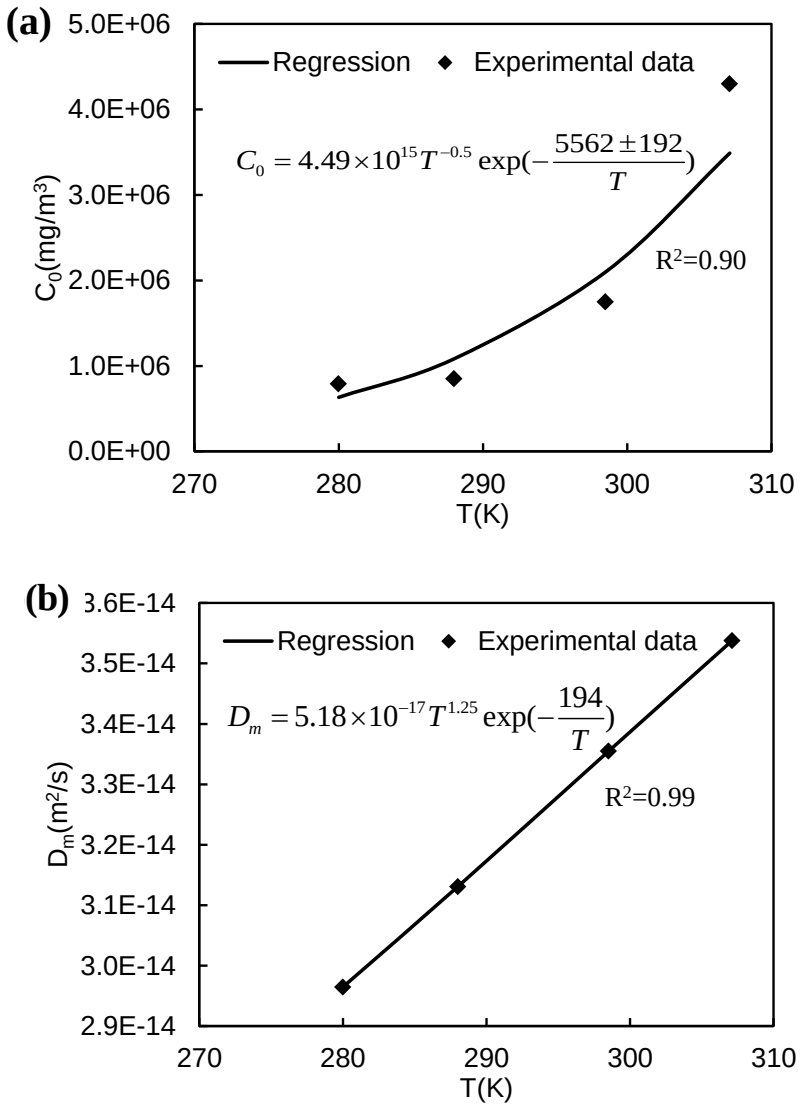

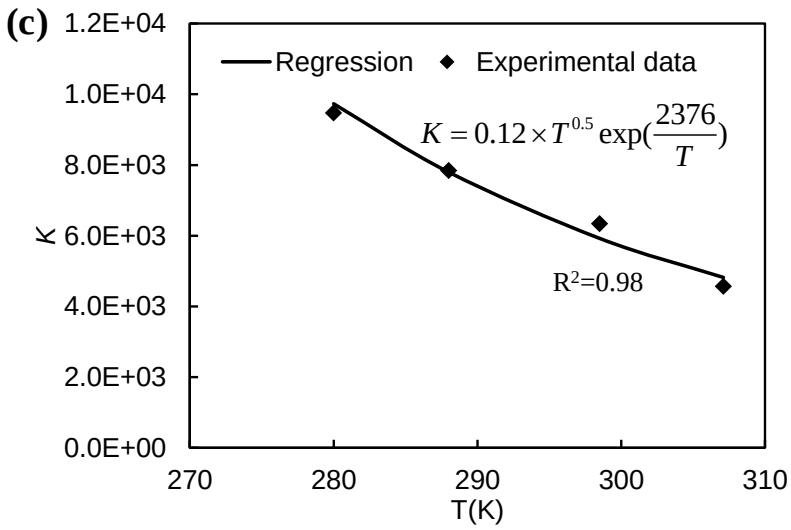

Figure 4-11: Correlations between C_0, D_m and temperature, K and temperature at identical absolute humidity (AH): (a) C_0 vs. T; (b) D_m vs. T; (c) K vs. T.

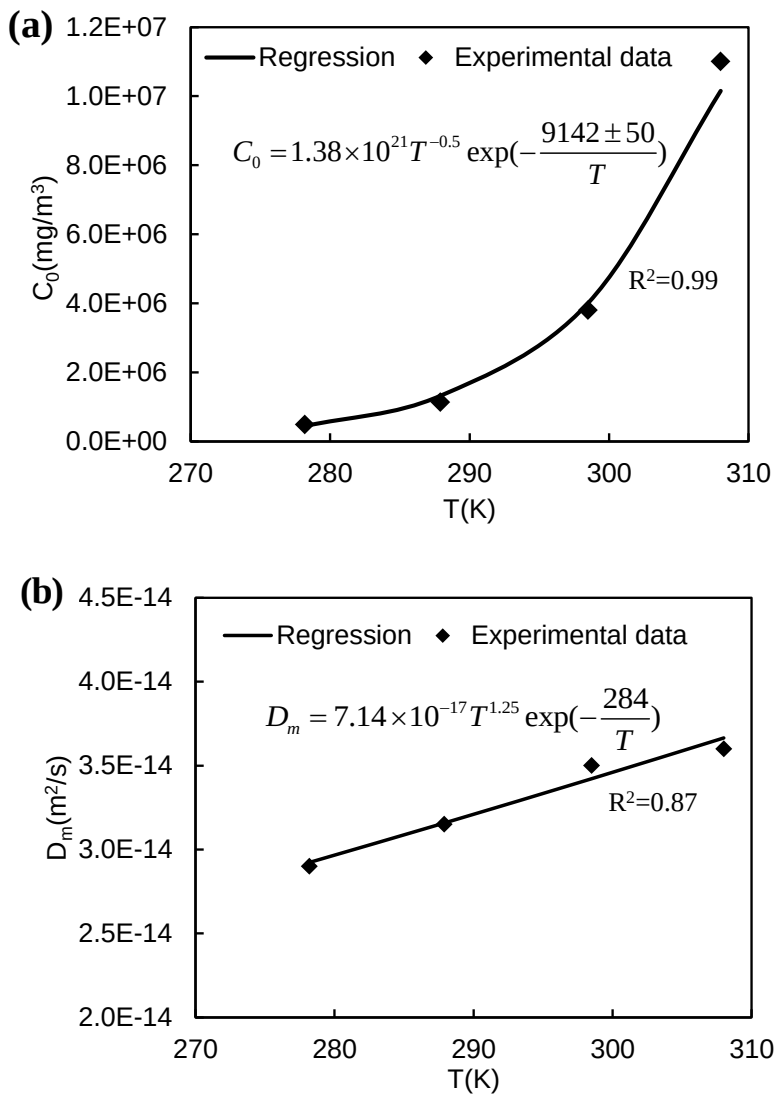

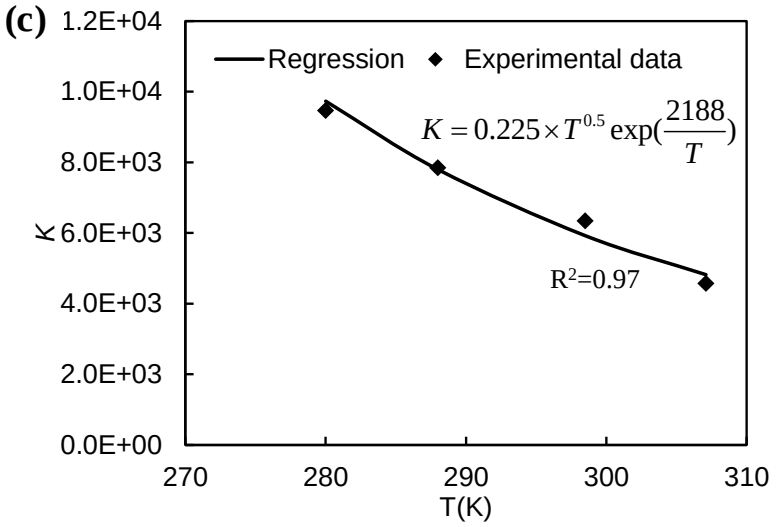

Figure 4-12: Correlations between C_0, D_m and temperature, K and temperature at identical relative humidity (RH): (a) C_0 vs. T; (b) D_m vs. T; (c) K vs. T.

The individual effect of temperature, C_0, D_m and K varied the same way with temperature no matter whether AH or RH were set as identical, and C_0 was the most sensitive parameter influenced by temperature. Moreover, the theoretical correlations between these emission parameters and temperature could both be validated by the experimental results at identical AH and RH. However, differences of C_0 among different temperatures were more pronounced at identical RH than AH as shown in

Table 4-5

Table 4-5, Figure 4-11(a) and Figure 4-12(a). The exponential constant C_2 in Eq. 4-12 is 9142 at identical RH, which is much larger than 5562 at identical AH.

4.3.2.3 The combined effects of temperature and humidity on formaldehyde emissions

4.3.2.3.1 Measurement results

Formaldehyde emission at the combined effects of temperature and AH, combined effects of temperature and RH are shown in S3, **Figure 4-9**(b) and S2, **Figure 4-9**(a). At the combined effects of temperature and AH as shown in **Figure 4-9**(b), formaldehyde concentration increased more significantly than that at individual effect of temperature. For instance, average formaldehyde concentrations at t=25.5 °C, AH=10.4 g/kg$_{air}$ were about 3.4 times as high as that at t=15.0 °C, AH=5.2 g/kg$_{air}$. At the individual effect of temperature as shown in **Figure 4-9**(a), average formaldehyde concentrations at t=25.5 °C, AH=4.0 g/kg$_{air}$ were about twice as high as the concentrations at t=15.0 °C, AH=4.1 g/kg$_{air}$. From the measurement results on humidity effect studies, formaldehyde emission increased with increase of AH. When RH was identical (S3), AH increased with temperature increase, and thus the effects of AH and temperature on formaldehyde emission were consistent in this occasion. Consequently, formaldehyde concentration increased more significantly at the combined effects of temperature and AH than the individual effect of temperature. Contrary to the approach by the representative parameter of AH, concentration differences at the combined effects of temperature and RH were smaller than that at the individual effect of temperature. The main reason was that the individual effects of RH and AH on formaldehyde emission shared the same pattern. When AH was identical (S2), RH decreased with increase of temperature, the effects of RH and temperature on formaldehyde emission were inverse to each other. Formaldehyde concentration differences in S3 were much larger than S2.

Generally speaking, concentration differences at the combined effects of temperature and RH (S2, **Figure 4-9**(b)) were smaller than that at the combined effects of temperature and AH (S3, **Figure 4-9**(a)). Thus, even though the qualitative conclusions of these two kinds of approaches were the same on the studies about the individual effect of temperature and the combined effects of temperature and humidity, the quantitative conclusions differed significantly.

4.3.2.3.2 Emission parameters

Initial emittable concentration (C_0) was the most sensitive parameter influenced by the combined effects of temperature and humidity among the three emission parameters. C_0 increased significantly at the consistent positive effect of temperature and AH (S2). For instance, C_0 increased from 4.93×10^5 mg/m^3 to 1.10×10^7 mg/m^3, which is a 22-fold increase when the condition changed from 5.2 °C, 2.8 g/kg$_{air}$ to 35.0 °C, 17.8 g/kg$_{air}$. Moreover, at the temperature of 15.0 °C, C_0 increased from 8.50×10^5 mg/m^3 to 1.14×10^6 mg/m^3 when RH increased 38.6% to 50% (AH increased from 4.0 g/kg$_{air}$ to 5.2 g/kg$_{air}$). Likewise, a more noticeable increase of C_0 had occurred when RH increased from 20% to 50% (AH increased from 4.0 g/kg$_{air}$ to 10.4 g/kg$_{air}$) at the temperature of 25.5 °C. These two pairs demonstrated the important contribution of humidity and the effect of hydrolysis reaction to formaldehyde emission.

D_m and K at the combined effects of temperature and AH did not significantly differ from the values at the individual effect of temperature. From our previous studies as well as the conclusions reported in the literature, humidity effects on D_m and K were not significant (Xu and Zhang 2011). Thus, the combined effects of temperature and humidity on these two emission parameters were supposed to share the same pattern as the individual effect of temperature. They were simplified to the correlations with individual effect of temperature.

4.3.2.3.3 Theoretical correlation

When formaldehyde emissions are influenced by the combined effects of temperature and humidity, total formaldehyde in the material would be influenced by and varied with humidity conditions. When humidity in the air increased, water molecules will transfer from the air, material-air surface to building materials, resulting a higher humidity content in the material and driving hydrolysis reactions. In our previous study on the individual humidity effect, an empirical positive linear correlation between C_0 and AH, C_0 and RH were obtained experimentally by using environmental chamber. Hydrolysis yielded formaldehyde concentration (m_2) is also linearly correlated with AH and RH of the air which gives as:

$$m_2 = a_1 \times AH + b_1 \tag{4-15}$$

By considering the correlation between m_2 and humidity, $C_{0,\,total}$ could also be expressed as the following equation.

$$C_{0,\,total} = m_1 + m_2 = m_1 + a_1 \times AH + b_1 \tag{4-16}$$

where m_1, a_1, b_1 are constants. When humidity is stabilized, $C_{0,\,total}$ inside the material is constant according to Eq. 16, in accordance with the aforementioned assumption in the analysis of the temperature effect. When humidity changes, material emissions are influenced by the combined effects of temperature and humidity and $C_{0,\,total}$ would vary the same way as humidity. Correlation between C_0 and the combined effects is given as

$$C_0 = \varepsilon C_a = \frac{\varepsilon C_{0,\,total}}{K} = \frac{\varepsilon(m_1 + m_2)}{K} = \frac{\varepsilon(m_1 + a_1 \times AH + b_1)}{K} = \frac{\varepsilon(m_1 + a_1 \times AH + b_1)}{A_1 T^{0.5} \exp\frac{A_2}{T}} \quad (4\text{-}17)$$

In which ε, m_1, a_1, b_1, A_1 and A_2 are constants, thus Eq 4-17 could be further simplified to

$$C_0 = (1 + C_1 \times AH) C_2 T^{-0.5} \exp(-\frac{C_3}{T}) \quad (4\text{-}18)$$

When humidity effect is characterized by RH, the correlation between C_0 and the combined effects follow the same derivation process and it could be expressed as

$$C_0 = (1 + C_1 \times RH) C_2 T^{-0.5} \exp(-\frac{C_3}{T}) \quad (4\text{-}19)$$

Equations 4-18 and 4-19 describe the correlation between the initial emittable concentration and the combined effects of temperature and humidity on formaldehyde emission. C_1, C_2 and C_3 are constants in Eqs. 4-18 and 4-19. They are associated with the physical properties of the material but independent of temperature and humidity conditions. These equations indicate physical principles and set a direction for future practical applications. They could be used to calculate C_0 at different temperature and humidity conditions. However, the constants (C_1, C_2 & C_3) cannot be directly estimated based on physical property measurements of the material. Multiple chamber tests under various temperature and humidity conditions and regression analysis need to be conducted to determine these constants. This requires a lot of work and may introduce some difficulties in the practical use of the correlations.

Correlation between C_0 and the combined effects of temperature and humidity are given in Figure 4-13. The correlation between C_0 and the combined effect of temperature and AH fit very well with the experimental data (R^2=0.99), indicating the correlation could well explain the combined effects of temperature and AH on C_0. Regression results of the correlation between C_0 and the combined effects of temperature and RH are presented in Figure 4-13(b). The degree of fitting is not as good as that between C_0 and the combined effects of temperature and AH, but it is still acceptable with R^2=0.90. Thus, the correlations between C_0 and the combined effects of temperature and humidity could also be validated by these two different approaches. But the constants regressed differed significantly from each other. These two different approaches and correlations could induce a big difference in the formaldehyde simulation in actual buildings.

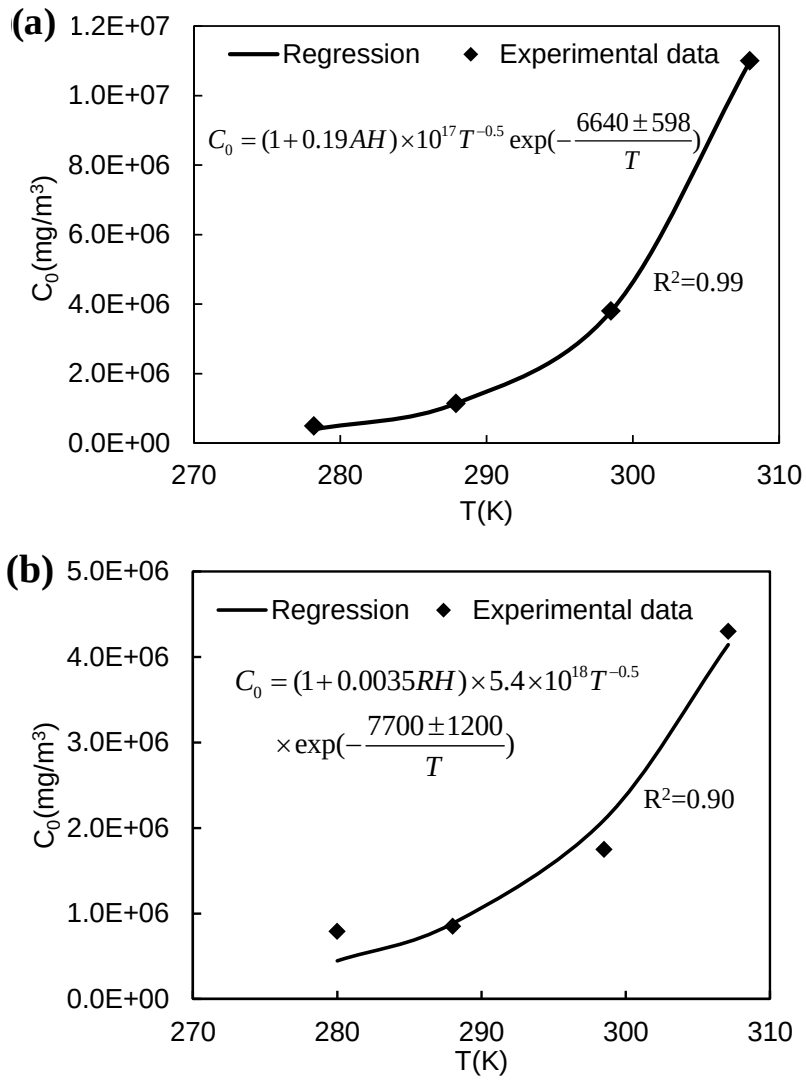

Figure 4-13: Correlation between initial emittable concentration (C_0) and the combined effects of temperature and humidity: (a) combined effects of temperature and AH (S3); (b) combined effects of temperature and RH (S2).

4.3.3 Conclusion on laboratory studies

The effects of temperature, humidity and their combined effects on formaldehyde emission parameters of a MDF were studied experimentally using the small-scale environmental chamber. The following conclusions could be drawn based on the measurement results and analysis:

(1) Humidity has a positive effect on formaldehyde emission from MDF. C_0 was the most sensitive emission parameter influenced by it. Linear relations between C_0 and RH, C_0 and AH were obtained. Humidity effects on D_m and K were found to be insignificant.

(2) A semi-empirical correlation between initial emittable concentration (C_0) and the combined effects of temperature (T) and humidity (absolute humidity AH or relative humidity RH) was derived, which was expressed as $C_0 = (1+C_1\times AH)C_2T^{-0.5}\exp(-C_3/T)$ and $C_0 = (1+C_1\times RH)C_2T^{-0.5}\exp(-C_3/T)$ by different representative parameters of humidity. Hydrolysis reactions affected by humidity and kinetic energy distribution of formaldehyde molecules affected by temperature were considered in the derivation process.

(3) A typical MDF was tested in three series of experiments with identical temperature, AH and RH, respectively, to validate the correlation. The good agreement between the correlation and measurement data demonstrated the effectiveness of these correlations.

(4) Differences of the conclusions between different representative parameter of humidity effect (AH vs. RH) were analyzed in the studies of the individual effect of temperature and the combined effects. The representative parameter of humidity has significant effects on the quantitative conclusions on the influencing factors studies.

It is understood that other VOCs may or may not follow the same trend. Additional quantitative studies are needed in the future, and the same method and procedure may be used.

5 Database of VOC emissions for IAQ simulation

(Zhenlei Liu, Andreas Nikolai, John Grunewald, Marc Abadie and Jensen Zhang)

5.1 Introduction

As we discussed in Section 3, in order to evaluate the impacts of VOC emissions from building materials on the indoor air quality beyond the standard chamber test conditions and test period, the model-based testing and evaluation (MBTE) method is needed. Mechanistic emission source models have been developed in the past. However, very limited data are available for the required model parameters including the initial concentration (C_{m0}), in-material diffusion coefficient (D_m), partition coefficient (K_{ma}), and convective mass transfer coefficient (h_m). In this section, we present two approaches that were developed for estimating the model parameters and establishing the database of model parameters for VOC emissions. Approach 1 is a procedure for estimating the model parameters using VOC emission data from standard small chamber tests. In the procedure, initial values of the model parameters were refined by multivariate regression analysis of the measured emission data. Approach 2 is a procedure based on empirical correlation and similarity method (Section 3) for estimating K_{ma} and D_m. We will introduce the emission source model and then discuss the details of the two approaches separately in the following sections.

The schematic of the small standard chamber test and governing equations were provided in Section 3.2. The analytical solution to the governing equations for the chamber system with a diffusion source was derived by Deng et al. (2004) as follows (Eq. 5-1and 5-2):

$$C_m(y,t) = 2C_{m0}\sum_{n=1}^{\infty}\frac{\alpha-q_n^2}{A_n}\cdot\cos\left(\frac{y}{L_m}q_n\right)e^{-D_mL_m^2q_n^2t} \quad (5\text{-}1)$$

$$\mathrm{C_a(t)} = 2\mathrm{C_{m0}}\beta\sum_{\mathrm{n=1}}^{\infty}\left(\frac{\mathrm{q_n}\sin\mathrm{q_n}}{\mathrm{A_n}}\right)\mathrm{e}^{-\mathrm{D_mL_m^2q_n^2t}} \quad (5\text{-}2)$$

$$A_n = [K_{ma}\beta + (\alpha - q_n)K_{ma}Bi_m^{-1} + 2]\,q_n^{2\cos}\,q_n + q_n\sin q_n\,[K_{ma}\beta + (\alpha - 3q_n^2)K_{ma}Bi_m^{-1}\alpha - q_n^2]$$

$$Bi_m = \frac{h_mL_m}{D_m}$$

$$\alpha = NL_m^2/D_m$$

$$\beta = L\cdot L_m$$

Where,

Bi_m is termed as the Biot number for mass transfer, which represents the ratio of in-material to on-surface mass transfer resistance;

α is the dimensionless air exchange rate, representing the ratio of dilution rate in the chamber air to the in-material diffusion rate;

L is loading ratio, surface area of the material divided by the volume of the chamber;

β is the ratio of the volume of the chamber to the volume of the material;

The q_n's are the positive roots of:

$$q_n \tan q_n = \frac{\alpha - q_n^2}{K_{ma}\beta + (\alpha - q_n^2) K_{ma} Bi_m^{-1}} \quad (5\text{-}3)$$

Obviously, C_{m0}, K_{ma} and D_m are species properties, and h_m is part of the characteristics of the chamber conditions. As we mentioned in Section 3.2.2, the mass transfer coefficient h_m may be estimated by CFD simulations or from established correlations between the mass transfer coefficient and air velocity over the surface. For example, the h_m-values of the two small-scale environmental chambers that were used to establish the material emission database (MEDB-IAQ) at the National Research Council Canada (NRC) were measured to be 1.0 and 1.5 m/h, respectively (Zhang et al., 1999). Some empirical relations were also adopted for the gas-phase mass transfer coefficient (Huang and Haghighat, 2002). For laminar flow, there exists (White, 1988)

$$Sh = 0.644 Sc^{\frac{1}{3}} Re^{\frac{1}{2}} \quad (5\text{-}4)$$

Where *Sh* is Sherwood number ($Sh = \frac{K_m}{D_m/L_m}$); *Sc* is Schmidt number ($Sc = \frac{\nu}{D_m}$), ν is the kinematic viscosity, m^2/s; Re is Reynolds number ($Re = \frac{v \cdot l}{\nu}$), *v* is the velocity of the fluid, m/s, *l* is the characteristic dimension, m.

Due to the consistent flow patterns in the standard chamber test condition, the h_m can be estimated independently from the chamber's test condition and extended to full-scale chamber condition.

The remaining three key parameters (C_{m0}, D_m and K_{ma}) need to be obtained from the emission test data, see the following Approach 1. If the emission data is insufficient, D_m and K_{ma} can also be estimated by the subsequent Approach 2.

5.2 Approach 1: Standard procedure by using emission data

An overview of the procedure to determine D_m, K_{ma} and C_{m0} will be shown as follows. There are four main steps of the procedure:

(1) Data pre-processing. Generation of the data with even time interval (Figure 5-1);
(2) Initial guesses as well as the lower and upper limits of the model parameters, C_{m0}, D_m and K_{ma} (Figure 5-3);
(3) Regression analysis to determine D_m and K_{ma} (Figure 5-4);
(4) Re-calculation of C_{m0} (Figure 5-4).

To verify the procedure and discuss the key issues involved, simulated chamber test data were generated by superposition of different levels of experimental uncertainties on the theoretical curve from the analytical solution to a mechanistic emission model, and then the procedure was used to estimate the model parameters from these data and determine how well the estimates converged to the original parameter values used for the data generation (data are provided in the Appendix).

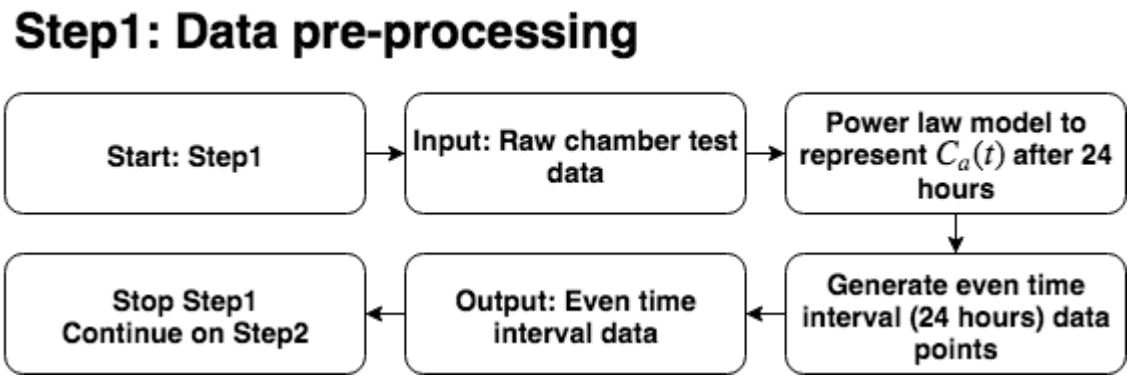

Figure 5-1 Step 1: Data pre-processing

5.2.1 Validated Region with Data Sets from the Literature

To better interpret the experimental results analyzed by the diffusion model, a sensitivity study was performed. The simulated cases for the sensitivity study were created by the analytical solution for the same standard small-chamber test condition. The total elapsed time was 672 hours (28 days), which is the common elapsed time in international standard emission tests for most dry building materials (ISO Standard Indoor air – part 6, 2011). Based on the range of D_m and K_{ma} from the cases found in the literature (Appendix), 7 levels of D_m and K_{ma} are selected to cover all the literature cases, totaling 49 sets of simulation cases evaluated. All the cases had good convergence so that the overall normalized residuals (defined as the root squared error divided by the square of the measured air concentration) were less than 4% between that modeled with the parameters estimated and the original concentration data used to obtain the model parameters. However, only the cases with original D_m and K_{ma} in the shaded area were able to obtain good estimates of the model parameters by the procedure (Figure 5-2). In the cases outside the shaded area, the 28 days concentration data did not yield good estimations of the model parameters although the predicted concentration agreed well with the original concentration data used by the procedure. This was because outside the range, the 28 days concentration data were not sensitive to further changes of D_m and/or K_{ma}. For example, when the partition coefficient is less than 10^3, and the diffusion coefficient is larger than 10^{-9} m^2/s, the emission rate from the surface is mainly controlled by the mass transfer resistance through the boundary layer and is insensitive to the D_m and K_{ma} used because there is little in-material resistance. Similarly, when K_{ma} is larger

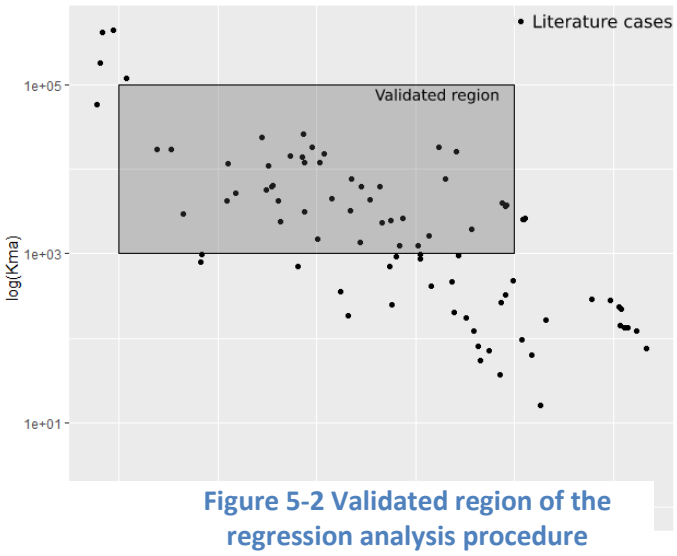

Figure 5-2 Validated region of the regression analysis procedure

than 10^5 and D_m is less than 10^{-13} m^2/s, there is abundant source at the surface and in-material diffusion resistance is relatively large, the emission rate is also primarily controlled by the mass transfer resistance in the material. It should be noted that significant variability also exists in the literature data. As a result, we limit the use of the current procedure for model parameter estimation to the validated range of D_m and K_{ma} (shaded area). When the regressed results are outside this range, we recommend setting the respective D_m and/or K_{ma} at the border line value for the purpose of estimating the concentrations within the 28 day period. Prediction beyond the 28 day test period for these cases would exhibit larger errors. In the implementation of the procedure, we focused on the emission factor to evaluate the IAQ. The error of the emission factor was less than 10% in reproducing the measured data.

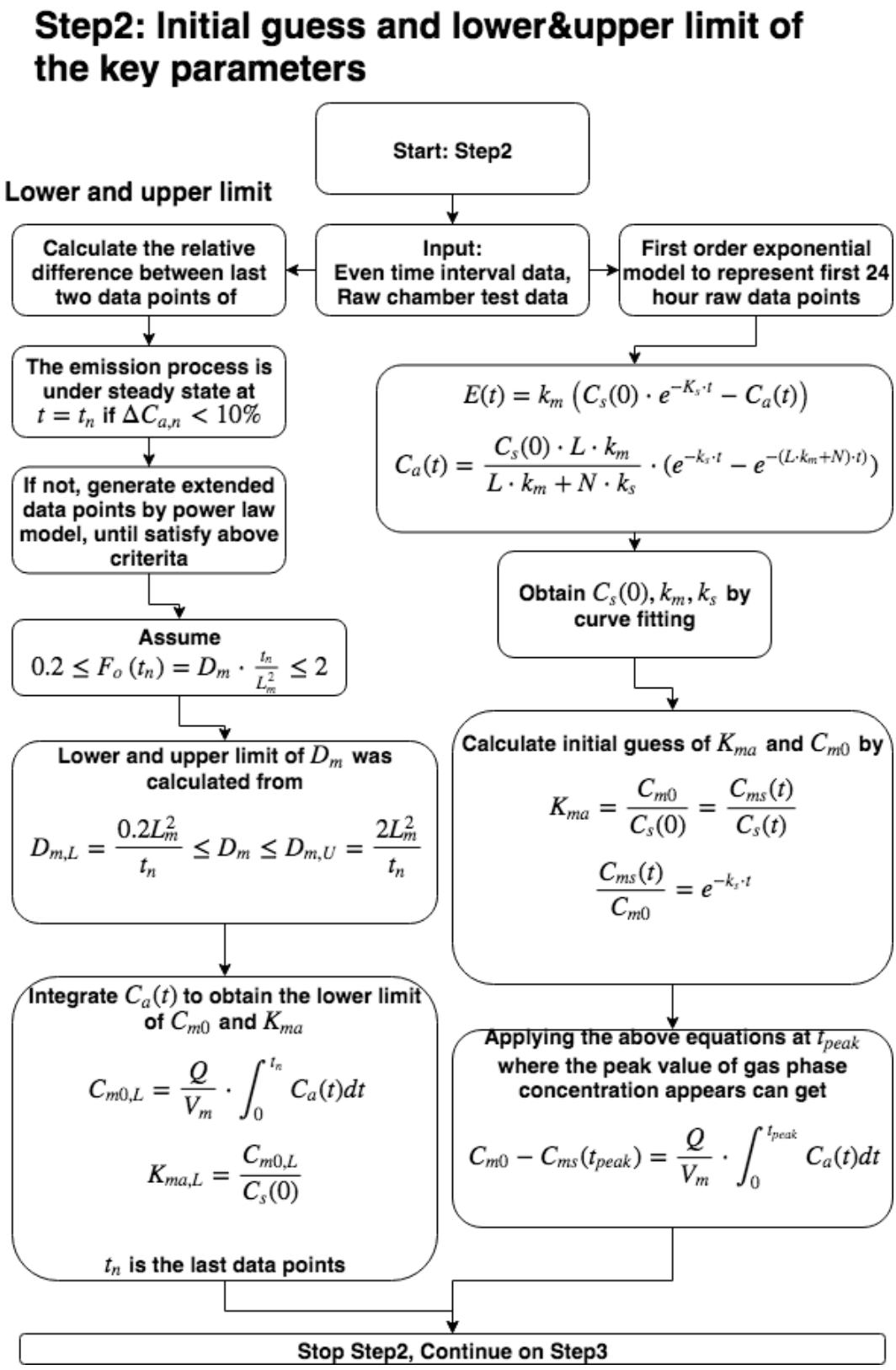

Figure 5-3 Step 2: Initial guesses and limitation of parameters

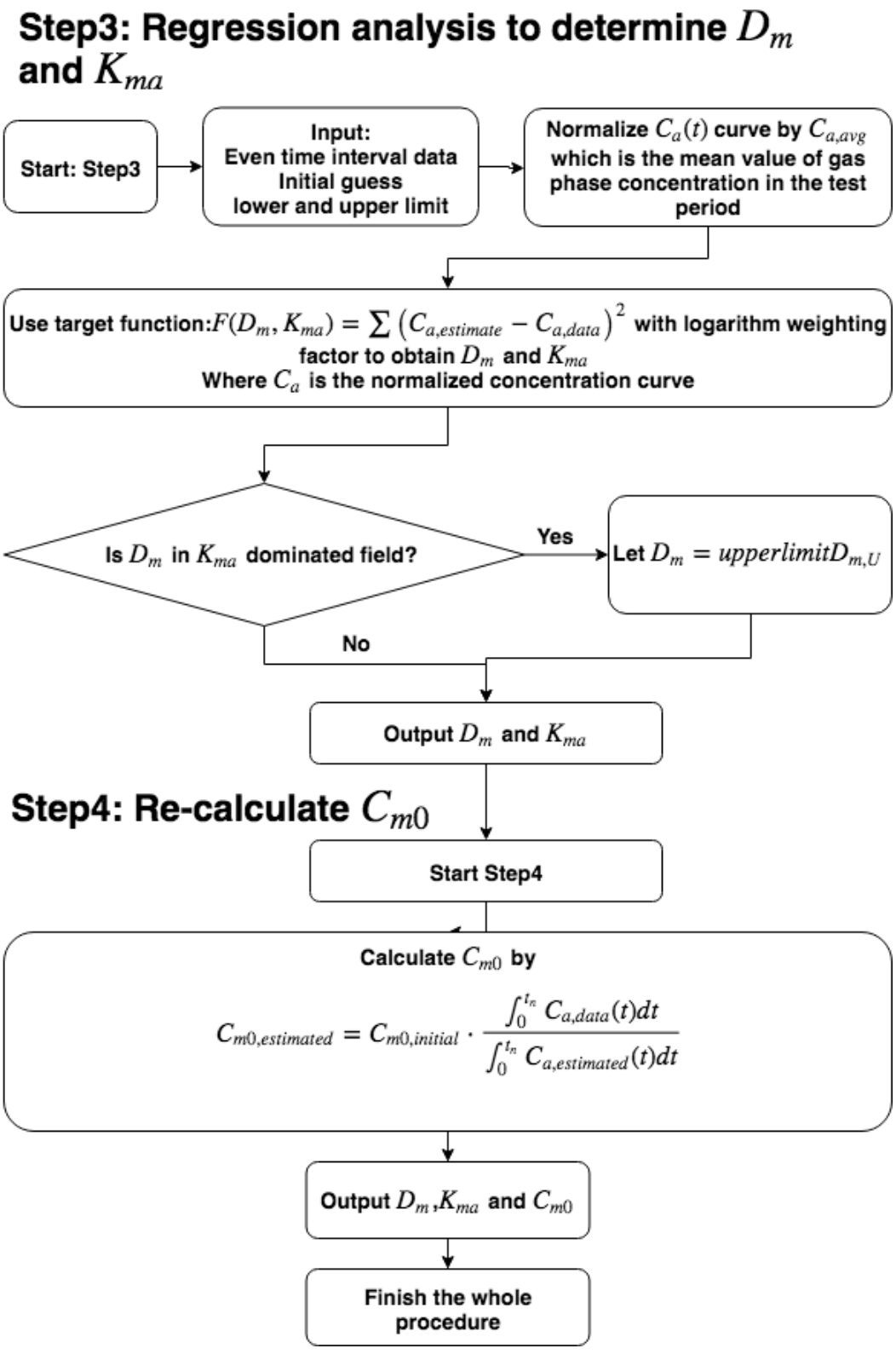

Figure 5-4 Step 3 and 4: Regression analysis and recalculation of C_{m0}

5.2.2 Application of the procedure

One material (particleboard ID: PB 6) was selected from the NRC database to illustrate the application of the procedure. Figure 5-5 shows the results of PB6 with the procedure implemented. The results show that all the regression analysis results represent the measured data in the test period very well. However, the concentration curve obtained with the model parameters that were estimated from 840 hours test data points were slight lower than the measured concentration in the initial emission period. This was because the procedure fits the evenly generated "sampling" data points from the power-law model which slightly underestimated the concentration curve in the initial emission period.

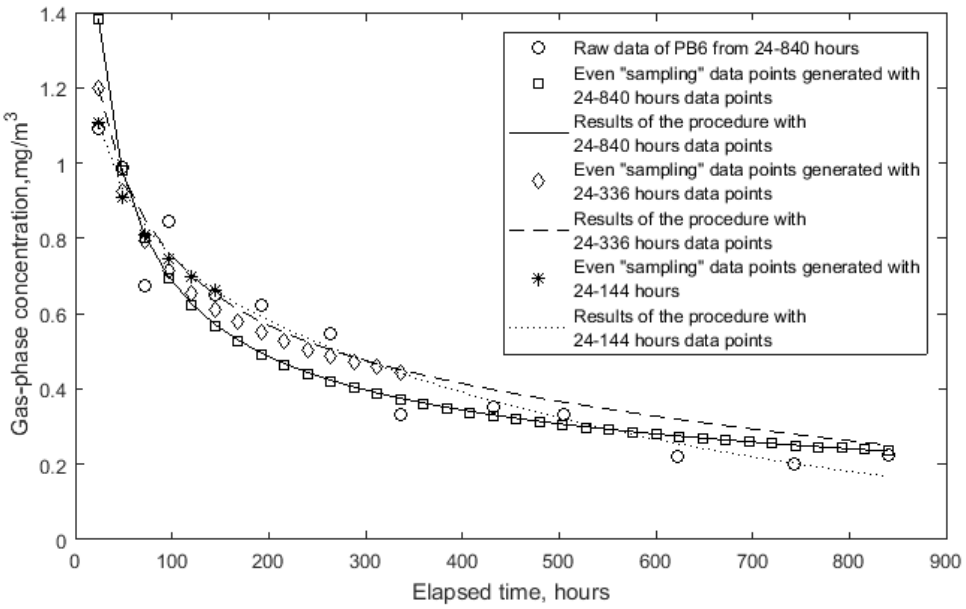

Figure 5-5 Measured data and regression analysis of PB6. (Estimated key parameters: (a) 144 hours: $D_m = 9.75 \times 10^{-11}$ m²/s, $K_{ma} = 8458$, $C_{m0} = 3.51\times10^4$ mg/m³; (b) 336 hours: $D_m = 4.18\times10^{-11}$ m²/s, $K_{ma} = 9134$, $C_{m0} = 5.49\times10^4$ mg/m³; (c) 840 hours: $D_m = 1.67\times10^{-11}$ m²/s, $K_{ma} = 2885$, $C_{m0} = 7.44\times10^4$ mg/m³.)

5.2.3 Conclusion

Based on the material emission test in the ventilated chamber and analytical solution of the diffusion model, a procedure has been developed to obtain key parameters (diffusion coefficient, partition coefficient, initial concentration, and convective mass transfer coefficient) for dry emitting materials. The procedure was suggested to be used in the validated region ($1\times10^{-13} < D_m < 1\times10^{-9}$ m²/s, $1000 < K_{ma} < 100{,}000$). Applying the procedure to literature cases, all the regression analysis had good convergence with residual less than 4%. When the procedure was applied to all the cases collected from literature, the error in reproducing the measured emission factor data was less than 10%. More discussions of the Approach 1 procedure are provided in the Appendix, which was published in the Building Simulation Journal as a contribution to Annex68 (Liu et al. 2020).

5.3 Approach 2: Empirical correlation and similarity method between VOCs and water vapor

In Section 3.2.3, we showed the molecular weight and vapor pressure were found to correlate well with the diffusion and partition coefficient, respectively when applied to the compounds with similar polarity (Eq.3-7 and 3-8). There was also a similarity theory-based approach in which D_m and K_{ma} may be estimated in theory based on the similarity between VOC and water vapor transport and storage in the porous media.

5.3.1 Diffusion coefficient and molecular weight

The correlation between D_m and molecular weight was well described by Eq.3-7 and verified by the measured results from literature. Figure 5-6 and Figure 5-7 are two examples that show the correlations of D_m and molecular weight for aromatic hydrocarbon and aldehyde in particleboard and gypsum board, respectively.

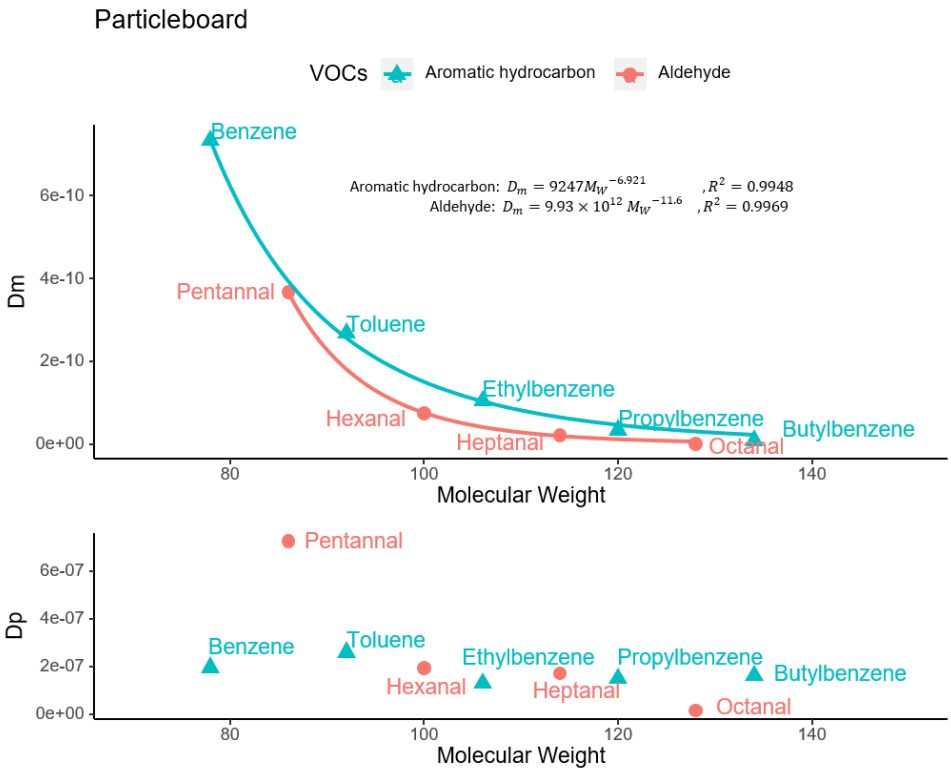

Figure 5-6 Diffusion coefficient vs. Molecular weight for particleboard: Top plot shows that the power law model is a good representation of the *Dm-MW* relationship; bottom plot shows a nearly constant *Dp* regardless of different VOCs except for Pentanal and Octanal, an indication that the pore diffusion is the primary transport mechanism for these VOCs. Data are from Bodalal et al., 1999

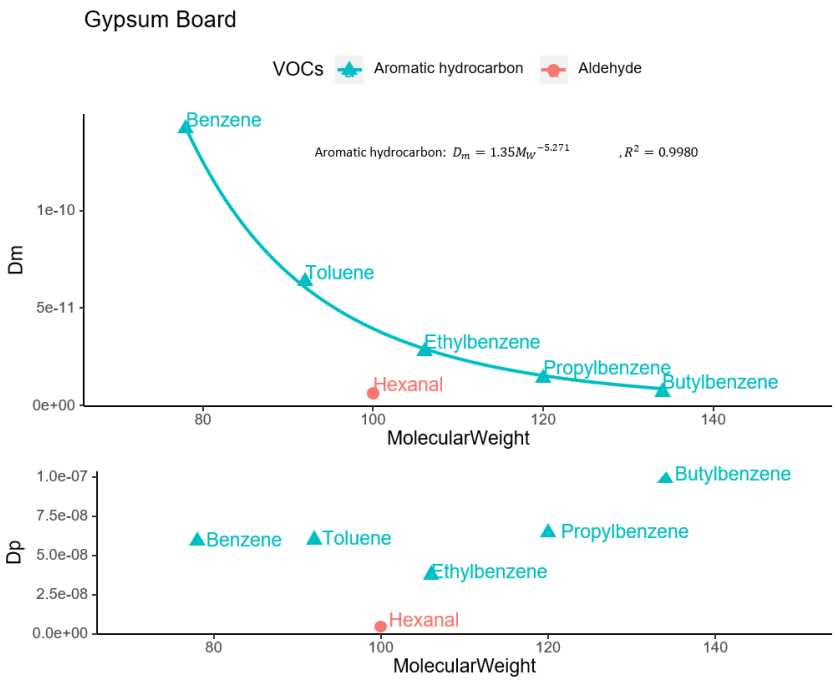

Figure 5-7 Diffusion coefficient vs. Molecular weight for gypsum board: Top plot shows that the power law model is a good representation of the D_m-MW relationship except for Hexanal; bottom plot show a nearly constant D_p regardless of different VOCs except for Hexanal and Butylbenzene, an indication that pore diffusion is the primary transport mechanism for these VOCs. Data are from Bodalal et al., 1999

The correlation of D_m and molecular weight was obtained by curve fitting, which has a high R-square value, over 0.98. The quality of the curve fitting indicates that a good correlation. Errors between measured data and estimated data is acceptable, which is due to the uncertainty of the insufficient data of the chamber test. The results prove the relation between D_m and molecular weight. The coefficients in Eq. 3-7 and 3-8 can be determined by the regression analysis. The plots also show that D_p had a weak dependence on the molecular weight for each material and the VOCs tested. This suggests that D_p and D_{air} (diffusion coefficient in free air) can be used to estimate the resistance factor of VOCs.

5.3.2 Partition coefficient and vapor pressure

Figure 5-8 and Figure 5-9show the correlations of K_{ma} and vapor pressure (Eq.3-8) for aromatic hydrocarbons and aldehydes in particleboard and gypsum board, respectively. The R-square value of the curve fitting is over 0.95, which also indicates a good correlation of the estimation.

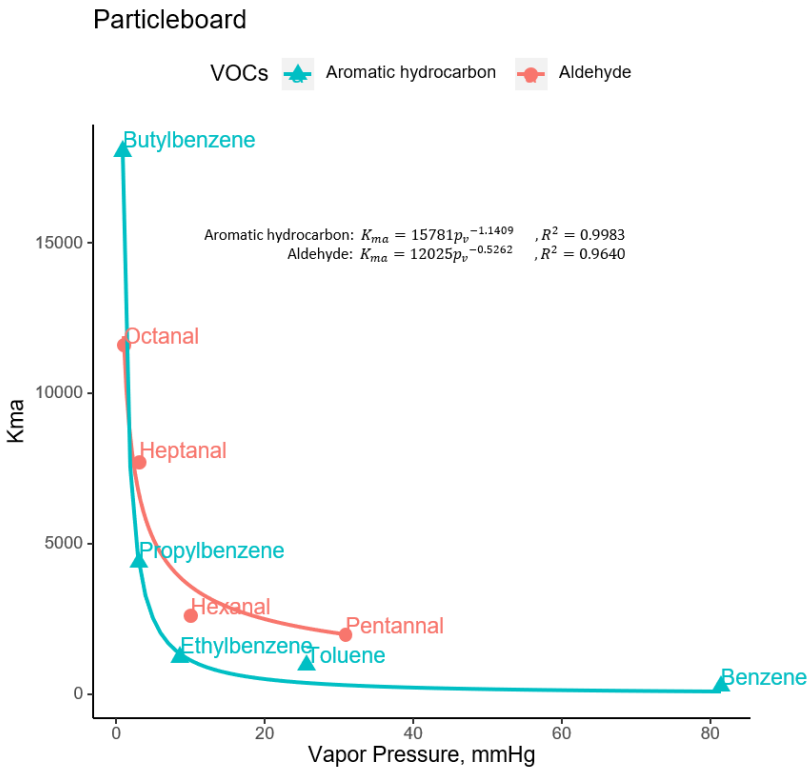

Figure 5-8 Partition coefficient vs. Vapor pressure for particleboard

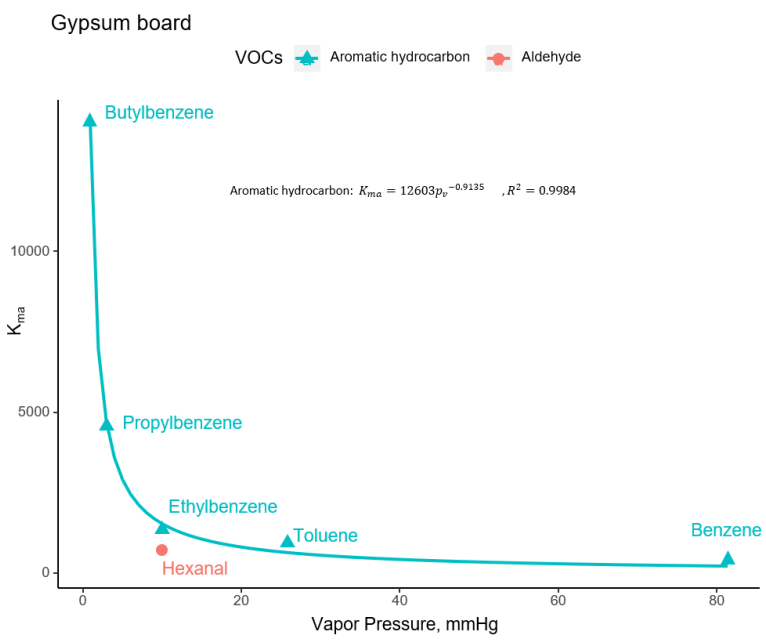

Figure 5-9 Partition coefficient vs. Vapor pressure for gypsum board

Based on the above two correlations, we can estimate D_m and K_{ma} when we have at least two measured data for this material. If the estimated data is in between the two measured data, the estimation is more accurate since the trend of D_m and K_{ma} change with molecular weight or vapor pressure is significant. If such measured data is not available for the specific material of interest, the estimation based on the similarity between water vapor and VOCs in porous media may be considered and used as a first approximation, as described below.

5.3.3 Similarity method

Xu (2011) developed the similarity method between VOC and water vapor transport in porous media. A similarity coefficient was defined as the ratio between the resistance factors for VOC transport and water vapor transport in porous media.

For the porous media, D_p can be calculated by

$$D_p = D_{air}\frac{\varepsilon}{\tau} = \frac{D_{air}}{\mu} \quad (5\text{-}5)$$

Where D_{air} is the diffusivity in free air in m^2/s; μ is a factor that accounts for both porosity and tortuosity of the material. The porosity ε and tortuosity τ were measured individually.

D_{air} can be calculated by

$$D_{air} = \frac{0.001T^{1.75}M_r^{0.5}}{P\left(V_A^{\frac{1}{3}}+V_B^{\frac{1}{3}}\right)^2} \quad (5\text{-}6)$$

$$M_r = (M_A + M_B)/(M_A M_B)$$

Where M_A was the molecular weight of dry air, g/mol; M_B was the molecular weight of VOC compound, g/mol; V_A was the molecular volume of dry air, mL/(g mol); V_B was the molecular volume of VOC compound, mL/(g mol); T was the temperature, K; and P was the pressure, atm.

The equations indicate that the heavier organic compounds in the same class has slightly lower diffusivity in free air that water vapor as illustrated in Figure 5-10.

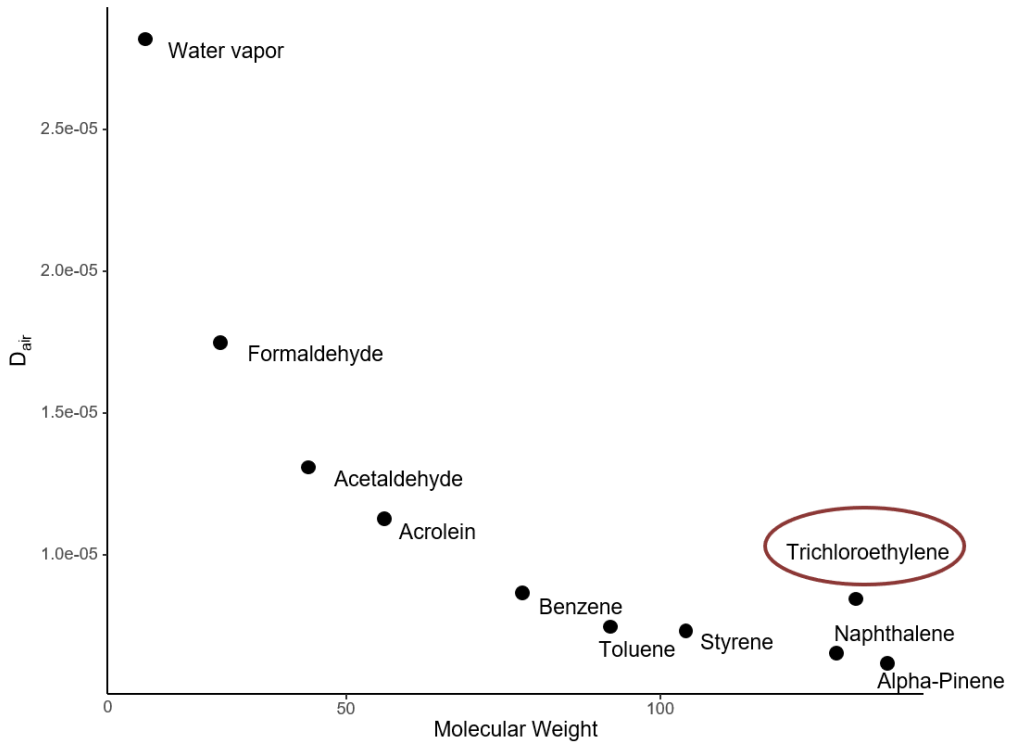

Figure 5-10 Air diffusivity of water vapor and target VOC compounds defined in Subtask 1 of IEA EBC Annex 68. The heavier compounds have lower diffusivity. Trichloroethylene is an outlier because the other VOC compound are aliphatic hydrocarbons, aromatic hydrocarbons or aldehyde.

The similarity coefficient (k_{VOC}) is defined by

$$\mathrm{k_{VOC}} = \frac{\mu_{\mathrm{VOC}}}{\mu_{\mathrm{vapor}}} \quad (5\text{-}7)$$

The water vapor transport properties of a large number of common building materials are well established in the database of Delphin/Champs-bes. μ_{vapor} was measured for all the materials in the database.

We use particleboard as an example to show the procedure that can be used to estimate D_p of an aromatic hydrocarbon compound by the similarity method.

- $D_{air,vapor}$ is calculated by Eq. 5-6 to be $2.82 \times 10^{-5} m^2/s$.
- μ_{vapor} is 30 in the Delphin6.0 database.
- $D_{p,vapor}$ is calculated by Eq. 5-5 to be $9.4 \times 10^{-7} m^2/s$.
- The resistance factor for VOCs can be assumed to be constant for the same type of compounds in the same material under the hygroscopic range where interaction with adsorbed water molecules may be negligible. The resistance factor of an aromatic hydrocarbon compound in particleboard is assumed to be 45 based on the mean value of the ratio of $D_{air,voc}$ to D_p in Figure 5-6 .
- The similarity coefficient can then be calculated by Eq. 5-7 as $k_{VOC} = 1.5$.
- $D_{p,VOC}$ can then be calculated by Eq. 5-5 and 5-6 for each compound.

The next step is the estimation of K_{ma}, which is also needed to calculate D_m. First, we can estimate K_{ma} of water vapor from moisture retention curve (included in Delphin/CHAMPS-BES database). Eq.5-8 shows the relationship between the *dMC/dRH* (from the moisture retention curve) and $K_{ma}=dC_m/dC_{air}$ for water vapor.

$$\frac{dMC}{dRH} = \frac{0.6219 * p_s \rho_a}{OEFF \times p_a \rho_w} \times \frac{d\frac{M_{water}}{V_m}}{d\frac{M_{water\ vapor}}{V_{air}}} = \frac{0.6219 * p_s \rho_a}{OEFF \times p_a \rho_w} K_{ma} \quad (5\text{-}8)$$

Where *MC* is the normalized volumetric moisture content, $\mathrm{m^3/m^3}$; 0.6219 is the constant coefficient representing the ratio of the molecular weight of water to the molecular weight of air; *OEFF* is the effective saturation moisture content which is a constant for each material representing the maximum moisture that can be stored in the material; p_s is saturated pressure of water vapor; p_a is the atmosphere pressure; ρ_a is the density of air; ρ_w is the density of liquid water. The last term shows the definition of K_{ma} for water vapor that is the ratio at equilibrium between the concentration of water in the material (comprising the pore air and solid matrix) and the concentration in the surrounding air. Based on Eq. 5-8 we can estimate K_{ma} by the slope (red line in Figure 5-11 and Figure 5-12) of the moisture retention curve under hygroscopic region. We suggest to use the data points between 0 and 20% RH to limit it to the mostly mono-layer vapor adsorption region with the assumption that sorption in the low vapor concentration region would be more applicable to the corresponding VOC sorption by the same material at low concentrations. The estimated K_{ma} of water vapor for particleboard and calcium silicate is 9368 and 896, respectively. The measured K_{ma} of water vapor for particleboard and calcium silicate is about 50% of the above estimated value. . Based on the sensitivity studies for approach 1, the error of the emission factor estimation would still be acceptable even if the estimated K_{ma} is doubled for this range of K_{ma}, as shown in Figure 5-13. The reason is the emission factor is dominated by the in-material diffusion process for the low K_{ma} case. On the other hand, the high K_{ma} case indicated abundant VOCs in the surface of material that the surface resistance is the dominating factor, and

only a thin layer of material participates in the emission process. The long-term emission process is also independent with the value of K_{ma} (Yang et al., 2001).

Given that K_{ma} and D_p are estimated, D_m can be calculated as $\frac{K_{ma}}{D_p}$.

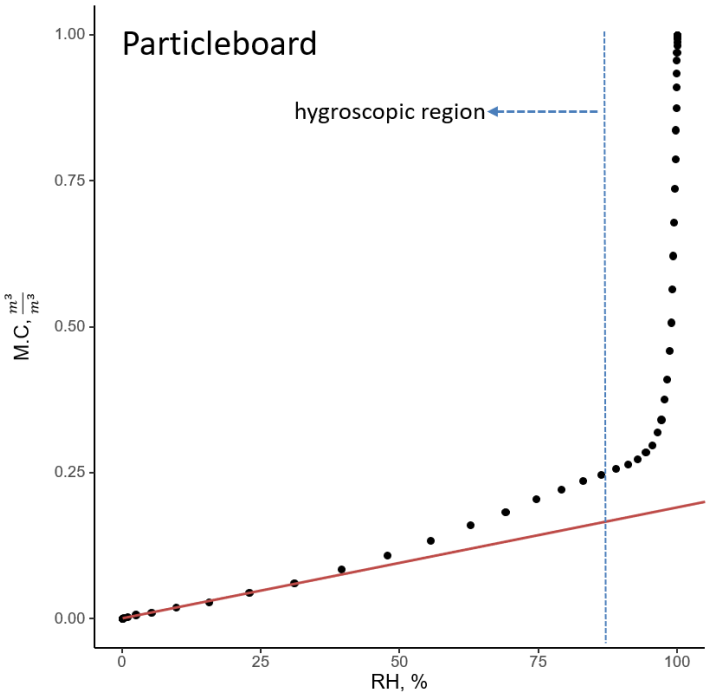

Figure 5-11 Moisture retention curve for particleboard. 0 -20% RH are used for estimating K_{ma} by the relation shown in Eq. 5-8.

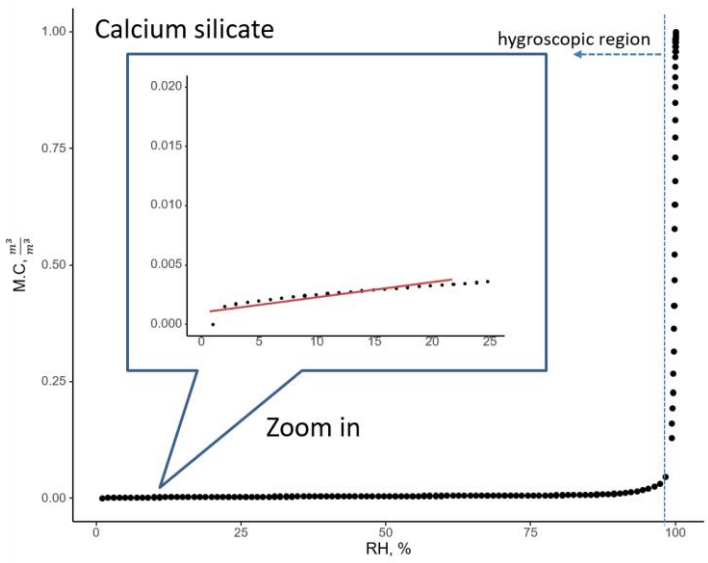

Figure 5-12 Moisture retention curve for calcium silicate. 0 -20% RH are used for estimating K_{ma} by the relation shown in Eq. 5-8.

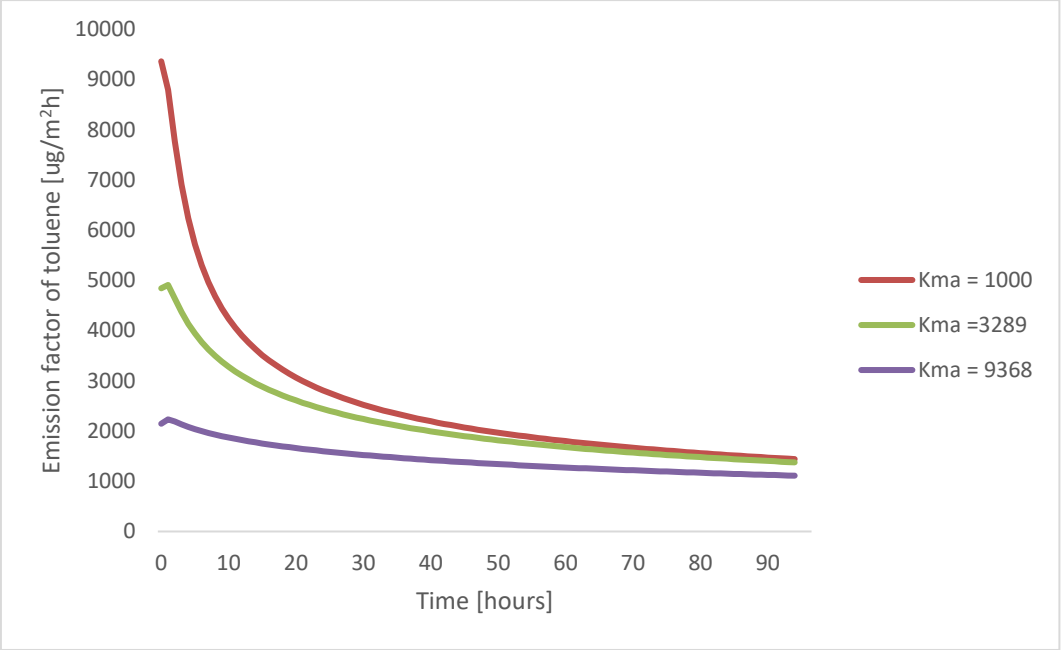

Figure 5-13 The influence of the partition coefficient on the resulting VOC emission factor

5.4 Results

Using the Approaches 1 and 2 above, we calculated the D_p, K_{ma}, and D_m for all the target VOCs (see the Appendix, Table 2). As an example, Figure 5-14 shows how the estimated D_p and D_m vary with the compounds ordered from low to high molecular weight for particleboard. Figure 5-15show how K_{ma} vary with the vapor pressure of the compounds for particleboard.

Figure 5-14 Diffusion coefficient [m²/s] distribution of target compounds

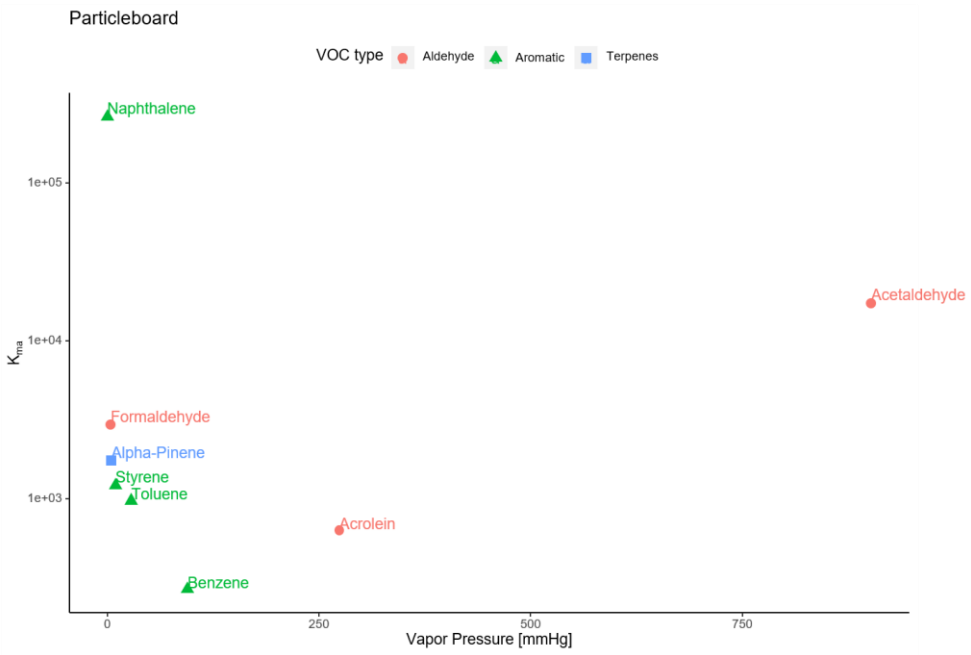

Figure 5-15 Partition coefficient distribution of target compounds

5.5 Conclusion

The good agreement between the estimated parameters and the measured data validates the effectiveness of the two approaches. The first approach provided a method to obtain the parameters of the diffusion model mathematically from the emission data of the well-established small chamber test. The second approach showed how the model parameters can be obtained empirically from correlation of the species properties and similarity with water vapor transport. Its adoption as a standard procedure for data analysis will result in a database of mechanistic model parameters for evaluating the impact of material emissions on indoor pollution load and IAQ. A data set of the model parameters for the materials used in the reference house and the target VOCs selected in IEA EBC Annex 68, Subtask 1 have been generated.

6 Conclusions and outlook

Indoor space air pollution loads depend on the emission rates of indoor source and rates of pollutant transport from outdoors much like the space cooling/heating loads that depend on external and internal heat gains/losses. Indoor sources include primary emissions from building materials and furnishing and occupant activities. Due to the large number of sources and pollutants and the effects of environmental conditions on the source emissions, determining the air pollution loads of an indoor space is arguably far more challenging than determining the space cooling/heating loads.

Limiting the scope to VOC emissions from building materials and furnishing, we have shown that a baseline space pollution load for a residential building can be determined by first defining a local reference building for the country or region of interest. The emission characteristics of the materials and furnishing used in the reference building can be obtained by standard small chamber testing in accordance with the well-established standard test methods. The emission test data can be used to determine the initial VOC concentrations and the material's diffusion and partition coefficients under standard test conditions (typically 23 ^{o}C and 50% RH) using the procedure developed in this study. A small database of such emission model parameters has been developed for the materials in a reference house based on data collected from the literature for a wide range of VOCs. The model parameters can be used in the mechanistic model to predict the emission rates of various building materials and their contributions to the indoor space air pollution loads for design.

Further it has been shown that the model parameters are significantly affected by temperature, but not significantly affected by relative humidity under typical 30-60% RH conditions. Air temperature affects the vapor pressure of the VOCs and hence affects the in-material diffusion and partition coefficients. An approach has been established to account for such effects in the pollutant load calculation model such as Delphin, which enables the prediction of the emission rates from building materials and furnishing beyond the standard test condition, and hence can be used to determine the material's contribution to the indoor pollution load during building operation.

Empirical correlations between the model parameters and the air temperature have also been obtained based on the experimental work presented. In particular, the dependence of the initial formaldehyde concentration on the air temperature indicates the pollutant release mechanism within the material need further study since a simple initial concentration parameter is not sufficient to account for the emission characteristics observed.

While the present study shows an approach and procedure to determine the indoor space pollution loads for VOCs emitted from building materials and furnishings, additional efforts are necessary for determining the indoor space pollution loads due to occupant activities, outdoor emission sources, for other type of pollutants such as SVOC, particles and biological contaminants, and for pollutants due to indoor air and surface chemistry.

7 Acknowledgments

The authors would like to thank all Annex 68 participants for sharing their time and experience, providing data and reviewing the present document. We would like to acknowledge the National Science Foundation of China for the financial support (Grant No. 51578278 and BK20170646).

8 References

Andersen, Ib, G. R. Lundqvist, and L. Mølhave. 1975. "Indoor Air Pollution Due to Chipboard Used as a Construction Material." Atmospheric Environment 9: 1121–27. https://doi.org/10.1016/0004-6981(75)90188-2.

ANSI/BIFMA M7.1 Standard Method For Testing VOC Emissions From Office Furniture Systems, Components and Seating. BIFMA® International., 2680 Horizon Drive Suite A1, Grand Rapids MI 49546.

ASHRAE Standards 62.2-2010 Ventilation and Acceptable Indoor Air Quality in Low-Rise Residential Bulidings American Society of Heating, Refrigerating, and Air-Conditioning Engineers, Inc.: Atlanta, GA.

ASHRAE Standards 90.2-2007 Energy-Efficient Design of Low-Rise Residential Buildings, American Society of Heating, Refrigerating, and Air-Conditioning Engineers, Inc.: Atlanta, GA.

ASTM 5116-1997. Standard Guide for Small-Scale Environmental Chamber Determinations of Organic Emissions from Indoor Materials/Products.

ASTM 6670-2001. Standard Pracice for Full-Scale Chamber Determination of Volatile Organic Emissions from Indoor Materials/Products.

ASTM. 2008. Standard Test Method for Determining Formaldehyde Concentrations in Air from Wood Products Using a Small-Scale Chamber. Vol. 02. https://doi.org/10.1520/D6007-02R08.Copyright.

Blondeau, P, a L Tiffonnet, a Damian, O Amiri, and J L Molina. 2003. "Assessment of Contaminant Diffusivities in Building Materials from Porosimetry Tests." Indoor Air 13 (3): 310–18. https://doi.org/10.1034/j.1600-0668.2003.00208.x.

Bodalal, A., Zhang, J.S. & Plett, E.G. 1999, A method for measuring internal diffusion and equilibrium partition coefficients of volatile organic compounds for building materials, Building and Environment, vol. 35, no. 2, pp. 101-110. Bodalal, A.,1999, A Fundamental Study of Volatile Organic Emissions from Building Materials. Ph.D. Thesis, Carleton University. Ottawa, ONT. Canada.

Brown, K. 2001. "Air Toxics in a New Australian over an 8-Month Period Dwelling" 3190: 160–66. https://doi.org/10.1177/1420326X0101000307.

Brown, Stephen K. 2001. "Air Toxics in a New Australian Dwelling over an 8-Month Period." Indoor and Built Environment 10 (3–4): 160–66. https://doi.org/10.1159/000049231.

California Department of Public Health (2017), Standard Method for The Testing and Evaluation of Volatile Organic Chemical Emissions from Indoor Sources Using Environmental Chambers Version 1.2

Christiansson, J., Yu T.W. and Neretnieks, I.,1993. Emission of VOCs from PVC-floorings - models for predicting the time dependent emission rates and resulting concentrations in the indoor air. Indoor Air '93, Proceedings of the 6th International Conference on Indoor Air Quality and Climate, Vol. 2, Helsinki, Finland, July 4-8, pp 389-394.

Cox, S.S., Little, J.C. & Hodgson, A.T. 2002, Predicting the Emission Rate of Volatile Organic Compounds from Vinyl Flooring, Environmental Science & Technology, vol. 36, no. 4, pp. 709-714. Crump, Derrick

R., Richard W. Squire, and Chuck W.F. Yu. 1997. “Sources and Concentrations of Formaldehyde and Other Volatile Organic Compounds in the Indoor Air of Four Newly Built Unoccupied Test Houses.” Indoor and Built Environment 6 (1): 45–55. https://doi.org/10.1177/1420326X9700600106.

Deng, B., Kim, C.N., 2004. An analytical model for VOCs emission from dry building materials. Atmospheric Environment 38, 1173–1180.

Deng, Q., Yang, X. & Zhang, J. 2009, Study on a new correlation between diffusion coefficient and temperature in porous building materials, Atmospheric Environment, vol. 43, no. 12, pp. 2080-2083.

Fabi, Valentina, Rune Vinther Andersen, Stefano P. Corgnati, and Bjarne W. Olesen. 2013. “A Methodology for Modelling Energy-Related Human Behaviour: Application to Window Opening Behaviour in Residential Buildings.” Building Simulation 6 (4): 415–27. https://doi.org/10.1007/s12273-013-0119-6.

Farajollahi, Yashar, Zhi Chen, and Fariborz Haghighat. 2009. “An Experimental Study for Examining the Effects of Environmental Conditions on Diffusion Coefficient of VOCs in Building Materials.” Clean - Soil, Air, Water 37 (6): 436–43. https://doi.org/10.1002/clen.200900053.

Frihart, C. R., J. M. Wescott, T. L. Chaffee, and K. M. Gonner. 2012. “Formaldehyde Emissions from Urea-Formaldehyde and No-Added_Formaldehyde-Bonded Particleboard as Influenced by Temperature and Relative Humidity.” Forest Products Journal 62 (7/8): 551–58. https://doi.org/10.13073/FPJ-D-12-00087.1.

Frihart, Charles R., James M. Wescott, Timothy L. Chaffee, and Kyle M. Gonner. 2012. “Formaldehyde Emissions from Urea-Formaldehyde– and No-Added-Formaldehyde–Bonded Particleboard as Influenced by Temperature and Relative Humidity.” Forest Products Journal 62 (7): 551–58. https://doi.org/10.13073/fpj-d-12-00087.1.

García, E., de Pablos, A., Bengoechea, M.A., Guaita, L., Osendi, M.I. & Miranzo, P. 2011, "Thermal conductivity studies on ceramic floor tiles", Ceramics International, vol. 37, no. 1, pp. 369-375.

GB/T18204.26-2000. n.d. “Methods for Determination of Formaldehyde in Air of Public Places. Beijing.Pdf.”

Haghighat, F., Huang, H. & Lee, C. 2005, Modeling Approaches for Indoor Air VOC Emissions from Dry Building Materials-A Review, ASHRAE Transactions, vol. 111, pp. 635. Hamami, A. A., Ph Turcry, and A. Aït-Mokhtar. 2012. “Influence of Mix Proportions on Microstructure and Gas Permeability of Cement Pastes and Mortars.” Cement and Concrete Research 42 (2): 490–498. https://doi.org/10.1016/j.cemconres.2011.11.019.

He, G., Yang, X. & Shaw, C.Y. 2005, Material Emission Parameters Obtained Through Regression, Indoor and Built Environment, vol. 14, no. 1, pp. 59-68.

Hooff, T. Van, and B. Blocken. 2013. “CFD Evaluation of Natural Ventilation of Indoor Environments by the Concentration Decay Method: CO2gas Dispersion from a Semi-Enclosed Stadium.” Building and Environment 61: 1–17. https://doi.org/10.1016/j.buildenv.2012.11.021.

Huang, H., Haghighat, F. & Blondeau, P. 2006, Volatile organic compound (VOC) adsorption on material: influence of gas phase concentration, relative humidity and VOC type, Indoor Air, vol. 16, no. 3, pp. 236-247.

Huang, H. & Haghighat, F. 2002, Modelling of volatile organic compounds emission from dry building materials, Building and Environment, vol. 37, no. 12, pp. 1349-1360.

Huang, Shaodan, Jianyin Xiong, and Yinping Zhang. 2015. "Impact of Temperature on the Ratio of Initial Emittable Concentration to Total Concentration for Formaldehyde in Building Materials: Theoretical Correlation and Validation." Environmental Science and Technology 49 (3): 1537–44. https://doi.org/10.1021/es5051875.

Huang, S., Xiong, J. & Zhang, Y. 2013, A rapid and accurate method, ventilated chamber C-history method, of measuring the emission characteristic parameters of formaldehyde/VOCs in building materials, Journal of Hazardous Materials, vol. 261, pp. 542-549

ISO 16000:2011(E), 2011. Indoor air – Part 6: Determination of volatile organic compounds in indoor and test chamber air by active sampling on Tenax TA sorbent, thermal desorption and gas chromatography using MS or MS-FID. Standard. International Organization for Standardization. Geneva, CH

Jianyin Xiong Shaodan Huang, Yinping Zhang, Wenjuan Wei. 2013. "Association between the Emission Rate and Temperature for Chemical Pollutants in Building Materials." Environmental Science & Technology 47 (15): 8540–47. https://doi.org/10.1021/es401173d.

Kim, Sumin, Jin A. Kim, Hyun Joong Kim, and Shin Do Kim. 2006. "Determination of Formaldehyde and TVOC Emission Factor from Wood-Based Composites by Small Chamber Method." Polymer Testing 25 (5): 605–614. https://doi.org/10.1016/j.polymertesting.2006.04.008.

Korjenic, Azra, Helene Teblick, and Thomas Bednar. 2010. "Increasing the Indoor Humidity Levels in Buildings with Ventilation Systems: Simulation Aided Design in Case of Passive Houses." Building Simulation 3 (4): 295–310. https://doi.org/10.1007/s12273-010-0015-2.

Langmuir, Irving. 1918. "The Adsorption of Gases on Plane Surfaces of Glass, Mica and Platinum." Journal of the American Chemical Society 40: 1361–1403. https://doi.org/10.1021/ja02242a004.

Laustsen J. 2008. Energy efficiency requirements in building codes, energy efficiency policies for new buildings. IEA information paper, OECD/IEA, March.

Lee, Chang Seo. 2003. "A Theoretical Study on VOC Source and Sink Behavior of Porous Building Materials." Ph.D. Dissertation, Concordia University, Montreal., Quebec, Canada.

Li, H. 2007, A modeling and experimental investigation of coupled heat, air, moisture and pollutants transport in building envelope systems. Ph.D. dissertation. Syracuse University Library. Syracuse, NY.

Liang, Weihui, Shen Yang, and Xudong Yang. 2015. "Long-Term Formaldehyde Emissions from Medium-Density Fiberboard in a Full-Scale Experimental Room: Emission Characteristics and the Effects of Temperature and Humidity." Environmental Science and Technology 49 (17): 10349–56.

Lin, Chi Chi, Kuo Pin Yu, Ping Zhao, and Grace Whei-May Lee. 2009. "Evaluation of Impact Factors on VOC Emissions and Concentrations from Wooden Flooring Based on Chamber Tests." Building and Environment 44: 525–533. https://doi.org/10.1016/j.buildenv.2008.04.015.

Little, J.C., Hodgson, A.T. and Gadgil, A.J., 1994. Modeling emissions of volatile organic compounds from new carpets. Atmospheric Environment, Vol. 28, pp. 227-234.

Liu, Yanfeng, Xiaojun Zhou, Dengjia Wang, Cong Song, and Jiaping Liu. 2015. "A Prediction Model of VOC Partition Coefficient in Porous Building Materials Based on Adsorption Potential Theory." Building and Environment 93 (2): 221–233. https://doi.org/10.1016/j.buildenv.2015.06.025.

Liu, Z., Nicolai, A., Abadie, M., Qin, M., Grunewald, J. & Zhang, J. 2020, "Development of a procedure for estimating the parameters of mechanistic VOC emission source models from chamber testing data", *Building Simulation*, .

Liu, Z., Zhang, J., Qin, M., Nicolai, A., and Abadie, M. 2018. Development of a procedure for estimating the parameters of mechanistic emission source models from chamber testing data. Proceedings of IBPC 2018 – 7th International Building Physics Conference, Sept. 23-26, Syracuse, New York, USA.

Lyman, W. J., Reehl, W. F., & Rosenblatt, D. H. (1990). Handbook of chemical property estimation methods: environmental behavior of organic compounds. Washington, DC, American Chemical Society.

Myers, G. E., and M Nagaoka. 1981. "Formaldehyde Emission: Methods of Measurement and Effects of Some Particleboard Variables." Journal of Wood Science 13 (3): 140–50.

Myers, George E. 1985. "The Effects of Temperature and Humidity on Formaldehyde Emission from UF-Bonded Boards: A Literature Critique." Forest Products Journal 35 (9): 20–31. https://doi.org/10.1002/path.4011.

Nazaroff, William W., and Charles J. Weschler. 2004. "Cleaning Products and Air Fresheners: Exposure to Primary and Secondary Air Pollutants." Atmospheric Environment. https://doi.org/10.1016/j.atmosenv.2004.02.040.

NorthPass. 2012. Very Low-Energy House Concepts in North European Countries. Intelligent Energy Report, 34p.

Nørgaard, A. W., V. Kofoed-Sørensen, C. Mandin, G. Ventura, R. Mabilia, E. Perreca, A. Cattaneo, et al. 2014. "Ozone-Initiated Terpene Reaction Products in Five European Offices: Replacement of a Floor Cleaning Agent." Environmental Science and Technology 48 (22): 13331–39. https://doi.org/10.1021/es504106j.

Parthasarathy, Srinandini, Randy L Maddalena, Marion L Russell, and Michael G Apte. 2011. "Effect of Temperature and Humidity on Formaldehyde Emissions in Temporary Housing Units." Journal of the Air & Waste Management Association (1995) 61 (6): 689–95. https://doi.org/10.3155/1047-3289.61.6.689.

Petitjean, Mélanie, György Hantai, Coline Chauvin, Philippe Mirabel, Stéphane Le Calvé, Paul N.M. Hoang, Sylvain Picaud, and Pál Jedlovszky. 2010. "Adsorption of Benzaldehyde at the Surface of Ice, Studied by Experimental Method and Computer Simulation." Langmuir 26 (12): 9596–9606. https://doi.org/10.1021/la100169h.

Qian, K., Zhang, Y., Little, J.C. & Wang, X. 2007, Dimensionless correlations to predict VOC emissions from dry building materials, Atmospheric Environment, vol. 41, no. 2, pp. 352-359.

Saeki, K, K Obayashi, J Iwamoto, N Tone, N Okamoto, K Tomioka, and N Kurumatani. 2014. "The Relationship between Indoor, Outdoor and Ambient Temperatures and Morning BP Surges from Inter-Seasonally Repeated Measurements." Journal of Human Hypertension 28 (8): 482–88. https://doi.org/10.1038/jhh.2014.4.

Salthammer, T., and F. Fuhrmann. 2007. "Photocatalytic Surface Reactions on Indoor Wall Paint." Environmental Science and Technology 41 (18): 6573–78. https://doi.org/10.1021/es070057m.

Sidheswaran, Meera, Wenhao Chen, Agatha Chang, Robert Miller, Sebastian Cohn, Douglas Sullivan, William J. Fisk, Kazukiyo Kumagai, and Hugo Destaillats. 2013. "Formaldehyde Emissions from Ventilation Filters under Different Relative Humidity Conditions." Environmental Science and Technology 47 (10): 5336–43. https://doi.org/10.1021/es400290p.

Smith, J.F., Gao, Z., Zhang, J.S. & Guo, B. 2009, "A New Experimental Method for the Determination of Emittable Initial VOC Concentrations in Building Materials and Sorption Isotherms for IVOCs", CLEAN – Soil, Air, Water, vol. 37, no. 6, pp. 454-458.Soutullo, S., R. Enríquez, M. J. Jiménez, and M. R. Heras. 2014. "Thermal Comfort Evaluation in a Mechanically Ventilated Office Building Located in a Continental Climate." Energy and Buildings 81: 424–29. https://doi.org/10.1016/j.enbuild.2014.06.049.

Sparks,L.E., Tichenor,B.A., Chang, J.C.S. and Guo, Z. 1996. Gas-phase mass transfer model for predicting volatile organic compound (VOC) emission rates from indoor pollutant sources. Indoor Air, 6:31-40.

Sun, Song, Jianjun Ding, Jun Bao, Chen Gao, Zeming Qi, and Chengxiang Li. 2010. "Photocatalytic Oxidation of Gaseous Formaldehyde on TiO2: An in Situ DRIFTS Study." Catalysis Letters 137: 239–246. https://doi.org/10.1007/s10562-010-0358-4.

Suzuki, Masaki, Hiroshi Akitsu, Kohta Miyamoto, Shin ichiro Tohmura, and Akio Inoue. 2014. "Effects of Time, Temperature, and Humidity on Acetaldehyde Emission from Wood-Based Materials." Journal of Wood Science 60 (3): 207–14. https://doi.org/10.1007/s10086-014-1397-z.

Thullner K. 2010. Low-energy buildings in Europe - Standards, criteria and consequences: a study of nine European countries. Report, ISBN 978-91-85147-42-7, 165p.

Trabelsi, A., R. Belarbi, P. Turcry, and A. Aït-Mokhtar. 2011. "Water Vapour Desorption Variability of in Situ Concrete and Effects on Drying Simulations." Magazine of Concrete Research 63 (5): 333–342. https://doi.org/10.1680/macr.9.00161.

Wei, Wenjuan, Cynthia Howard-Reed, Andrew Persily, and Yinping Zhang. 2013. "Standard Formaldehyde Source for Chamber Testing of Material Emissions: Model Development, Experimental Evaluation, and Impacts of Environmental Factors." Environmental Science and Technology 47 (14): 7848–7854. https://doi.org/10.1021/es400721j.

Wiglusz, Renata, Elzbieta Sitko, Grazyna Nikel, Irena Jarnuszkiewicz, and Barbara Igielska. 2002. "The Effect of Temperature on the Emission of Formaldehyde and Volatile Organic Compounds (VOCs) from Laminate Flooring - Case Study." Building and Environment 37 (1): 41–44. https://doi.org/10.1016/S0360-1323(00)00091-3.

White, F., 1988. Heat and Mass Transfer (Series in Mechanical Engineering), Addison-Wesley.

Wilson, E., Engebrecht-Metzger, C., Horowitz, S., Hendron, R., . 2014 Building America House Simulation Protocols doi:10.2172/1126820.

Wolkoff, P., P. A. Clausen, P. A. Nielsen, and L. Mølhave. 1991. "The Danish Twin Apartment Study; Part I: Formaldehyde and Long-Term VOC Measurements." Indoor Air 1 (4): 478–90. https://doi.org/10.1111/j.1600-0668.1991.00012.x.

Xiong, J. & Zhang, Y. 2010, Impact of temperature on the initial emittable concentration of formaldehyde in building materials: experimental observation, Indoor Air, vol. 20, no. 6, pp. 523-529.

Xu, J. & Zhang, J.S. 2011, An experimental study of relative humidity effect on VOCs' effective diffusion coefficient and partition coefficient in a porous medium, Building and Environment, vol. 46, no. 9, pp. 1785-1796.

Xu, J., Zhang, J., Grunewald, J., Zhao, J., Plagge, R., Ouali, A. & Allard, F. 2009, A Study on the Similarities between Water Vapor and VOC Diffusion in Porous Media by a Dual Chamber Method, CLEAN – Soil, Air, Water, vol. 37, no. 6, pp. 444-453.

Yang, M., Zhang, J.S., Li, H., Dang, T.Q. & Gao, X.F. 2005, "Determination of Building Materials' Transport Properties for Modeling VOC Emissions", ASHRAE Transactions, vol. 111, pp. 88.

Yang, X., Chen, Q., Zeng, J., J.S. Zhang, and C.Y. Shaw. 2001. A mass transfer model for simulating volatile organic compound emissions from 'wet' coating materials applied to absorptive substrates, International Journal of Heat and Mass Transfer. 44(9), pp1803-1815.

Yang, X., Chen, Q., Zhang, J.S., Magee, R., Zeng, J. & Shaw, C.Y. 2001, Numerical simulation of VOC emissions from dry materials, Building and Environment, vol. 36, no. 10, pp. 1099-1107.Yang, X.,1999. Study of building material emissions and indoor air quality, Ph.D. Thesis, Massachusetts Institute of Technology, Cambridge, Massachusetts.

Ye, W., Little, J.C., Won, D. & Zhang, X. 2014, "Screening-level estimates of indoor exposure to volatile organic compounds emitted from building materials", Building and Environment, vol. 75, pp. 58-66.

Yu, Kuo Pin, Whei May Grace Lee, and Guan Yi Lin. 2015. "Removal of Low-Concentration Formaldehyde by a Fiber Optic Illuminated Honeycomb Monolith Photocatalytic Reactor." Aerosol and Air Quality Research 15 (3): 1008–1026. https://doi.org/10.4209/aaqr.2014.09.0202.

Zhang, J., Zhang, J.S., Chen, Q., and Yang, X. 2002b. A critical review on VOC sorption models. Transactions of ASHRAE, Vol. 108(1), pp162-174.

Zhang, J.S., Zhu, J.P., Shaw, C.Y., Zeng, J., Plett, E.G., Bodalal, A., Chen, Q., Yang, X., 1999. Development of Standard Small Chamber Test Methods

Zhang, J., Zhang, J. & Chen, Q. 2002, Effects of environmental conditions on the VOC sorption by building materials--part 1: Experimental results, ASHRAE Transactions, vol. 108, pp. 273

Zhang, J.; J.S. Zhang; and Q. Chen. 2003. Effects of environmental conditions on the VOC sorption by building materials – Part II: Model evaluations. Transactions of ASHRAE. 109(1), pp.

Zhang, Y., Luo, X., Wang, X., Qian, K. & Zhao, R. 2007, Influence of temperature on formaldehyde emission parameters of dry building materials, Atmospheric Environment, vol. 41, no. 15, pp. 3203-3216

Zhang,J.S., Yang, M., Li, H., and Salonvaara, H.M.. 2004. Toward a Model-Based Test Methodology for Evaluating VOC Emissions from Building Materials and Indoor Products. Proceedings of ASTM Conference on Indoor Emissions Testing—Methods and Interpretation. October 4-5, Washington, DC.

Zhang J.S., Zhu J.P., Shaw C.Y., Plett E., Bodalal A., Chen Q. and Yang X. 1999 Models for Predicting Volatile Organic Compound (VOC) Emissions from Building Materials CMEIAQ Report 3.1, IRC/NRC (Ottawa, Canada)

Zhou, X., Liu, J. & Liu, Y. 2018, Alternately airtight/ventilated emission method: A universal experimental method for determining the VOC emission characteristic parameters of building materials, Building and Environment, vol. 130, pp. 179-189.

9 Appendix

Table A-1 Estimation of saturated VOC vapor pressure and saturated density at 293.15K with Eq. 3-10

			MW	Vapor pressure calculation coefficient				temperature range, K		$p_{voc,sat}$	$\rho_{g,sat}^{m_{voc}}$
Cas. No.	Molecular Formula	Name	(g/mol)	A	B	C	D	from	to	kPa	kg/m^3
71-41-0	C5H12O	1-pentanol	88.15	-19.38194	-12196.4	149.3463	9.39571E-06	195.56	588.00	0.2115	0.0076
75-07-0	C2H4O	Acetaldehyde	44.05	-18.27131	-7241.251	130.8048	2.63363E-05	150.15	461.00	96.834	1.7501
64-19-7	CH3COOH	Acetic Acid	60.05	-7.798528	-7029.721	68.22937	5.931E-06	289.81	592.71	1.5811	0.039
71-43-2	C6H6	Benzene	78.11	-8.433613	-6281.04	71.10718	6.19841E-06	278.68	562.16	10.025	0.3213
104-51-8	C10H14	n-Butyl-benzene	134.22	-14.25732	-10104.4	112.4329	7.81134E-06	185.30	660.55	0.0948	0.0052
110-82-7	C6H12	Cyclohexane	84.16	-9.200978	-6354.898	75.65058	7.37481E-06	279.69	553.54	10.366	0.3579
124-18-5	C10H22	Decane	142.3	-7.768817	-8163.335	69.76469	2.62033E-06	243.49	618.45	0.1368	0.008
112-40-3	C12H26	Dodecane	170.3	-13.98384	-11200.45	112.7229	5.78857E-06	263.57	658.20	0.012	0.0008
100-41-4	C8H10	Ethylbenzene	106.2	-9.553983	-7638.082	79.79371	5.65318E-06	178.15	617.17	0.9523	0.0415
50-00-0	CH2O	Formaldehyde	30.03	-7.881614	-4425.491	64.846	1.30872E-05	164.15	408.00	446.47	5.5011
111-71-7	C7H14O	Heptanal	114.19	-14.45804	-9973.079	114.3643	7.0694E-06	230.15	603.00	0.3072	0.0144
142-82-5	C7H16	Heptane	100.21	-14.12388	-8030.07	108.1461	1.20486E-05	182.56	540.26	4.7391	0.1949
66-25-1	C6H12O	Hexanal	100.16	-10.6744	-7962.359	87.30592	7.04921E-06	217.15	579.00	1.119	0.046
71-36-3	C4H10O	n-Butanol	74.12	-9.882614	-9127.496	86.72214	1.42848E-06	183.85	563.00	0.6498	0.0198
111-84-2	C9H20	Nonane	128.2	-8.327399	-7739.415	72.54661	3.89483E-06	219.63	595.65	0.4383	0.0231
629-62-9	C15H32	n-Pentadecane	212.42	-24.79227	-16463.11	187.8062	1.09741E-05	283.10	706.80	0.0003	2E-05
629-59-4	C14H30	n-Tetradecane	198.39	-24.98538	-15806.55	187.8225	1.21628E-05	279.01	692.40	0.0009	8E-05
124-13-0	C8H16O	Octanal	128.22	-37.3436	-16088.37	262.5051	2.99392E-05	246.00	621.00	0.1437	0.0076
111-65-9	C8H18	Octane	114.23	-7.37874	-6981.936	65.77825	3.38092E-06	216.38	568.83	1.3987	0.0656
110-62-3	C5H10O	Pentanal	86.1	-13.24588	-8057.739	103.0526	1.08453E-05	182.00	554.00	3.498	0.1236
108-95-2	C6H5OH	Phenol	94.11	-11.04001	-10003.05	93.27452	4.31995E-06	314.06	694.25	0.0411	0.0016
79-09-4	C3H6O2	Propanoic acid	74.08	-8.903315	-8375.112	77.77671	4.15966E-06	252.45	604.00	0.3634	0.011
103-65-1	C9H12	Propyl-benzene	120.19	-10.94494	-8512.487	89.57939	6.16532E-06	173.67	638.38	0.3317	0.0164
108-88-3	C7H8	Toluene	92.14	-8.79548	-6918.798	74.1358	5.75491E-06	178.18	591.79	2.8992	0.1096
1120-21-4	C11H24	Undecane	156.3	-17.37222	-11585.21	134.0873	9.45325E-06	247.57	638.76	0.0367	0.0024

Table A-2: Database of VOC and material properties

- Approach 1: The diffusion model parameters are estimated by the procedure with VOC emission data of chamber test of the cited works.
- Approach 2: The coefficients for the correlation of D_m and molecular weight, K_{ma} and vapor pressure, respectively, are based on the cited works. If the cited works provide emission data of VOC compound out of the defined target compound in ST1, approach 1 was applied to obtain the diffusion model parameter first.
- Approach L: The diffusion model parameters are provided directly by the cited work.
- Polarity of compounds:
    - Polar: Acetaldehyde, Acrolein, Alpha-pinene, Formaldehyde, Styrene, Toluene, Trichloroethylene
    - Non-polar: Benzene, Naphthalene

Material:	particleboard									
VOC	CAS NO.	VOC type	D_m (m^2/s)		K_{ma}		C_{m0} ($\mu g/m^3$)		Approach	Source
			Mean	SD	Mean	SD	Mean	SD		
Acetaldehyde	75-07-0	Aldehyde	1.67E-11	0.00E+00	1.73E+04	8.39E+03	3.80E+05	6.44E+04	1	Suzuki et al., 2014
Acrolein	107-02-8	Aldehyde	5.16E-08		6.27E+02				2	
Alpha-pinene	80-56-8	Terpenes	1.74E-10	1.33E-10	1.74E+03	2.45E+03	7.04E+03	3.41E+03	1	NRC reprot 4-1, 1999
Benzene	71-43-2	Aromatic	7.33E-10		2.66E+02		-		L	Bodalal et al., 1999
Formaldehyde	50-00-0	Aldehyde	4.84E-10	6.80E-11	2.94E+03	1.30E+03	2.74E+07	6.00E+05	L	Xiong et al., 2011
Naphthalene	91-20-3	Aromatic	2.39E-11		2.63E+05				2	
Styrene	100-42-5	Aromatic	1.00E-10		1.21E+03				2	
Toluene	108-88-3	Aromatic	2.68E-10		9.68E+02				L	Bodalal et al., 1999
Trichloroethylene	79-01-6	Halocarbon								

Material:	carpet									
VOC	CAS NO.	VOC type	D_m (m^2/s)		K_{ma}		C_{m0} ($\mu g/m^3$)		Approach	Source
			Mean	SD	Mean	SD	Mean	SD		
Acetaldehyde	75-07-0	Aldehyde	6.40E-12		1.00E+00		1.30E+06		L	Little et al., 1994
Acrolein	107-02-8	Aldehyde	4.27E-10		1.00E+00				2	Zhang et al., 2001
Alpha-pinene	80-56-8	Terpenes	1.46E-10		1.38E+02				2	Zhang et al., 2001
Benzene	71-43-2	Aromatic	3.50E-10		1.15E+00				2	Zhang et al., 2001
Formaldehyde	50-00-0	Aldehyde	2.00E-08	2.00E-08	5.83E+03	5.17E+03	4.50E+06	-	L	Little et al., 1994 Xu et al., 2012
Naphthalene	91-20-3	Aromatic	1.74E-10		8.64E+04				2	Zhang et al., 2001
Styrene	100-42-5	Aromatic	3.60E-12	4.08E-13	5.47E+03	9.53E+02	1.02E+07	1.12E+07	L	Little et al., 1994
Toluene	108-88-3	Aromatic	1.12E-10		4.98E+00		3.56E+05		1	Elkilani et al., 2003
Trichloroethylene	79-01-6	Halocarbon								

Material:	gypsum									
VOC	CAS NO.	VOC type	D_m (m^2/s)		K_{ma}		C_{m0} (µg/m^3)		Approach	Source
			Mean	SD	Mean	SD	Mean	SD		
Acetaldehyde	75-07-0	Aldehyde	4.94E-11		5.00E+01				2	Xu et al., 2012 Yang et al., 2001
Acrolein	107-02-8	Aldehyde	2.62E-11		1.31E+02				2	Xu et al., 2012 Yang et al., 2001
Alpha-pinene	80-56-8	Terpenes	9.44E-11	3.88E-11	2.97E+04	1.30E+04	1.17E+06	6.56E+05	1	NRC reprot 4-1, 1999
Benzene	71-43-2	Aromatic	1.42E-10		4.16E+02				L	Bodalal et al., 1999
Formaldehyde	50-00-0	Aldehyde	1.40E-10	2.01E-12	4.63E+02	1.65E+01			L	Xu et al., 2012
Naphthalene	91-20-3	Aromatic	1.05E-11		9.34E+04				2	Bodalal et al., 1999
Styrene	100-42-5	Aromatic	3.13E-11		2.02E+03				2	Bodalal et al., 1999
Toluene	108-88-3	Aromatic	6.17E-11	2.02E-11	8.98E+03	1.26E+04	8.23E+06	4.20E+06	L and 1	Bodalal et al., 1999 NRC report 4-1, 1999
Trichloroethylene	79-01-6	Halocarbon								

Material:	painting									
VOC	CAS NO.	VOC type	D_m (m^2/s)		K_{ma}		C_{m0} ($\mu g/m^3$)		Approach	Source
			Mean	SD	Mean	SD	Mean	SD		
Acetaldehyde	75-07-0	Aldehyde	1.52E-07		2.88E+03				2	NRC reprot 4-1, 1999
Acrolein	107-02-8	Aldehyde	4.67E-08		1.21E+03				2	NRC reprot 4-1, 1999
Alpha-pinene	80-56-8	Terpenes	6.13E-10		6.24E+01				2	NRC reprot 4-1, 1999
Benzene	71-43-2	Aromatic	4.04E-10		1.70E+01		6.29E+04		1	BEESL Lab, 2019
Formaldehyde	50-00-0	Aldehyde	8.40E-07		5.39E+01				2	NRC reprot 4-1, 1999
Naphthalene	91-20-3	Aromatic	2.02E-09		1.05E+03				2	NRC reprot 4-1, 1999
Styrene	100-42-5	Aromatic	8.64E-10		5.54E+01				2	NRC reprot 4-1, 1999
Toluene	108-88-3	Aromatic	9.67E-11		1.31E+02		3.22E+10		L	Xiong et al., 2011
Trichloroethylene	79-01-6	Halocarbon								

Material:	plywood									
VOC	CAS NO.	VOC type	D_m (m^2/s)		K_{ma}		C_{m0} (µg/m^3)		Approach	Source
			Mean	SD	Mean	SD	Mean	SD		
Acetaldehyde	75-07-0	Aldehyde	5.19E-11		1.98E+01				2	Bodalal et al., 1999
Acrolein	107-02-8	Aldehyde	3.93E-11		6.15E+01				2	Bodalal et al., 1999
Alpha-pinene	80-56-8	Terpenes	1.45E-10	6.49E-11	3.57E+03	3.15E+03	1.84E+06	1.91E+06	1	NRC reprot 4-1, 1999
Benzene	71-43-2	Aromatic	2.08E-11		1.84E+02				L	Bodalal et al., 1999
Formaldehyde	50-00-0	Aldehyde	7.76E-11		3.50E+03				2	Bodalal et al., 2000
Naphthalene	91-20-3	Aromatic	1.52E-11		1.32E+05				2	Bodalal et al., 1999
Styrene	100-42-5	Aromatic	1.93E-11		1.50E+03				2	Bodalal et al., 1999
Toluene	108-88-3	Aromatic	1.19E-10	3.83E-11	9.89E+03	9.16E+03	8.52E+06	5.66E+06	1	NRC reprot 4-1, 1999
Trichloroethylene	79-01-6	Halocarbon								